Universidade do Minho
Escola de Ciências

Francisco Manuel de Oliveira Magalhães

Metabolic engineering for the production of branched-chain fatty acids from D-xylose in *Saccharomyces cerevisiae*

julho de 2023

Metabolic engineering for the production of branched-chain fatty acids from D-xylose in *Saccharomyces cerevisiae*
Francisco Magalhães
UMinho | 2023

Universidade do Minho
Escola de Ciências

Francisco Manuel de Oliveira Magalhães

Metabolic engineering for the production of branched-chain fatty acids from D-xylose in *Saccharomyces cerevisiae*

Dissertação de Mestrado
Mestrado em Bioquímica Aplicada

Trabalho efetuado sob a orientação de
Professor Doutor Björn Fredrik Johansson
Doutorando Paulo César Fernandes da Silva

julho de 2023

Acknowledgements

First of all, I would like to thank my supervisors Professor Björn Fredrik Johansson and Paulo César Fernandes da Silva for their availability and help in carrying out this work, and also for the teachings and sharing of scientific knowledge.

I would like to thank my LGM colleagues, Humberto, João, Vitor, Rosana, Alexandra, Cláudia, Inês and Faezeh for their companionship and help, and for all the moments spent.

I would also like to thank all the other colleagues and technicians of the Biology Department, in particular Sr. Luís, Inês, D. Manuela and Sr. Amaro for their assistance provided in this work.

And lastly, I would like to thank my family and friends for all the moral support, and for being there in the worst and best moments of my life.

This work was supported by project FatVal PTDC/EAM-AMB/32506/2017 (POCI-01-0145-FEDER032506) from which I also received a three month scholarship.

STATEMENT OF INTEGRITY

I hereby declare having conducted this academic work with integrity. I confirm that I have not used plagiarism or any form of undue use of information or falsification of results along the process leading to its elaboration.

I further declare that I have fully acknowledged the Code of Ethical Conduct of the Universidade do Minho.

Resumo

Engenharia metabólica para a produção de ácidos gordos de cadeia ramificada a partir de D-xilose em *Saccharomyces cerevisiae*

Os ácidos gordos de cadeia ramificada (BCFAs) são um grupo específico de ácidos gordos e são produtos de grande interesse dado as recentes aplicações clínicas descobertas. Os ácidos gordos são sintetizados em vários organismos, incluindo a *Saccharomyces cerevisiae*. As leveduras utilizam principalmente a glucose como principal fonte de carbono. No entanto, existem outras alternativas como a xilose, que é abundante na biomassa lignocelulósica. Ainda assim, esta espécie de levedura não tem a capacidade de assimilar naturalmente a xilose. Por isso, são necessárias estratégias de engenharia metabólica para obter estirpes de levedura capazes de assimilar xilose e crescer eficientemente em meios contendo xilose. O intuito da engenharia metabólica é modificar o metabolismo celular para promover ou melhorar o consumo de substratos e a produção de metabolitos. Uma estratégia é a expressão heteróloga da via da xilose isomerase (XI) para converter a xilose em xilulose, que pode ser metabolizada pelas leveduras. Neste trabalho, estirpes de levedura foram transformadas com um plasmídeo usado como vetor de expressão contendo a cassete de expressão da XI. Além disso, integração genómica desta via foi tentada pelo método CRISPR/Cas9. Após a expressão da via XI, as leveduras foram submetidas a evolução laboratorial adaptativa para melhorar o consumo da xilose e o crescimento em meios com este açúcar. As leveduras foram também evoluídas sob depleção de nitrogénio para aumentar a acumulação de lípidos. Neste trabalho, a expressão heteróloga da via XI e a evolução adaptativa levaram ao desenvolvimento de estirpes de levedura consumidoras de xilose. A combinação de vias heterólogas para a consumo de xilose com a produção de ácidos gordos expandiria as aplicações da engenharia metabólica em leveduras, levando a um processo sustentável de produção de combustíveis e outros produtos químicos.

Palavras-chave: Ácidos gordos de cadeia ramificada; D-Xilose; Engenharia metabólica; *Saccharomyces cerevisiae*; Xilose isomerase.

Abstract

Metabolic engineering for the production of branched-chain fatty acids from D-xylose in *Saccharomyces cerevisiae*

Branched-chain fatty acids (BCFAs) are a specific group of fatty acids and are products of great interest since clinical applications were recently found. Fatty acids are synthesized in various organisms, including the *Saccharomyces cerevisiae* yeast. Yeasts uses mainly glucose as the main carbon source. Nevertheless, there are other alternatives like xylose, which is abundant in lignocellulosic biomass. However, this yeast specie does not have the ability to naturally assimilate xylose. Therefore, metabolic engineering strategies are required to obtain yeast strains capable to assimilate xylose and grow efficiently on xylose-containing media. The aim of metabolic engineering is to modify the cellular metabolism to enable or improve the substrate consumption and metabolite production. One strategy is the heterologous expression of xylose isomerase (XI) pathway to convert xylose into xylulose, which can be metabolized by yeasts. In this work, yeast strains were transformed with a plasmid used as an expression vector containing the XI expression cassette. Besides, the genomic integration of XI pathway was also attempted by the CRISPR/Cas9 method. After the expression of the XI pathway, yeasts were subjected to adaptive laboratorial evolution to improve the xylose consumption and growth on xylose-containing media. In addition, yeasts were evolved under nitrogen depletion in order to enhance the lipid accumulation. In this work, the heterologous expression of XI pathway and the adaptive evolution led to the development of xylose-consuming yeast strains. The combination of heterologous pathways for the xylose consumption with the production of fatty acids would expand the applications of metabolic engineering in yeasts, leading to an sustainable process for the production of fuels and other chemicals.

Keywords: Branched-chain fatty acids; D-Xylose; Metabolic engineering; *Saccharomyces cerevisiae*; Xylose isomerase.

Table of Contents

List of Abbreviations

6-PGL	6-phosphogluconolactone
6-PG	6-phosphogluconate
A-ALD	Acetylating acetaldehyde dehydrogenase
ACC	Acetyl-CoA carboxylase
ACK	Acetate kinase
ACP	Acyl carrier protein
ACS	Acetyl-CoA synthetase
ADH	Alcohol dehydrogenase
ADP	Adenosine diphosphate
ALD	Acetaldehyde dehydrogenase
ALE	Adaptive laboratorial evolution
ATP	Adenosine triphosphate
BCAA	Branched-chain amino acid
BCAT	Branched-chain amino acid transferase
BCFA	Branched-chain fatty acid
BKD	Branched-chain-α-ketoacid dehydrogenase
bp	Base-pairs
CRISPR	Clustered regularly interspaced short palindromic repeats
DNA	Deoxyribonucleic acid
Ery-4-P	Erythrose-4-phosphate

F-6-P	Fructose-6-phosphate
FA	Fatty acid
FAEE	Fatty acid ethyl ester
FAL	Fatty alcohol
FAR	Fatty acyl-CoA reductase
FAS	Fatty acid synthases
FFA	Free fatty acid
Fru-6-P	Fructose-6-phosphate
G-6-P	Glucose-6-phosphate
GA-3-P	Glyceraldehyde-3-phosphate
GC-MS	Gas chromatography - mass spectrometry
Gly-3-P	Glyceraldehyde-3-phosphate
Gnd	Phosphogluconate dehydrogenase
GPD	Glyceraldehyde-3-phosphate dehydrogenase
GRAS	Generally regarded as safe
gRNA	Guide RNA
HULT	Histidine uracil leucine tryptophan
LB-Amp	Lysogeny broth with ampicillin
LC-MS	Liquid chromatography - mass spectrometry
LCFA	Large-chain fatty acid
MCFA	Medium-chain fatty acid
MPT	Malonyl:palmitoyl transferase
NAD	Nicotinamide adenine dinucleotide
OD	Optical density

PBH	Polyhydroxybutyrate
PCR	Polymerase chain reaction
PDC	Pyruvate dehydrogenase complex
PDH	Pyruvate dehydrogenase
PFL	Pyruvate:formate lyase
PFO	Pyruvate:ferrodoxin oxidoreductase
Pi	Inorganic phosphate
PNO	Pyruvate: NADP+ oxidoreductase
PPP	Pentose phosphate pathway
RNA	Ribonucleic acid
Rpe1	Ribulosephosphate epimerase
SCFA	Short-chain fatty acid
SC-U	Synthetic complete medium without uracil
SDX	Synthetic defined xylose medium
Sed-7-P	Sedoheptulose-7-phosphate
SOC	Super optimal broth with catabolite repression
Tal1	Transaldolase
TALEN	Transcription activator-like effector nucleases
TE	Thioesterase enzyme
Tkl1	Transketolase
Tm	Melting temperature
VLCFA	Very large-chain fatty acid
WS	Wax-ester synthase
XDH	Xylitol dehydrogenase
XI	Xylose isomerase
XK	Xylulokinase

XR Xylose reductase

YNB Yeast nitrogen base
YPD Yeast peptone dextrose
YPK Yeast pathway kit
YPX Yeast peptone xylose

ZFN Zinc-finger nucleases
Zwf1 Glucose-6-phosphate dehydrogenase

List of Figures

List of Tables

Chapter 1

Introduction

1.1 Metabolic engineering of *Saccharomyces cerevisiae*

1.1.1 Metabolic engineering concept

Metabolic engineering is a practice in which the cellular metabolism is modified in order to improve the cellular activities by manipulation of enzymatic, transport, and regulatory functions of the cell (Bailey, 1991). It can be applied to various organisms including bacteria, yeast, filamentous fungi, plants, and animals. Metabolic engineering strategies are used to enable or improve the product formation, substrate consumption or to enhance cellular properties, by modification of specific metabolic pathways or introduction of new ones (Stephanopoulos et al., 1998). The metabolism is modified through genetic engineering techniques based on the use of the recombinant DNA technology.

Metabolic engineering encompasses two stages of synthesis and analysis. The synthetic component involves genetic engineering strategies used to modify certain metabolic pathways in a host organism, enabling the creation of engineered strains with improved properties. These engineering strategies can include the introduction of heterologous genes, or the modification and deletion of native genes. Furthermore, the obtained engineered organisms are evaluated for their ability to consume or produce a desired metabolite. Thus, the analysis component comes with various methods to evaluate the outcome of the modifications made in the host organism. The most common analytic techniques include: DNA array technology for transcriptome analysis; two-dimensional gel electrophoresis for proteome analysis; chromatographic techniques coupled to mass spectrometry for metabolite level measurements; ^{13}C-labelling experiments for metabolic flux analysis; advanced fermentation experiments; and bioinformatics (Ostergaard et al., 2000).

Prior to the existence of genetic engineering techniques, the biotechnology relied on the natural ability of a cell to produce valuable products, and strain improvement was based on random mutagenesis and selection strategies (Wuest et al., 2011). However, the advances in genetics and molecular biology led to

the emergence of genetic manipulation tools that enabled the construction of new engineered strains with improved traits. The first attempt to manipulate microbial DNA happened with the experiment done in 1973 by Stanley Cohen, Herbert Boyer and their colleagues (Cohen et al., 1973). In this experiment, they produced recombinant human insulin from bacteria through the introduction of foreign genes into bacterial cells, which allowed the transfer of genes from one organism to another. Then, it became apparent that bacteria and other microorganisms could be engineered to use genes for the overproduction of chemicals and pharmaceutical products (Woolston et al., 2013). This discovery was crucial for the appearance of the genetic engineering and it was the basis of the recombinant DNA technology. The development of that technique was essential to the beginning of metabolic engineering since it introduced a way to modify specific biochemical reactions in cells (Stephanopoulos et al., 1998). During the 1980s, researchers investigated fundamental questions of design and functioning of chemical networks. This led to the publication of the first scientific papers enumerating all possible routes connecting a substrate with a target product, the thermodynamic analysis of pathways, the distribution of kinetic control, and the design of genetic circuits to bring about a desired pattern of gene expression and product synthesis (Woolston et al., 2013). Then, the first works towards the metabolic engineering concept were published in the beginning of the 1990s by James Bailey, Gregory Stephanopoulos and Joseph Vallino (Bailey, 1991; Stephanopoulos and Vallino, 1991). These works laid the groundwork for the systematic engineering of metabolic pathways in microorganisms and established the field as an relevant area of research in biotechnology and synthetic biology.

Currently, metabolic engineering has many applications, specially in bacteria and yeasts since they have historically been the easiest to study and manipulate (Wuest et al., 2011). These applications include the synthesis of new heterologous products, the increase of native product yields, and the use of less expensive feedstocks. Besides, metabolic engineering has the potential to play a significant role in promoting an environment-friendly economy. By harnessing the power of living cells and their metabolic activities, it is possible to develop more sustainable and efficient manufacturing processes for a wide range of products, including advanced biofuels and industrial chemicals (Kwak and Jin, 2017). The high selectivity and specificity of biological catalysts, including enzymes and microbial cells, is one of their main advantages. Biological catalysts are highly suited to certain chemical processes, lowering the amount of undesirable byproducts and waste that are produced by the traditional chemical synthesis, and improving the overall process efficiency (Sheldon and Woodley, 2017). Moreover, many biological reactions can be carried out at lower temperatures and pressures in comparison to the traditional chemical processes, minimizing the energy consumption required for manufacturing. This not only reduces the environmental impact of the manufacturing process, but it can also lead to cost savings and increased competitiveness.

1.1.2 Metabolic engineering in *S. cerevisiae*

Saccharomyces cerevisiae, also known as baker's yeast, is a eukaryotic unicellular organism belonging to the kingdom Fungi and an important model organism in biological studies. Yeasts share similarities with higher eukaryotes in cellular organization, making them a suitable model for eukaryotic organisms including humans. It has remarkable features such as rapid growth, ease of replica plating and mutant isolation, ease of genetic manipulation, and highly versatile DNA transformation system (Sherman, 2002). Besides, it is non-pathogenic and it has a great commercial availability. In addition, the *S. cerevisiae* genome is well-studied and it was the first eukaryotic genome to be sequenced in 1996 (Engel et al., 2014). The complete sequence of its genome is regarded as a reference to the sequences of other higher eukaryotic genes including the human ones (Meisinger et al., 2006).

Yeasts has been instrumental in the production of foods and alcoholic beverages by the fermentation process for millennia (Lahue et al., 2020). However, the existence of yeasts and their role in alcoholic fermentation remained undiscovered for a long time. In the 19^{th} century, Louis Pasteur began his work on alcoholic fermentation, in which it was established that the cause of the fermentation process is associated with vital activity exerted by yeasts (Barnett, 2003). The Pasteur's work was a fundamental contribution to biology and it changed the understanding about fermentation. Nowadays, yeasts are still used to this process, making them a relevant object of study. Furthermore, the latest advances of genetic engineering enabled the emergence of new applications of yeasts in biotechnology (Mattanovich et al., 2014).

S. cerevisiae is one of the most studied organisms and it is widely used in both fundamental research and industry. In fundamental research, yeasts are used in various fields of biology, including the study of ageing, regulation of gene expression, signal transduction, cell cycle, metabolism, apoptosis, neurodegenerative disorders, and many other biological processes (Karathia et al., 2011). Moreover, *S. cerevisiae* is widely used in biotechnology, specially in microbial production of recombinant proteins, chemicals, and metabolites. This is possible due to the genetic manipulation of yeasts, which is relatively easy and it has a large collection of genetic tools available (Nandy and Srivastava, 2018). Some yeast traits such as high substrate uptake rates, high metabolic rates, and resistance against various stresses, including low pH, high osmotic pressure, high alcohol concentration, and phage contamination, make this yeast specie an optimal choice for metabolite production (Kwak and Jin, 2017). Besides, due to the long history of application in the production of consumable products, *S. cerevisiae* has been classified as a GRAS (Generally Regarded As Safe) organism (Ostergaard et al., 2000).

The improvement of yeast strains has largely been accomplished by metabolic engineering strategies. In comparison to traditional methods of genetic strain improvement such as selection, mutagenesis, mating, and hybridization, metabolic engineering is more advantageous for two reasons: the directed modification of strains without the accumulation of unfavorable mutations, and the introduction of foreign genes into *S. cerevisiae* that endow them with novel traits (Nevoigt, 2008).

Although ethanol is the most relevant product of yeast metabolism, metabolic engineering allowed the synthesis of new products and the increase of native products yields. The most common metabolic products obtained from engineered yeasts include alcohols like butanol and isobutanol (Branduardi et al., 2013), organic acids like lactic acid and succinic acid (Porro et al., 1999; Xiberras et al., 2020), flavonoids (Wang et al., 2011), stilbenoids (Wang et al., 2011), isoprenoids (Paddon et al., 2013), polyketides (Gao et al., 2013), and penicillins (Gidijala et al., 2009). Additionally, there were attempts to develop yeasts strains for the production of fatty acids in large quantities, as well as derivatives, such as fatty alcohols (FALs), fatty acid ethyl esters (FAEEs), and alkanes (Lian and Zhao, 2015). Besides, engineered yeasts can be used for recombinant protein synthesis. For example, the human leukocyte interferon was the first recombinant protein produced by recombinant *S. cerevisiae* (R. A. Hitzeman et al., 1981). Other recombinant proteins, including human insulin and hepatitis B antigen, have also been produced by yeasts (Kjeldsen et al., 2001; R. Hitzeman et al., 1983). Another application of engineered yeasts is the whole-cell biocatalysis. This is a process where the metabolic reactions of cells are used to carry out desired chemical reactions with the use of whole cells in bioreactors. The biochemical reactions are usually employed in intracellular medium, but secreted enzymes may also contribute to biocatalytic activity through *in vivo* biotransformations (Mattanovich et al., 2014). Yeasts have been used for whole-cell biocatalysts, specifically for the reduction of α-keto esters (Kratzer et al., 2008), and conversion of cephalosporins and steroids (Abad et al., 2010; Braun et al., 2012).

1.1.3 Genetic engineering strategies in yeasts

The availability of tools for genetic modification is one of the key requirements of metabolic engineering (Nielsen and Keasling, 2016). The genetic modifications can include the introduction of heterologous genes encoding new metabolic pathways, deletion, mutation or overexpression of native genes in the host organism. These techniques usually involve the transformation of host organisms with recombinant DNA, or directed mutagenisis techniques. Some genetic engineering strategies in yeasts use the homologous recombination, which is a process where two similar DNA molecules exchange genetic material and it is used by cells as a repair mechanism of DNA breaks (Li and Heyer, 2008). This technique can be used to make precise changes in the genome, including the insertion and deletion of specific nucleotides or genes.

Heterologous genes can be introduced through the transformation of host organisms with recombinant DNA, which is composed by the vector and the insert DNA. The insert is a heterologous gene to be expressed, and it can be isolated by fragmentation of foreign genomic DNA with restriction enzymes or amplification by the polymerase chain reaction (PCR) (Brown, 2016). Then, the heterologous gene is cloned in a host organism, using a cloning vector to replicate the recombinant DNA in the host cell. Consequently, multiple copies of the recombinant DNA, including the vector and the heterologous gene, are obtained.

The cloned gene is then inserted into an expression vector and incorporated by the host organism through transformation. In *S. cerevisiae*, this is typically done using the PEG-LiAc-ssDNA method, where yeast cells are treated with a mixture of polyethylene glycol, lithium acetate, and a single stranded DNA carrier, in order to make them more permeable to foreign DNA (Gietz, 2014).

The gene inactivation is done through insertional mutagenesis (knock-out), where a gene construction is introduced into the host organism to inhibit the expression of a specific gene (Sitnicka et al., 2010). It starts with the insertion of a DNA fragment from a vector into a targeted gene in the host DNA. This insertion causes the discontinuation of the gene and block its expression. Deletion cassettes can be used for gene inactivation, which is inserted into a vector DNA and incorporated in the host cell. Then, the cassette is integrated into the host chromosomal DNA via homologous recombination, causing the disruption of gene expression.

Furthermore, strain engineering can be performed by other genome edition techniques, such as meganucleases (Paques and Duchateau, 2007), transcription activator-like effector nucleases (TALENs) (Christian et al., 2010), and zinc-finger nucleases (ZFNs) (Carroll, 2011). These technologies utilize double-stranded DNA breaks for site-directed genome edition. However, especially when multiple genetic manipulations are required, strain construction is a time-consuming and labour-intensive process (Mans et al., 2015). A recently developed method for genome editing is the CRISPR/Cas9. It offers improvements over the aforementioned methods, and it has the potential to be employed in gene therapy (Xiao-Jie et al., 2015). This method is based on a bacterial defense mechanism against viruses that consists of a DNA segment containing alternating repeating DNA sequences called CRISPR (Clustered Regularly Interspaced Palindromic Repeats). These sequences are spaced by viral DNA collected from previous phage infections (Barrangou et al., 2007). The Cas proteins cut the viral DNA at specific sequences to neutralize the virus and collect a part that is added to the CRISPR array. This mechanism enables the recognition of foreign DNA from invading viruses and gives an embedded memory of the virus infection, enabling bacteria to defend themselves against future phage invasions. The CRISPR/Cas9 system requires two components for its function, the Cas9 protein and the guide RNA (gRNA) (Mans et al., 2015). The gRNA directs the Cas9 to cut a selected region of the host genomic DNA where the guide RNA is complementary. Whereas, the Cas9 cuts the double stranded DNA at a specific location, more precisely in a region called protospacer adjacent motif (PAM). After the DNA cut, the DNA is repaired via two pathways: non-homologous end joining (NHEJ), typically leading to a random insertion or deletion of DNA; or homology directed repair (HDR), where a homologous piece of DNA is used as a repair template (Redman et al., 2016). The CRISPR/Cas9 is an efficient approach for strain construction and explores their potential for simultaneous introduction of multiple genetic modifications on yeasts. In *S. cerevisiae*, a plasmid expressing the Cas9 and a selected guide RNA target sequence can be introduced in yeasts through transformation (Generoso et al., 2016). This enables a simple and rapid way to introduce modifications on yeast DNA, since the Cas9 and the guide RNA are expressed on a single plasmid.

1.2 Yeast xylose catabolism

1.2.1 Xylose catabolism

The traditional carbon sources used by yeasts are glucose and sucrose, which are primarily produced from cane sugar and corn starch (Mattanovich et al., 2014). Nevertheless, there are other alternative carbon sources that can be used by yeasts. The best examples are glycerol, a by-product from biodiesel production, and the main constituents of hemicellulose, xylose and arabinose (Mattanovich et al., 2014). Xylose is an aldopentose and it is the second most abundant sugar in nature after glucose, being 30-40% of the lignocellulosic biomass (Mosier et al., 2005). Since xylose is predominant in lignocellulosic materials, it is an attractive substrate for production of fuels and chemicals (Kwak and Jin, 2017). However, most microorganisms, including *S. cerevisiae*, are unable to metabolize xylose and use it as a carbon source. Therefore, genetic engineering approaches are required in order to enable the xylose assimilation in such organisms.

Xylose assimilation requires the conversion of xylose into xylulose and subsequent phosphorylation of xylulose to xylulose-5-phosphate (Figure 1). The most widely used metabolic engineering strategies for the xylose consumption in *S. cerevisiae* involves the expression of heterologous genes that encode enzymes for xylose conversion. Two metabolic pathways for xylose assimilation are the xylose isomerase (XI) and the oxidoreductase (XR/XDH) pathways. In the XI pathway, xylose is directly converted into xylulose via xylose isomerase. In the oxidoreductase pathway, xylose is first reduced to xylitol via xylose reductase (XR), which is then oxidized into xylulose via xylitol dehydrogenase (XDH). Xylose reductase uses NADPH or NADH for reduction, whereas xylitol dehydrogenase only requires NAD+ for oxidation. The oxidoreductase pathway is predominant in fungi, while the xylose isomerase pathway is more common in prokaryotes (Silva et al., 2021). The enzymes XR and XDH are encoded by the genes *XYL1* and *XYL2*, respectively, and the XI is encoded by the *xylA* gene (Ostergaard et al., 2000).

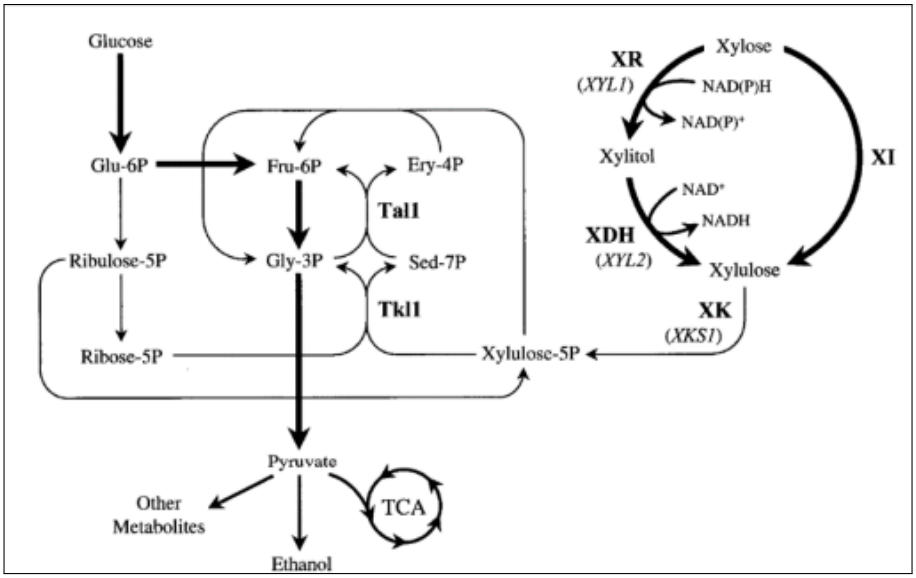

Figure 1: Overview of glucose and xylose catabolism in *S. cerevisiae*. The bold lines represent the glycolytic pathway, where glucose catabolism occurs, and the xylose assimilation pathway. The remaining lines represent the PPP. Abbreviations: TCA = tricarboxylic acid cycle; Tkl1 = transketolase; Tal1 = transaldolase; Glu-6P = glucose-6-phosphate; Fru-6P = fructose-6-phosphate; Gly-3P = glyceraldehyde-3-phosphate; Ery-4P = erythrose-4-phosphate; Sed-7P = sedoheptulose-7-phosphate. The *XYL1*, *XYL2* and *XKS1* genes are shown in parentheses. XR - xylose reductase; XDH - xylitol dehydrogenase; XI - xylose isomerase, XK - xylulokinase. Obtained from Ostergaard *et al.* (2000).

Although the oxidoreductase pathway expression in *S. cerevisiae* provides faster xylose assimilation rates in comparison with the xylose isomerase pathway (Karhumaa et al., 2007), it is susceptible to a cofactor imbalance under anaerobic conditions (Wahlbom et al., 2001). This cofactor imbalance occurs due to the differential coenzyme preference between xylose reductase and xylitol dehydrogenase, where XR preferably uses NADPH over NADH for xylose reduction (Cunha et al., 2019). Consequently, it leads to an accumulation of xylitol that reduces the carbon assimilation and ethanol production in yeasts (Hahn-Hägerdal et al., 2007). One solution to this cofactor imbalance is to increase the activity of xylitol dehydrogenase by overexpressing the *XYL2* gene (Karhumaa et al., 2007). Other strategies have been employed to solve this problem, which involve the redirection of carbon fluxes from NADPH to NADH-consuming reactions (Moysés et al., 2016). These strategies encompasses the addition of an external electron acceptor to the fermentation media (Ohgren et al., 2007), the connection of furaldehyde reduction with xylose metabolism (Almeida et al., 2009), the modification of ammonium assimilation pathway (Roca et al., 2003), the channelling of carbon fluxes through a recombinant phosphoketolase pathway in a xylose-consuming strain (Sonderegger et al., 2004), and the change of cofactor preference for the XR and XDH enzymes (Almeida et al., 2011).

The development of efficient xylose-consuming yeast strains is critical to the production and commercialization of advanced biofuels and chemicals (Kwak and Jin, 2017). This has the potential to reduce the reliance on fossil fuels and to promote the production of yeast metabolic products by a sustainable and

environment-friendly process. In this process, renewable feedstocks like the lignocellulosic biomass can be used, where xylose is abundant. Therefore, metabolic engineering strategies applied for the production of metabolites derived from the xylose conversion in yeasts can contribute to the implementation of a sustainable production process in a future green economy.

1.2.2 Xylose isomerase pathway

The xylose isomerase is an enzyme that catalyzes the conversion of D-xylose into D-xylulose in a single-step reaction. It belongs to the family of isomerases, specially those involved in the interconversion of aldoses and ketoses. Xylose isomerases are also referred to as glucose isomerases because of their ability to convert D-glucose into D-fructose (Singh and Kumar, 2019). Currently, this enzyme has been successfully industrialized and it has a extensive market in the food industry due its application in production of high-fructose corn syrup (Mu et al., 2018).

As mentioned before, the xylose isomerase pathway is one of the metabolic routes for xylose degradation in yeasts. In *S. cerevisiae*, the heterologous expression of XI pathway is necessary since the xylose isomerase enzyme is not present in this yeast specie. In contrast to the oxidoreductase pathway, the XI pathway is a redox neutral reaction and does not suffer from a cofactor imbalance. For this reason, the currently most promising xylose metabolic pathways are based on the XI pathway (Silva et al., 2021). However, this metabolic pathway has been proven to be difficult to express in *S. cerevisiae*. Several attempts have been made, which include XIs from *Escherichia coli* (Briggs et al., 1984; Sarthy et al., 1987), *Bacillus subtilis* (Amore et al., 1989), *Actinoplanes missouriensis* (Amore et al., 1989), *Lactobacillus pentosus* (Hallborn, 1996) and *Clostridium thermosulfurogenes* (Moes et al., 1996). This difficulty to express the XI pathway in yeasts was attributed to several reasons, such as protein misfolding, post-translational modifications, improper disulfide bridge formation, sub-optimal internal pH, and absence of specific metal ions (Van Maris et al., 2007). The first successfully expressed XIs in *S. cerevisiae* were extracted from *Thermus thermophilus* and *Piromyces sp.* (Walfridsson et al., 1997; Kuyper et al., 2003). Furthermore, other XIs were expressed in yeasts, being currently fifteen which have been actively expressed (Silva et al., 2021). Among these, it is included the most recent xylose isomerase to be expressed and tested on yeasts, a novel xylose isomerase extracted from the gut of the wood feeding beetle *Odontotaenius disjunctus*. This new XI, denominated as 8054_2, displays higher growth rates on xylose under aerobic conditions and better kinetic properties, in comparison with its homolog from *Piromyces sp.*. Besides, this new XI provides 50% faster growth on xylose to yeasts, 72% higher xylose isomerization rate than the XI from *Piromyces*, it has 2.6 times higher specific activity, 37% higher affinity for D-xylose, and it exhibits higher activity over a broader temperature range, retaining 51% of maximal activity at 30°C, when compared with only 29% activity of the *Piromyces* XI (Silva et al., 2021). Therefore, this novel XI is a highly valuable addition to the yeast metabolism, enabling an efficient assimilation and conversion of xylose in *S. cerevisiae*.

1.3 Optimization of yeast metabolism by adaptive laboratorial evolution

1.3.1 Adaptive laboratorial evolution

Adaptive laboratorial evolution (ALE) is a useful technique for the development of evolved microbial strains with a desired phenotype, implementing the same principles of natural selection in laboratorial settings (Mavrommati et al., 2021). During an ALE experiment, a certain organism is cultivated under clearly defined conditions for prolonged periods of time, in the range of weeks to years, in order to allow the selection of improved phenotypes by selecting those that undergo advantageous mutations (Dragosits and Mattanovich, 2013). ALE has become a valuable tool in metabolic engineering for strain development and optimization by reliably facilitating microbial fitness improvements (Sandberg et al., 2019). Adaptive evolution is a powerful method to improve certain features in microbial strains without required previous knowledge of underlying genetic mechanisms, as long as the desired trait can be coupled and achieved with the microbial growth (Winkler et al., 2013).

The ALE experiments can be performed by serial batch cultivation in shake flasks, in chemostat continuous cultures, or in turbitostat cultures (Figure 2). The most common procedure for adaptive evolution is in serial batch cultivations since it is a simple and inexpensive method. In this particular case, microbial cells are cultivated in media and grown until reach a certain optical density. Then, the cells are successively transferred to new cultures where there is a gradual variation of the environmental conditions, to adapt the microorganisms to the desired conditions (Mavrommati et al., 2021). Alternatively, the ALE experiment can be carried out in continuous culturing devices like chemostats and turbidostats. However, the use of chemostats and turbidostats is expensive as it requires specific equipment and expertise. Chemostats are continuous culture vessels, where the nutrient supply and the microbial population are kept constant under a controlled environment (Ziv et al., 2013). In order to maintain a constant working volume over time, fresh medium is continuously introduced to the vessel while the microbial culture is withdrawn at the same rate as the media enters. The growth conditions are controlled by a single limiting nutrient that is added to the system at a constant rate, and evolution occurs under nutrient limitation. A turbidostat is a reactor similar to a chemostat, in which an optical sensor measures the turbidity of the fluid (Li and Heyer, 2008). When an ALE experiment is carried out using a turbidostat, new media is continuously fed to the culture while the microbial culture is withdrawn, in the same way as in a chemostat culture. In turbidostat cultures, the cell density is maintained at a certain level by the continuous dilution with fresh medium (Dragosits and Mattanovich, 2013). In contrast to chemostat cultures, the growth rate in turbidostats does not depend on a single component of the culture medium, neither does the flow rate remains constant.

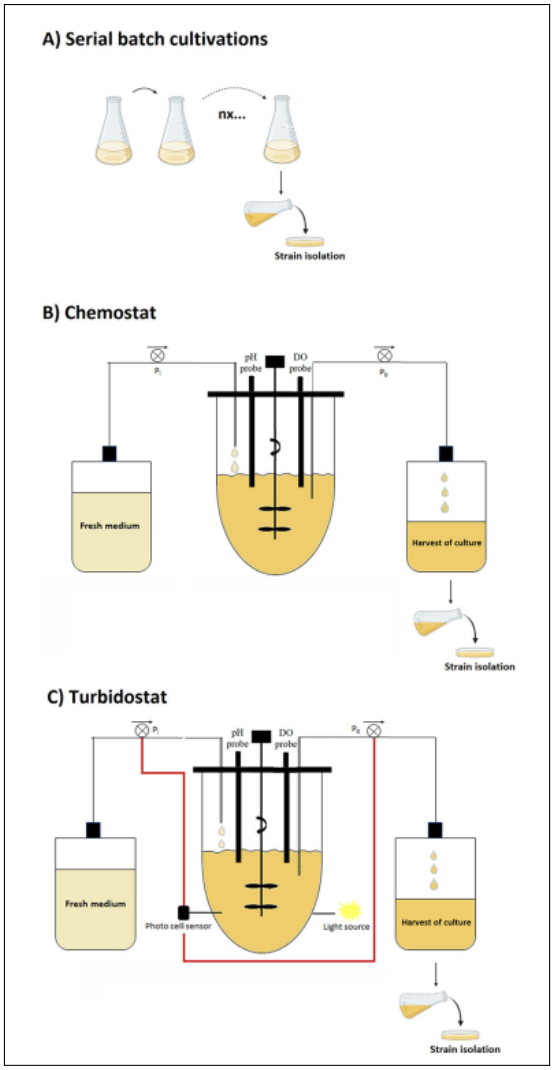

Figure 2: Experimental devices used for ALE experiments. (A): Serial batch cultivation is performed in shake flasks where growth conditions change during microbial growth. In each adaptation cycle, the stress factor is kept constant or increasing. (B): Chemostat continuous culture is performed in bioreactor where growth conditions are kept constant during microbial growth. Steady state conditions are controlled by the limiting growth factor and evolution occurs under nutrient limitation. The stress factor is kept constant or increasing during evolution. (C): Turbitostat continuous culture is performed in bioreactor where growth conditions are kept almost constant during microbial growth. Steady state conditions are controlled by the optical density in the reactor and evolution occurs under balanced growth conditions. The stress factor is kept constant or increasing during evolution. Adapted from Mavrommati *et al.* (2021).

The main applications of ALE may include: the activation of latent pathways to utilize novel substrates or to produce new products (D.-H. Lee and Palsson, 2010; Fischer et al., 2010); the increase of the substrate uptake rate (Wisselink et al., 2007); the improvement of growth rate and product titers (Fong et al., 2005); and the adaptation of microbial strains to different environmental conditions (Portnoy et al., 2008). ALE strategies have been proven highly effective for the optimization of producing strains, making it a valuable method in metabolic engineering (Chatterjee and Yuan, 2006). Besides, ALE has also become

a widely used tool for biotechnological applications, improving the yields and reducing costs in industrial settings (Portnoy et al., 2011).

1.3.2 Adaptive evolution of yeasts for the optimization of xylose assimilation

Adaptive evolution have been the most commonly used and the most effective approach to improve xylose assimilation by yeasts (Jeong et al., 2020). The introduction of the xylose isomerase pathway in *S. cerevisiae* is not enough to promote an efficient conversion of xylose, since all reported XI-based pathways in yeasts suffer from low xylose consumption rates and ethanol productivity, as well as poor cell growth when compared with the oxidoreductase pathway (S.-M. Lee et al., 2012). Thus, adaptive evolution has been used to the improve xylose assimilation in yeasts expressing this pathway. This process involves the cultivation of yeasts in culture media with glucose and xylose, where the sugar concentration ratio varies gradually over various cell generations. During the evolution experiment, the glucose concentration decreases while the concentration of xylose increases, until the culture media has solely xylose and no glucose at the end of the evolution experiment. In this way, yeasts can use both sugars as carbon sources, which increases the yeast overall growth rate in sugar mixed culture media (Papapetridis et al., 2018). Besides, yeasts will evolve through random mutations and natural selection, resulting in the generation of mutant strains that are capable to ferment xylose more efficiently.

The co-fermentation of glucose and xylose can improve the overall sugar conversion rate and the growth on culture media with both sugars. In an evolution experiment conducted by Papapetridis, various yeast strains were created and cultivated in batch culture media with glucose and xylose, where the xylose concentration was gradually increased (Papapetridis et al., 2018). The simultaneous consumption of both sugars was forced in a XI-engineered yeast strain with a modified oxidative pentose phosphate pathway (Kuyper et al., 2005), through the deletion of genes encoding the glucose-6-phosphate isomerase (*PGI1*) and the ribulose-5-phosphate epimerase (*RPE1*). The inactivation of *PGI1* prevents the metabolization of glucose-6-phosphate into glycolysis, while the inactivation of *RPE1* prevents the entry of ribulose-5-phosphate into the non-oxidative pentose phosphate pathway (PPP). Furthermore, to reduce the impact of these modifications on NADP+/NADPH redox cofactor balancing, the native NADP+-dependent 6-phosphogluconate dehydrogenases, Gnd1 and Gnd2, were replaced by a heterologous NAD+-dependent enzyme. Then, yeasts were cultivated in serial batch cultures with a mixture of glucose and xylose, in order to obtain yeast strains that rapidly consumed both sugars. After the evolution experiment, some mutations were identified by the whole-genome sequencing of the evolved strains, including mutations in *HXK2*, *RSP5* and *GAL83*. Upon their combined introduction into an engineered xylose-fermenting yeast strain, these mutations strongly promoted a simultaneous utilization of glucose and xylose, yielding a strain with a 2.5-fold higher sugar conversion ratio in comparison to its non-evolved xylose-fermenting parental strain

(Papapetridis et al., 2016). Therefore, the laboratorial evolution of XI-engineered yeasts on sugar mixed cultures with glucose and xylose has the potential to generate yeast strains that are capable to assimilate xylose more efficiently and to grow more rapidly on xylose-containing culture media.

1.3.3 Enhancement of lipid production by nitrogen depletion

In general, the metabolism of carbohydrates in yeasts merges into the glycolysis pathway. The pyruvate produced from glycolysis can be converted into acetyl-CoA via aerobic respiration, or it can be directed to the alcoholic fermentation to produce ethanol. In addition, the acetyl-CoA can also be used for the lipid biosynthesis, including fatty acids (FAs), triacylglycerols (TAGs) and lipid droplets (LDs). The relationship between the nitrogen depletion and the increase of storage lipid production was studied in a experimental work where it was intended to understand the role of nitrogen starvation in autophagy (Dan et al., 2015). The autophagy is a cellular mechanism for intracellular degradation and quality control in eukaryotes, in which cytosolic components are sequestrated into double membrane autophagosomes and the internal content is then degraded when autophagosomes fuse with endosomal or lysosomal compartments (Mizushima and Komatsu, 2011). The synthesis of storage lipids is essential to autophagy since they are involved in the autophagosome biogenisis. One universal physiological stimulus of autophagy is nutrient limitation, specially nitrogen starvation. It was found that the depletion of nitrogen sources in yeasts has an impact on carbon metabolism, as it led to a continued consumption of glucose, a downregulation of fermentation, an increase of TAG synthesis and proliferation of LDs (Dan et al., 2015). In that experiment, yeasts were cultivated in two culture media, a rich glucose medium and a synthetic glucose medium with a minimal amount of nitrogen, in which aminoacids and ammonium sulfate were removed. The cellular TAG content was measured in both yeast cultures. According to the obtained results, the yeasts cultivated under nitrogen starvation produced a larger amount of TAG accompanied by a rapid proliferation of LDs, in comparison with the yeasts cultivated in the rich glucose medium. Thus, the cultivation of yeasts in culture media with nitrogen depletion provided an improvement of lipid production. The adaptive evolution of yeasts in culture media with the removal of nitrogen sources could be an optimal strategy to enhance the lipid biosynthesis, enabling the development of yeast strains that are optimized for the production of lipids in large quantities.

1.4 Fatty acid production from D-xylose in *S. cerevisiae*

1.4.1 Production of acetyl-CoA from xylose

Acetyl-CoA plays an important role in cells since it is involved in various essential metabolic pathways. It is produced from the breakdown of carbohydrates, lipids, and proteins, serving as a key intermediate for biosynthetic pathways, such as fatty acids, sterols, amino acids and polyketides biosynthesis. In *S.*

cerevisiae, acetyl-CoA is produced from the conversion of pyruvate in mitochondria or in the cytosol (Lian and Zhao, 2015). In mitochondria, the pyruvate is converted to acetyl-CoA by the pyruvate dehydrogenase complex (PDC), initiating the TCA cycle. In the cytosol, acetyl-CoA is produced through the pyruvate dehydrogenase bypass pathway, where is generally used for the fatty acid production (Figure 3). This pathway involves the decarboxylation of pyruvate into acetaldehyde by PDC, and reduction of acetaldehyde into ethanol via alcohol dehydrogenase (ADH). Alternatively, acetaldehyde can be converted to acetate via acetaldehyde dehydrogenase (ALD). Then, the acetate can be activated by the acetyl-CoA synthetase (ACS), producing acetyl-CoA with a cost of two ATP molecules.

However, due to the feedback inhibition of ACS and high energy input requirement, the activation of acetate is a rate-limiting step (Lian and Zhao, 2015). Besides, the metabolic flux is directed toward ethanol production and the supply of acetyl-CoA is very limited, causing the low levels of cytosolic acetyl-CoA in yeasts. Some metabolic engineering strategies can be applied to redirect the metabolic fluxes and to increase acetyl-CoA levels, including the inactivation of competing pathways and the introduction of heterologous pathways that are more efficient and less energy consuming (Lian and Zhao, 2015). These strategies include the expression of heterologous pathways, including the phosphoketolase (PK), the phosphate acetyltransferase (PTA), the pyruvate:formate lyase (PFL), the pyruvate:ferrodoxin oxidoreductase (PFO), the pyruvate: NADP+ oxidoreductase (PNO), a engineered PDH-bypass pathway, the ATP-dependent citrate lyase (ACL), and the acetylating aldehyde dehydrogenase (A-ALD) pathways. Additionally, the deletion of ADH and GPD (glyceraldehyde-3-phosphate dehydrogenase) pathways can redirect the glycolytic fluxes to the acetyl-CoA biosynthesis.

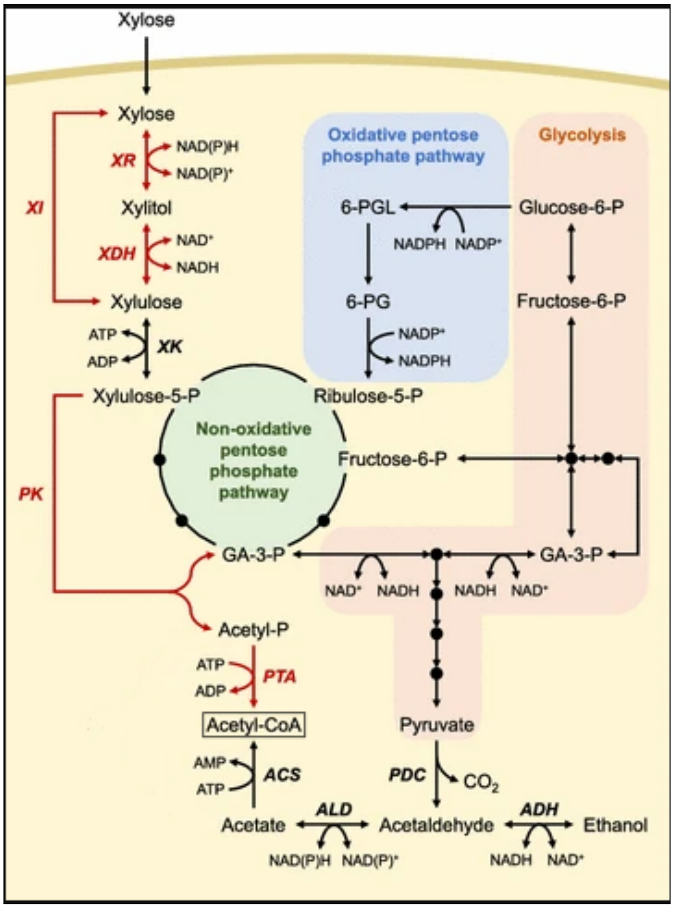

Figure 3: Overview of xylose assimilation pathways in yeasts. Black lines represent endogenous pathways in *S. cerevisiae*, and red lines represent heterologous pathways that can be introduced in these yeasts. Abbreviations: XR = xylose reductase; XI = xylose isomerase; XDH = xylitol dehydrogenase; XK = xylulokinase; PK = phosphoketolase; ACK = acetate kinase; PTA = phosphate acetyltransferase; ACS = acetyl-CoA synthase; ALD = acetaldehyde dehydrogenase; ADH = alcohol dehydrogenase; 6-PGL = 6-phosphoglucono-1,5-lactone; 6-PG = 6-phosphogluconate; GA-3-P = glyceraldehyde-3-phosphate. Adapted from Kwak and Jin (2017).

1.4.2 Phosphoketolase/Phosphate acetyltransferase pathway

As mentioned before, in *S. cerevisiae*, the conversion of xylose into xylulose and subsequent phosphorylation to xylulose-5-phosphate is followed by its metabolization through the pentose phosphate pathway. Alternatively, xylulose-5-phosphate can be metabolized in yeasts by the heterologous PK pathway (Figure 3). In this case, xylulose-5-phosphate is converted into acetyl phosphate and glyceraldehyde-3-phosphate. Glycerldehyde-3-phosphate is metabolized through either the non-oxidative phase of PPP or glycolysis, while acetyl phosphate can be phosphorylated into acetyl-CoA via phosphate acetyltransferase (PTA). The PK/PTA pathway lead to a more efficient way to convert xylulose-5-phophate in acetyl-CoA in comparison with the native metabolic route (Kwak and Jin, 2017). The reason for this is the carbon loss associated to the decarboxylation of pyruvate to acetaldehyde and the consumption of two ATP molecules in the

native metabolism. Whereas, in the PK/PTA pathway, the carbon is conserved and only one ATP unit is consumed.

The expression of PK combined with the PTA pathway results in a enhancement of acetyl-CoA production and its derivatives. The heterologous expression of the PK pathway in a yeast strain that produce polyhydroxybutyrate (PHB), a product derived from acetyl-CoA, improved the production from 4 mg/g dry cell weight into 28 mg/g dry cell weight (Kocharin et al., 2013). The PK was also expressed in yeasts for FAEEs production, which was increased by 5.7-fold relatively to the parental yeast strain (de Jong et al., 2014). Thus, the expression of the PK/PTA pathway is an appropriate strategy to enhance the acetyl-CoA production in *S. cerevisiae*. Consequently, this pathway can also promote an improved production of fatty acids in yeasts, since acetyl-CoA is a precursor of the FAs biosynthesis. In addition, this pathway establishes a link between the xylose catabolism and fatty acid production, through the xylulose-5-phosphate that is obtained from the xylose conversion and it is further metabolized into acetyl-CoA by the PK/PTA pathway.

1.4.3 Fatty acid biosynthesis

Fatty acids are essential macromolecules due to their roles in living organisms, acting as the building blocks of phospholipidic bilayers in cell membranes, storing energy, and signaling (Trotter, 2001). FAs can be classified in various types according to the length, bond and chain. In terms of bond type, FAs are separeted in two groups: saturated and unsaturated. Those which have solely simple bonds are saturated, while those with at least one double bond are unsaturated. Depending on the acyl-chain length, FAs have variable lengths ranging from 2 to 36 carbons (Cox and Nelson, 2021). There are four groups of FAs, including very long-chain fatty acids (VLCFAs), long-chain fatty acids (LCFAs), medium-chain fatty acids (MCFAs), and short-chain fatty acids (SCFAs). VLCFAs have an acyl-chain of 22 or more carbons and are used as food supplements (Rezanka, 1989). LCFAs have a length between 14 to 20 carbons, and are used mainly for biofuels production, specially biodiesel (Knothe, 2010). MCFAs have a chain ranging of 6 to 12 carbon molecules, whereas SCFAs have 2 to 4 carbons. Both MCFAs and SCFAs are used as precursors for biofuels and platform chemicals (Nikolau et al., 2008; Rude and Schirmer, 2009). Depending on chain type, FAs can be linear or branched, being the latter denominated as branched-chain fatty acids (BCFAs).

The biosynthesis of FAs is carried out by fatty acid synthases (FAS), which can be divided into two types, FAS I and FAS II. Both FAS I and II are predominant in eukaryotes and prokaryotes, respectively (Chan and Vogel, 2010). Despite being mostly found in bacteria, FAS II can also be found in eukaryotic organelles like mitochondria and plastids (Tehlivets et al., 2007). The FAS I consists of large multifunctional polypeptides that carry all the proteins necessary for FA biosynthesis on one or two large polypeptide chains, whereas FAS II is composed by discretely expressed monofunctional proteins (Lian and Zhao, 2015). In yeasts, FA biosynthesis can occur via FAS I in the cytosol, or in mitochondria via FAS II (Hu et al., 2019). In

S. cerevisiae, the FAS I comprise two subunits, α-subunit Fas2 and β-subunit Fas1. Six copies of eight independent functional domains are assembled into an $\alpha 6\beta 6$ molecular complex of 2.6 MDa (Lomakin et al., 2007).

FA synthesis begins with the conversion of acetyl-CoA into malonyl-CoA by acetyl-CoA carboxylase (ACC), with the cost of one ATP molecule (Figure 4). Then, malonyl-CoA:ACP transacylase transfers malonyl-CoA to the acyl carrier protein (ACP). Malonyl-ACP is generated and employed as an extender unit, combining with acyl-ACP to produce β-ketoacyl-ACP. The extended β-ketoacyl-ACP is reduced in a NADPH-dependent reaction to produce β-hydroxyacyl-ACP, which is then converted to trans-2-enoyl-ACP by the removal of a hydroxyl group. Then, the trans-2-enoyl-ACP reductase reduces the double bond in another NADPH-dependent reaction. Each elongation cycle results in the synthesis of acyl-ACP with the fatty acyl chain extended by two carbon units. The fatty acyl-CoA elongation cycle ends with the formation of palmitoyl-CoA, which is released from the FAS complex by the malonyl:palmitoyl transferase domain (MPT). The released fatty acyl-CoAs can be converted into various products, such as free fatty acids (FFAs), fatty alcohols (FALs), and fatty acid ethyl esters (FAEEs) by the enzymes thioesterase (TE), fatty acyl-CoA reductase (FAR), and wax-ester synthase (WS), respectively (Lian and Zhao, 2015).

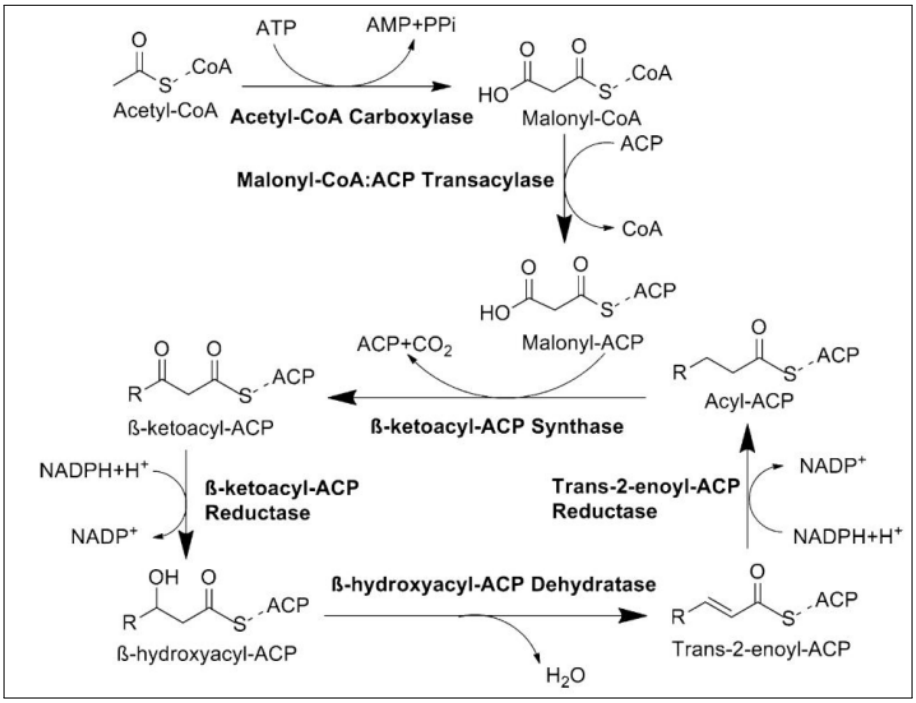

Figure 4: Overview of the fatty acid biosynthesis. Malonyl-ACP is used as the extender unit, and fatty acyl chain is extended by two carbon units after each elongation cycle including condensation, reduction, dehydration, and reduction. Obtained from Lian and Zhao (2015).

Fatty acids, specifically when they are in form of free fatty acids (FFAs), are present at low concentrations, as most FAs are bound to proteins, cofactors or other functional groups (Fernandez-Moya and Silva, 2017). However, FFAs are often desired for the conversion of FAs into derivatives, which serve as biofuels and fine chemicals (Kwak and Jin, 2017). In order to produce high levels of FAs, large amounts of FA synthesis precursors, such as acetyl-CoA, ATP and NADPH, are required. This can be achieved through metabolic engineering strategies that enhance the production of these precursors. One example is the aforementioned PK/PTA pathway, which has been proven to increase the acetyl-CoA levels in *S. cerevisiae*, leading to an enhanced production of FAs in yeasts.

1.4.4 Branched-chain fatty acids

Branched-chain fatty acids (BCFAs) are fatty acids substituted with one or more methyl branches on the linear carbon chain (Taormina et al., 2020). Usually, BCFAs have an *iso* structure where the FA has the branch point on the penultimate carbon atom, or an *anteiso* structure, in which the branch point is located on the ante-penultimate carbon atom (Figure 5).

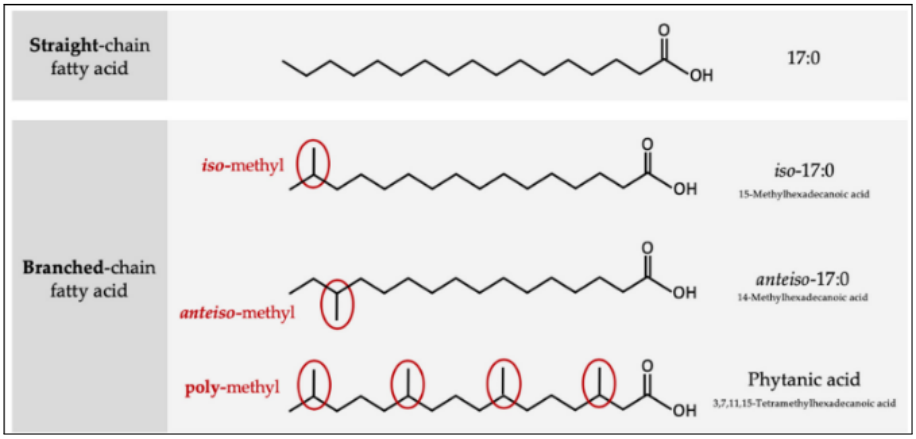

Figure 5: Structural differences between different types of FAs, including linear-chain fatty acids, and iso, anteiso, and multi-methyl branched-chain fatty acids. Obtained from Taormina *et al.* (2020).

The biosynthesis of BCFAs initiates with the production of branched-chain α-ketoacids, including α-ketoisovalerate, α-keto-β-methylvalerate, and α-ketoisocaproate, which are derived from the branched-chain amino acids (BCAAs) valine, leucine and isoleucine, respectively (Figure 6). These α-ketoacid products are obtained by the removal of the BCAA amino group via transferase enzyme. Then, the α-ketoacids are subsequently decarboxylated by branched-chain-α-ketoacid dehydrogenase, producing the respective branched short-chain carboxylic acids isobutyril-CoA, isovaleryl-CoA, and 2-methylbutyril-CoA. Finally, branched short-chain carboxylic acids are elongated by the branched-chain fatty acid synthase, where malonyl-CoA acts as the chain extender in each elongation cycle. After various cycles of chain enlogation, BCFAs with *iso* or *anteiso* structures are produced.

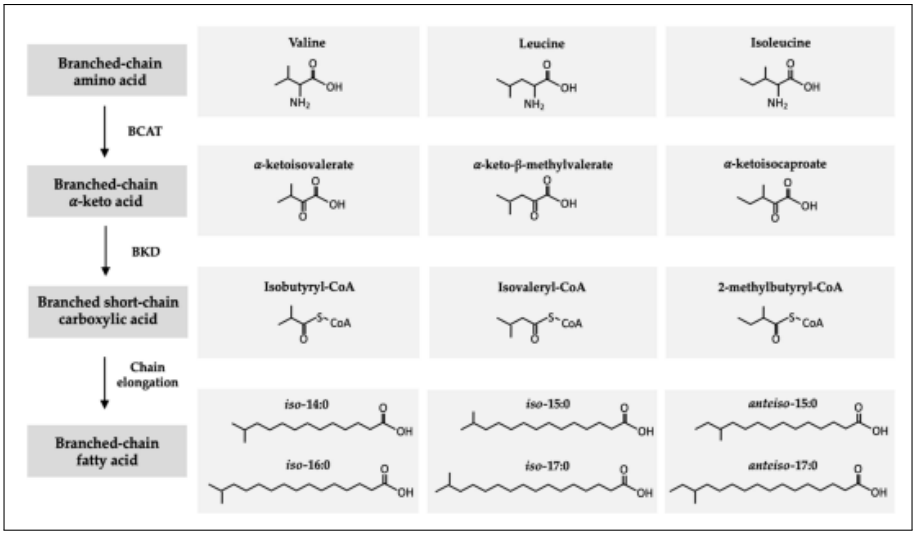

Figure 6: Biosynthetic pathways of branched-chain fatty acids. Abbreviations: BCAT, branched-chain amino acid transferase; BKD: branched-chain-α-ketoacid dehydrogenase. Obtained from Taormina *et al.* (2020).

BCFAs are typically found in dairy products, constituting 2% of dairy fat (Taormina et al., 2020). In particular, they are abundant in ruminant animals since they are produced by the bacterial fermentation of feed in the rumen (Allison and Bryant, 1963). Besides, BCFAs are common lipidic constituents of certain groups of bacteria such as the gram-positive genera *Bacillus*, *Streptomyces* and *Staphylococcus* (Christie and Han, 2012). They are particularly prominent in *Bacillus*, constituting 95% of the FAs in many species of *Bacillus* and *Lactobacillus* (Kaneda, 1991). In addition, BCFAs are important structural lipidic constituents of bacterial cell membranes since they regulate their fluidity and permeability (Taormina et al., 2020). BCFAs are also rarely found in internal human tissues, although they are present in higher concentrations in the skin and vernix caseosa, the unique waxy white substance coating the skin of term newborns (Ran-Ressler et al., 2008). Moreover, BCFAs have potential health benefits, including improved reduced inflammation, anticarcinogenic properties, energy homeostasis, improved insulin sensitivity, and improved gut health (Taormina et al., 2020). For example, capsaicin and many related compounds, which only differ by the BCFA moiety, give to chili peppers heat and have recently found clinical applications (McCarty et al., 2015). The capsaicin biosynthesis has been engineered in *S. cerevisiae*, but the production of BCFAs is still to be achieved. Due to their biological effects and possible health benefits, BCFAs are a new class of FAs that have attracted the attention of scientists (Taormina et al., 2020).

1.5 Objectives

The main purpose of this work is to optimize the xylose assimilation in *S. cerevisiae* and to rewire the metabolism towards the fatty acid biosynthesis. It is intended to establish a link between the production of fatty acids and the xylose catabolism, in which xylose is assimilated by yeasts via the xylose isomerase

pathway. The ultimate goal is the improvement of the titer, rate, and yield of fatty acids, specifically branched-chain fatty acids with pharmaceutical application, through combination of additional metabolic pathways recently developed in Björn Johansson lab. In order to achieve this aim, xylose-consuming *S. cerevisiae* strains were constructed and characterized by performing the following tasks:

- Transformation of *S. cerevisiae* with the xylose isomerase gene to integrate and express the XI pathway in yeasts. Two yeasts strains, CEN.PK2-1C and IMX994, were transformed with the plasmid pYPK0_TDH3_8054_2_ENO2, which is a expression vector that contains the xylose isomerase gene to be expressed. Besides, CEN.PK21-C yeasts were also transformed with the plasmid pRCC-K and the xylose isomerase expression cassette, in order to integrate the xylose isomerase gene on yeasts genome by the CRISPR/Cas9 method.

- Adaptive laboratorial evolution of XI-expressing yeasts to improve the xylose assimilation and growth on xylose-containing media. Yeasts were cultivated in culture media with glucose and xylose, where the concentration of xylose was gradually increased until the medium contained solely xylose and no glucose. Then, the evolved yeasts were also cultivated in two types of synthetic xylose media, one containing an aminoacid drop-out mix and another where the drop-out mix was removed to evolve yeasts under nitrogen depletion.

- Cultivation of evolved yeasts in rich glucose medium for plasmid loss, in yeasts previously transformed with the plasmid pYPK0_TDH3_8054_2_ENO2.

- Spot assay analysis for characterization of three groups of different types of yeasts: parental yeast strains, including wild-type and non-evolved transformed yeasts; evolved yeast strains; and yeasts without the plasmid pYPK0_TDH3_8054_2_ENO2. These yeast strains were tested in various cultures, such as glucose and xylose synthetic complete media without uracil, synthetic defined xylose medium, and rich xylose medium.

Chapter 2

Materials and Methods

2.1 Yeast and bacterial strains

In this experimental work, three *S. cerevisiae* strains were used: CEN.PK113-5D, CEN.PK2-1C and IMX994. The strains CEN.PK2-1C and IMX994 were used during all experimental work, while CEN.PK113-5D was used as a positive control for a colony PCR. The CEN.PK113-5D and CEN.PK2-1C strains belong to the CEN.PK family. Both CEN.PK strains are auxotrophic to uracil, and the CEN.PK2-1C strain is also auxotrophic for the aminoacids histidine, leucine and tryptophan (Entian and Kötter, 2007). IMX994 is a yeast strain that is derived from the CEN.PK113-5D yeast strain that expresses a *S. pyogenes* Cas9 (Mans et al., 2015). Besides, the IMX994 strain has the non-oxidative pentose phosphate pathway genes overexpressed, which are inserted in the aldose reductase locus (Papapetridis et al., 2018). In addition, the *E. coli* strain XL1-Blue was used specially for plasmid DNA extraction and transformation. This strain has the selective marker *AmpR*, which gives antibiotic resistance to ampicillin. All microbial strains used in this work and their respective relevant features are listed in table 1.

Table 1: Yeast and *E. coli* strains used in this experimental work.

Specie	Strain	Genotype	Source
S. cerevisiae	CEN.PK113-5D	*MATa ura3-52 MAL2-8c SUC2*	Entian and Kötter, 2007
S. cerevisiae	CEN.PK2-1C	*MATa ura3-52 his3-Δ1 leu2-3,112 trp1-289 MAL2-8c SUC2*	Entian and Kötter, 2007
S. cerevisiae	IMX994	*MATa ura3-52 MAL2-8c SUC2 can1::cas9-natNT2, gre3::RPE1, TKL1, TAL1, RKI1, XKS*	Papapetridis et al., 2018
E. coli	XL1-Blue	*recA1 endA1 gyrA96 thi-1 hsdR17 supE44 relA1 lac [F´ proAB lacIqZΔM15 Tn10 (Tetr)]*	Stratagene

2.2 Plasmids

In this work, two plasmids were used, pYPK0_TDH3_8054_2_ENO2 and pRCC-K. The plasmid maps are represented in Appendix A.

The plasmid pYPK0_TDH3_8054_2_ENO2 is a pYPK0 expression vector that contains the xylose isomerase expression cassette (TDH3_8054_2_ENO2), which is composed by the promoter TDH3, the xylose isomerase gene 8054_2, and the terminator ENO2. This plasmids contains the selection marker *URA3*, which enables the selection of transformant cells with this plasmid in uracil auxotrophic culture media. Besides, it also contains the *AmpR* marker, enabling the cultivation and selection of cells with this plasmid in selective media with ampicillin. The 8054_2 is the xylose isomerase gene extracted from the gut of the wood feeding beetle *Odontotaenius disjunctus* (Silva et al., 2021).

The plasmid pRCC-K is a CRISPR/Cas9 plamsid that expresses the Cas9 protein and has the sequence for the guide RNA scaffold, where a specific DNA target sequence with usually around 20 nucleotides in length can be inserted to determine the location of the Cas9 DNA cut (Generoso et al., 2016). The guide RNA expression cassette consists of a SNR52 promoter sequence, the gRNA scaffold, and the CYC1 terminator. The specific gRNA target sequence is chosen to be complementary to a specific DNA sequence of interest where the DNA will be cut. In this case, the gRNA was designed to specify the Cas9 break in the upstream region of the HXT11 gene (Appendix B), using the web tool ATUM (https://www.atum.bio/eCommerce/cas9/input). For the insertion of the target sequence on pRCC-K plasmid, the plasmid was amplified in three fragments by PCR to obtain the plasmid pRCC-K_gDNA_HXT11. This plasmid contains the DNA sequence that encodes the specific target sequence of the gRNA (5'-CACGAACAATGCATACACTC-3'). For this, three primer pairs were used to amplify three plasmid fragments, including the primer pairs 1646/253, 473/576, and 196/1645. The primers 1645 and 1646 contain the reverse and forward nucleotide sequences of the gRNA-coding DNA target, respectively. Furthermore, the amplified plasmid fragments share homologous ends so that the plasmid parts can be assembled by homologous recombination, generating the plasmid pRCC-K_gDNA_HXT11. After the plasmid amplification, the three resulting fragments were treated with the restriction enzyme *Dpn*I for enzymatic digestion, in order to get rid of any remaining template plasmid in the PCR samples. The pRCC-K plasmid has the selection marker *KanR*, which gives antibiotic resistance to geneticin. Thus, the selection of yeast transformants with this plasmid was done with rich glucose medium with geneticin. This plasmid also has the *AmpR* selection marker, enabling the bacterial transformation in selective media with ampicillin.

2.3 Culture media and growth conditions

During this experimental work, various cultures were used for different purposes. All yeast solid cultures were prepared in Petri dishes and incubated at 30°C. The yeast liquid cultures were also incubated at 30°C and with agitation in a rotatory shake of 200 revolutions/minute (rpm). The pre-cultures were prepared using Falcon tubes, whereas the growth cultures were prepared in glass tubes or Erlenmeyer flasks. In the case of *E. coli* cultures, they were prepared using the same materials and conditions, but the incubation temperature used was 37°C.

For short-term storage, microbial solid cultures were prepared and stored in the fridge at 4°C. Yeast cultures were maintained in solid rich glucose medium (YPD; 2% glucose, 2% peptone, 1% yeast extract, and 2% agar), while *E. coli* cultures were cultivated in solid lysogeny broth with ampicilin (LB-Amp; 1% NaCl, 1% yeast extract, 2% peptone, 2% agar, and 100 µg/mL Ampicilin). For long-term storage, fresh overnight cultures of each microbial culture were added to 25% glycerol in equal volume and stored in cryogenic vials at -80°C in the deep freezer. Yeasts were cultivated in liquid rich glucose medium (YPD; 2% glucose, 2% peptone, and 1% yeast extract), whereas *E. coli* cultures were prepared with liquid lysogeny broth with ampicilin (LB-Amp; 1% NaCl, 1% yeast extract, 2% peptone, and 100 µg/mL Ampicilin).

For plasmid DNA extraction, *E. coli* cells were cultivated in liquid lysogeny broth (LB-Amp; 1% NaCl, 1% yeast extract, 2% peptone, and 100 µg/mL Ampicilin). In yeasts, the cells were cultivated and grown in liquid rich glucose medium (YPD; 2% glucose, 2% peptone, and 1% yeast extract).

Before yeast transformation, yeasts were cultivated in pre-cultures of liquid rich medium (YPD; 2% glucose, 2% peptone, and 1% yeast extract). For transformant selection, yeasts were cultivated in two solid media, rich medium supplemented with geneticin (YPD+G418; 2% glucose, 2% peptone, 1% yeast extract, and 2% agar + 200 µg/mL geneticin) and synthetic complete medium without uracil (SC-U; 2% glucose, 0.67% yeast nitrogen base (YNB) + 0.07% amino acid dropout mix, 50 mM potassium hydrogen phtalate, 2% agar, 80 mg/L tryptophan, 80 mg/L histidine, 80 mg/L leucine). Yeasts transformed with the pYPK0_TDH3_8054_2_ENO2 plasmid were cultivated in SC-U, while yeasts transformed with the pRCC-K_gDNA_HXT11 plasmid were cultivated in YPD+G418. Before *E. coli* transformation, cells were cultivated in pre-cultures of liquid LB-Amp medium (1% NaCl, 1% yeast extract, 2% peptone, and 100 µg/mL Ampicilin). For the recovery of transformed *E. coli* cells, super optimal broth with catabolite repression medium (SOC; 2% tryptone, 0.5% yeast extract, 10 mM NaCl, 2.5 mM KCl, 10 mM MgCl2, 10 mM MgSO4, and 20 mM glucose) was added to the transformation mix. For *E. coli* transformant selection, plates with solid LB-Amp (LB-Amp; 1% NaCl, 1% yeast extract, 2% peptone, 2% agar, and 100 µg/mL Ampicilin) were used.

Before the ALE experiments, the transformed yeasts were cultivated in pre-cultures of liquid synthetic complete medium without uracil (SC-U; 2% glucose, 0.67% YNB + 0.07% amino acid dropout mix, 50 mM potassium hydrogen phtalate, 80 mg/L tryptophan, 80 mg/L histidine, 80 mg/L leucine), in which the

pH was adjusted to 5.5 with addition of 5M and 1M NaOH drops. The pH of culture media was measured by a pH electrode at room temperature. Then, in the first ALE experiment, yeasts were cultivated in liquid synthetic complete media (SC-U; 0.67% YNB + 0.07% amino acid dropout mix, 50 mM potassium hydrogen phtalate, 80 mg/L tryptophan, 80 mg/L histidine, 80 mg/L leucine, pH = 5.5) with initial concentrations of 0.5% glucose and 1.5% xylose. The glucose/xylose ratio was changed during the ALE experiment, in accordance with the table 2. In the second evolution experiment, yeasts were cultivated in synthetic media without uracil (0.67% YNB without amino acids, 0.07% amino acid dropout mix, 50 mM potassium hydrogen phtalate, 80 mg/L tryptophan, 80 mg/L histidine, 80 mg/L leucine, pH = 5.5), with and without drop-out. The drop-out is an aminoacid mix, which its composition is presented in table 13 (Appendix C). All previously evolved yeast strains were initially cultivated in culture media with 0.25% glucose + 1.75% xylose. Then, yeast cells were transferred to culture media with 1.9 % xylose + 0.1 % glucose with and without drop-out. Afterwards, yeast cells were cultivated to cultures with solely xylose (2%) until the end of the evolution experiment. After the evolution experiment, the evolved yeasts were cultivated in solid synthetic xylose medium without uracil (SX-U; 2% xylose, 0.67% YNB + 0.07% amino acid dropout mix, 50 mM potassium hydrogen phtalate, 2% agar, 80 mg/L tryptophan, 80 mg/L histidine, 80 mg/L leucine, pH = 5.5).

Table 2: SC-U media composition during the first ALE experiment with glucose and xylose concentrations expressed in percentage.

	Concentration (%)			
Glucose	0.5	0.25	0.1	0
Xylose	1.5	1.75	1.9	2

For the growth curves, yeast cultures were cultivated in liquid synthetic xylose medium without uracil (SX-U; 2% xylose, 0.67% YNB + 0.07% amino acid dropout mix, 50 mM potassium hydrogen phtalate, 80 mg/L tryptophan, 80 mg/L histidine, 80 mg/L leucine, pH = 5.5). Before the growth curves, yeasts were cultivated in pre-cultures of liquid synthetic complete medium (SC-U; 2% glucose, 0.67% YNB + 0.07% amino acid dropout mix, 50 mM potassium hydrogen phtalate, 80 mg/L tryptophan, 80 mg/L histidine, 80 mg/L leucine, pH = 5.5).

For plasmid loss, previously evolved yeast cells were cultivated in liquid rich medium (YPD; 2% glucose, 2% peptone, and 1% yeast extract). In order to select the yeasts that lost the plasmid, yeast cells were transferred in solid rich medium (YPD; 2% glucose, 2% peptone, 1% yeast extract, and 2% agar). Then, yeast colonies were isolated and re-transferred to two culture media, solid rich medium (YPD; 2% glucose, 2% peptone, 1% yeast extract, and 2% agar) and synthetic xylose medium without uracil (SX-U; 2% xylose, 0.67% YNB + 0.07% amino acid dropout mix, 50 mM potassium hydrogen phtalate, 2% agar, 80 mg/L tryptophan, 80 mg/L histidine, 80 mg/L leucine, pH = 5.5).

Before the spot assay experiments, yeast cells were cultivated in pre-cultures of liquid rich medium

(YPD; 2% glucose, 2% peptone, and 1% yeast extract). During the spot assay analysis, four culture media were used: synthetic complete medium without uracil (SC-U; 2% glucose, 0.67% YNB + 0.07% amino acid dropout mix, 50 mM potassium hydrogen phtalate, 2% agar, 80 mg/L tryptophan, 80 mg/L histidine, 80 mg/L leucine, pH = 5.5); synthetic xylose medium without uracil (SX-U; 2% xylose, 0.67% YNB + 0.07% amino acid dropout mix, 50 mM potassium hydrogen phtalate, 2% agar, 80 mg/L tryptophan, 80 mg/L histidine, 80 mg/L leucine, pH = 5.5); synthetic defined xylose medium (SDX; 2% xylose, 0.67% YNB without amino acids, 50 mM potassium hydrogen phtalate, 40 mg/L uracil, 2% agar, pH = 5.5); and rich xylose medium (YPX; 2% xylose, 2% peptone, 1% yeast extract, and 2% agar).

2.4 Plasmid DNA extraction

The plasmid DNA was extracted from *E. coli* cultures using the NZYTech Miniprep kit. For the plasmid extraction, fresh *E. coli* cells were cultivated in 10 mL of liquid culture LB-Amp in 50 mL Falcon tubes. Then, the cultures were incubated overnight at 37 °C. In the next day, the cultures were centrifuged for 30 seconds, the supernatant was removed and discarded, and the pellet was resuspended in 500 µL of buffer A1 (resuspension buffer with RNase) by vortexing. The cells were then lysed by adding 500 µL of buffer A2 (lysis buffer) and mixing by inverting the tube 6-8 times. Following a 4-minute incubation, 600 µL of buffer A3 (neutralization buffer) was added to the lysate and mixed by inverting again the tube 6-8 times. The lysate was then centrifuged for 10 minutes, and the resulting supernatant transferred to a spin column and centrifuged for 1 minute at 11000 g. With the flow-through discarded, 500 µL of pre-warmed buffer AY (wash buffer) was then added to the spin column and centrifuged for 1 minute. The flow-through was discarded again and 600 µL of buffer A4 (wash buffer with ethanol) added to the column, before being centrifuged for 1 minute. After discarding the flow-through, the columns were dried by centrifugation for 2 minutes. The spin column was then transferred to an empty 1.5 mL microcentrifuge tube and 50 µL of buffer AE (elution buffer) was added. After 1 minute of incubation at room temperature, the tubes were centrifuged for 1 min at 12000 g. Finally, the tubes with purified plasmid DNA were stored at -20 °C in the freezer for further utilization.

The plasmid extraction in *S. cerevisiae* followed the same protocol used in bacterial plasmid DNA extraction. However, it was used an extra step before the extraction, where cells were subjected to disruption by mechanical lysis. For this, yeast cells were first cultivated in YPD pre-cultures of 10 mL, and glass beads were added to the culture for cell disruption. The cell lysis was carried out using a disruptor during 5 minutes and with maximum rotation (5000 rpm).

After plasmid extraction, the extracted plasmid DNA was quantified and the DNA purity was measured by Nanodrop. The DNA purity was determined based on absorbance ratios at 260/280 nm and 260/230 nm (Lucena et al., 2016).

2.5 PCR conditions

During the experimental work, various PCR reactions were carried out for different purposes. For each PCR, the conditions were calculated using the WebPCR (https://pydna.pythonanywhere.com). This web tool allows to preview the PCR conditions, including the melting temperature (Tm), the extension time, the PCR product and its size expressed in base-pairs (bp). All primer sequences used for the PCR reactions are listed in table 14 (Appendix D). All PCRs were run under 35 cycles.

For conventional PCRs, the following reagents were added per 10 µL of reaction mix: 3 µL of ultra-pure water; 5 µL of Master Mix (1x Phusion HF Buffer, 0.02 U/µL Phusion polymerase, 200 µM of each dNTP); 0.5 µL of each primer (forward and reverse); and 1 µL of template DNA. Before the PCR, the DNA was diluted to a 1:10 dilution with ultra-pure water. The negative controls have the same reagents as the other reactions, but without DNA and 4 µL of H_2O. The DNA polymerase enzyme used was the Phusion High-Fidelity DNA Polymerase (ThermoFisher).

For colony PCRs, the following reagents were added per 10 µL of reaction mix: 4 µL of ultra-pure water; 5 µL of Master Mix (1x Taq polymerase Buffer, 0.05 U/µL Taq polymerase, 4 mM MgCl2, 0.4 mM of each dNTP); 0.5 of each µL primer (forward and reverse); and cell colonies used as template for PCR reactions. In colony PCRs, the initial denaturation time was raised to 15 minutes, in order to disrupt the cells by heating and to release the cell DNA to be used as template for the PCR reactions. The negative controls for the colony PCR have the same components as the other reactions, but without cells. The Taq DNA polymerase was used for all colony PCRs.

For the xylose isomerase expression cassette amplification, the primers 1643 and 1644 were used. The conditions used for this PCR are described in Table 3. The expected product size is 2731 bp.

Table 3: PCR conditions for the xylose isomerase expression cassette amplification.

PCR Phase	Temperature (ºC)	Time (Min:Sec)
Initial denaturation	98	0:30
Denaturation	98	0:10
Annealing	57.3	0:10
Extension	72	0:40
Final extension	72	5:00

For the pRCC-K_gDNA_HXT11 amplification, three PCR reactions were carried out to amplify three fragments of the plasmid, with the following primer pairs: 1646/253, 473/576, and 196/1645. The melting temperature (Tm), extension time and PCR product size for each of the three primer pairs used for pRCC-K amplification are indicated in table 4. The three PCR reactions were run simultaneously, in which the conditions used for PCR are described in Table 5. The selected annealing temperature was the lowest temperature of the three reactions (54.5°C) and the extension time used was the longest one (1

minute and 19 seconds). In addition, the plasmid DNA used as template was diluted three times, with dilutions of 1:100, 1:1000 and 1:10000.

Table 4: Primer pairs used for pRCC-K_gDNA_HXT11 PCR amplification. For each primer pair, the Tm (°C), the extension time, and prodcut size (bp) are represented.

Pimer pair	Tm (ºC)	Extension time (Min:Sec)	PCR product size (bp)
1646/253	64	1:19	5315
473/576	54.5	0:45	3020
196/1645	58.5	0:31	2068

Table 5: PCR conditions for the pRCC-K_gDNA_HXT11 plasmid amplification.

PCR Phase	Temperature (ºC)	Time (Min:Sec)
Initial denaturation	98	0:30
Denaturation	98	0:10
Annealing	54.5	0:10
Extension	72	1:19
Final extension	72	5:00

A colony PCR was performed in order to detect and confirm the presence of xylose isomerase gene in yeast transformants with the plasmid pYPK0_TDH3_8054_2_ENO2. The primers used were the 1287 and 1341. The expected PCR product size is 685 bp. The conditions used for this PCR are described in Table 6. For this colony PCR, it was used CEN.PK113-5D yeast cells as positive control, which had been previously transformed with the plasmid pYPK0_TDH3_8054_2_ENO2.

Table 6: Colony PCR conditions for the xylose isomerase detection on yeasts transformed with the pYPK0_TDH3_8054_2_ENO2 plasmid.

PCR Phase	Temperature (ºC)	Time (Min:Sec)
Initial denaturation	95	15:00
Denaturation	95	0:30
Annealing	59	0:30
Extension	72	0:30
Final extension	72	5:00

Furthermore, another colony PCR was done for the detection and confirmation of the xylose isomerase expression cassette integration on yeasts by the CRISPR/Cas9 method. The primers used were the 1354 and 1653 (Figure 7). The expected PCR product size is 1384 bp. The conditions used for this PCR are described in Table 7.

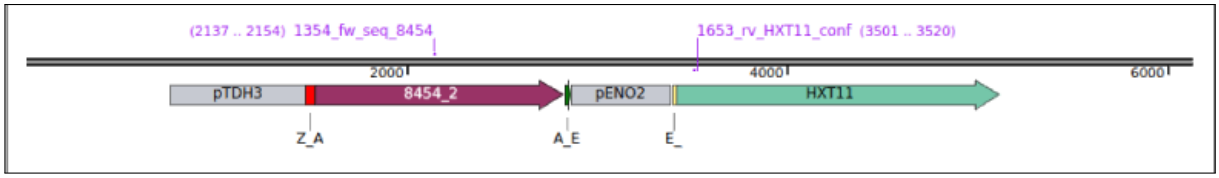

Figure 7: Schematic representation of the xylose isomerase cassette expression integrated on yeast genome, specifically in the upstream region of the HXT11 gene. In this image, the primers 1354 and 1653 used to confirm the genomic integration of XI expression cassette are represented. This image was generated using the software SnapGene®.

Table 7: Colony PCR conditions for the confirmation of the genomic integration of xylose isomerase expression cassette on yeasts.

PCR Phase	Temperature (ºC)	Time (Min:Sec)
Initial denaturation	95	15:00
Denaturation	95	0:30
Annealing	56	0:30
Extension	72	1:02
Final extension	72	5:00

In addition, another colony PCR was done for the detection of wild-type sequence on yeasts transformed for the integration of XI expression cassette. The primers used were the 1653 and 1654 (Figure 8). The expected PCR product size is 760 bp. The conditions used for this PCR are described in Table 8.

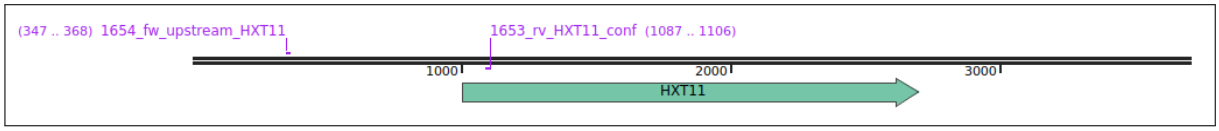

Figure 8: Schematic representation of the wild-type sequence of the HXT11 upstream region. The primers 1653 and 1654 used to detect the wild-type sequence are represented. This image was generated using the software SnapGene®.

Table 8: Colony PCR conditions for the detection of wild-type sequence on yeasts transformed for the XI expression cassette integration.

PCR Phase	Temperature (ºC)	Time (Min:Sec)
Initial denaturation	95	15:00
Denaturation	95	0:30
Annealing	55.7	0:30
Extension	72	0:34
Final extension	72	5:00

Moreover, another colony PCR was carried out to detect and confirm the pRCC-K plasmid, after yeast transformation. The primers used were the 473 and 474. The expected PCR product size is 1333 bp. The conditions used for this PCR are described in Table 9.

Table 9: Colony PCR conditions for the pRCC-K detection on transformant yeasts.

PCR Phase	Temperature (ºC)	Time (Min:Sec)
Initial denaturation	95	15:00
Denaturation	95	0:30
Annealing	56.4	0:30
Extension	72	0:59
Final extension	72	5:00

The PCR products were analyzed by agarose gel (1%, TAE 1x), and electrophoresis was performed at 200 V (7 V/cm) during 25 minutes. The molecular weight marker used were the home made pPSU marker or the Generuler 1 kb DNA ladder (ThermoFisher). Each sample loaded on gel was made of 1x loading buffer solution (5% glycerol and 0.05% bromophenol blue), Midori Green Direct (diluted from 1:500 to 1:1000, approximately). The agarose gels were visualized and photographed in the GenoView/GenoSmart UV transilluminator. At the end of PCR reactions, all PCR products were stored at 4°C in the fridge.

2.6 pRCC-K enzymatic digestion

For the pRCC-K enzymatic digestion, the resulting PCR products from the amplification of three pRCC-K fragments were treated with *Dpn*I enzyme. 1 µL of each PCR product was transferred to 1.5 mL Eppendorff tubes, and the following reagents were added to each tube: 16 of µL nuclease-free water; 2 of µL 10X Buffer Tango; and 2 of µL *Dpn*I enzyme. Then, the digestion reaction tubes were gently mixed and spin down for a few seconds. Afterwards, the digestion mixes were incubated at 37°C for 1 hour. After the incubation, the digestion reactions were heated at 80°C for 20 minutes to inactivate the enzyme and stop the digestion. Finally, the digested samples of the plasmid were stored at -20°C in the freezer.

2.7 Transformation of *S. cerevisiae*

The transformation of yeast strains was performed through an high efficiency yeast transformation protocol, based on PEG-LiAc-ssDNA method (Gietz, 2014). For the transformation, pre-cultures of 5 mL YPD for both yeast strains, CEN.PK2-1C and IMX994, were prepared in 50 mL Falcon tubes and incubated overnight at 30°C. Then, the pre-cultures grew until next day, and the optical density (OD) at 600 nm of each culture was measured through a spectrophotometer. 1 mL samples of each culture was collected and transferred to a cuvette to measure the optical density (OD) at 600 nm through a spectrophotometer,

with a dilution of 1:20. Before the transformation, yeast cultures grew until reach a OD = 1.2. Then, the cultures were centrifuged and washed with sterile water. The centrifugation was carried out at 5000 rpm for 5 minutes. After centrifugation, supernatant was discarded and the pellet leaved in each tubes was washed two times with 10 mL of sterile distilled water. The pellet was resuspended with sterile water, centrifuged in same conditions as before, and the supernatant was discarded. This procedure was repeated two times for the washing of cells. After the washing, the pellet was resuspended in 1 mL of sterile water and the liquid content in Falcon tubes were transferred to 1.5 mL Eppendorff tubes. Then, the cell suspensions were centrifuged at 3200 g during 30 seconds. For each tube, 300 µL of PLS mixture was added, which contains 1M lithium acetate, PEG 3500 (polyethylene glycol), and boiled single stranded carrier DNA (ssDNA). Afterwards, the DNA was added for each cell suspension, making up 60 µL of DNA in total for each transformation. In total, three yeast transformations were carried out, including: CEN.PK2-1C yeasts transformed with 5 µL of each one of the three pRCC-K_gDNA_HXT11 fragments + 45 µL of XI expression cassette DNA; CEN.PK2-1C yeasts transformed with 1 µL of pRCC-K_gDNA_HXT11 DNA + 59 µL of XI expression cassette; and CEN.PK2-1C and IMX994 yeasts transformed with 1 µL of pYPK0_TDH3_8054_2_ENO2 plasmid and 59 µL of distilled water. In addition, negative controls were made for each yeast strain, in which yeast cells were transformed with 60 µL of distilled water. The transformation mixtures were mixed by vortexing, and then, the tubes were incubated in warmed water bath, at 42°C, during 40 minutes. Furthermore, the tubes were centrifuged at 3200 g during 30 seconds, and supernatant was discarded. The pellet cells were resuspended in 1 mL YPD liquid media through up and down with a micropipettor. The suspensions on tubes were transferred to new Falcon tubes to incubate at 30°C during 2 hours for recovery time. Then, 100 µL of each transformation mix was transferred to new sterile Eppendorff tubes for three serial dilutions of 1:1, 1:10 and 1:100. Finally, the transformed cells with respective dilutions were plated in Petri dishes with solid SC-U media, and incubated at 30°C for 3 days.

2.8 *E. coli* transformation

The *E. coli* transformation was performed by the heat shock transformation protocol (Inoue et al., 1990). First, 150 µL of *E. coli* XL1-blue competent cells were first defrosted on ice. Then, 50 µL of competent cells were aliquoted to Eppendorff tubes, in which 1 µL of plasmid DNA was added for two transformations. Besides, another tube was used for the negative control, where no DNA was added. Then, the transformation tubes were incubated on ice for 20 minutes. Afterwards, cells were subjected to heat shock at 42°C during 45 seconds, and then immediately returned to the ice for 10 minutes. Furthermore, 200 µL of SOC medium was added to the tubes, and cells were allowed to recover at 37°C for 1 hour. Then, 100 µL of transformation mix was transferred to new sterile Eppendorff tubes for serial dilutions of 1:1, 1:10 and 1:100. Finally, the cells were plated in plates with solid LB-Amp media and incubated

overnight at 37°C.

2.9 DNA sequencing

For sequencing, the plasmid pRCC-K_gDNA_HXT11 previously extracted from *E. coli* cells was mixed with the primer 1356. 6.5 µL of two DNA samples of the same plasmid were transferred to two 10 µL Eppendroff tubes. Then, the plasmid DNA was mixed with 2.5 µL of primer, which was previously diluted to 1:10, and 1 µL of water. Afterwards, the tubes were sent to Eurofins genomics for sequencing.

2.10 Adaptive laboratorial evolution

For the first ALE experiment, three transformant colonies of CEN.PK2-1C and IMX994 strains were picked from the previous transformations and used as biological replicates. Yeast colonies were cultivated in pre-cultures with 5 mL of SC-U in 50 mL Falcon tubes and incubated overnight at 30°C. In the next day, 1 mL of pre-cultures samples were collected and transferred to a cuvette to measure the optical density at 600 nm through a spectrophotometer, with a dilution of 1:20. Each batch culture was inoculated with yeast cells to a OD value of 0.05, and yeast cells were successively transferred to new batches through serial passages. The batch cultures grew until the culture reached an observable amount of biomass, and the OD at 600 nm was measured and registered before the subsequent transfer. Then, cells were re-transferred to a new batch, and this process was repeated until the end of the evolution experiment. Yeasts were cultivated in glass tubes with 3 mL of culture media, where the concentration of glucose and xylose was gradually changed over the time, as indicated in table 2. The evolution experiment ended after 10 successive transfers for CEN.PK2-1C yeast cells and 11 for IMX994 yeasts. Afterwards, 100 µL from each yeast culture was plated in solid SX-U media, with dilutions of 10^{-2} and 10^{-3} for CEN.PK2-1C cells, and 10^{-3} and 10^{-4} dilutions for IMX994 cells. The plates were then incubated at 30°C for 4 days. Finally, the evolved cells from both yeast strains were stored in glycerol tubes for long-term storage in deep-freezer at -80°C. In addition, the non-evolved parental yeast colonies were also stored at -80°C in the deep freezer for further comparison with the evolved yeasts.

Furthermore, another ALE experiment was done with the previously evolved CEN.PK2-1C and IMX994 yeast strains. The evolution was carried out with two types of synthetic xylose cultures without uracil, one with the drop-out aminoacid mix and other without drop-out. The previous yeast colony with the highest growth for each strain was selected and cultivated in plates with solid SC-U, and the cultures were incubated at 30°C during 3 days. Then, two isolated colonies from each evolved yeast strain were obtained and used as biological replicates for the evolution experiment. Two technical replicates were made for each isolated yeast colony, giving a total of four replicates for each yeast strain. Pre-cultures with both yeast strains were prepared with 5 mL of SC-U in 50 mL Falcon tubes. In the next day, 1 mL of pre-cultures samples were

collected to measure the OD value in the spectrophotometer, with a dilution of 1:20. Each batch culture was inoculated with yeast cells to a OD = 0.05, and yeast cells were successively transferred to new batches by serial passages over the evolution experiment. Yeast cells were cultivated in glass tubes with 3 mL of culture media, where the concentration of xylose was gradually increased. Initially, the first two serial batches had concentrations of 0.25% glucose and 1.75% xylose. Then, yeast cells were transferred to new batch cultures with 1.9 % xylose + 0.1 % glucose in the next two transfers. From the fifth transfer, yeast cells were cultivated in medium with 2% xylose and no glucose until the end of this evolution experiment. The evolution was performed over 33 days and ended after 11 successive transfers for CEN.PK2-1C and IMX994 yeasts cultivated in medium with drop-out, and 6 transfers for CEN.PK2-1C cells and 11 transfers for IMX994 in medium without drop-out. 100 µL samples of evolved yeast cells were plated in solid SX-U media, with dilutions of 10^{-3} and 10^{-4}. The SX-U plates were incubated at 30°C during 4 days. At the end, the evolved yeast cells were re-transferred to a new solid SX-U media and stored at 4°C in the fridge for short-time storage, and stored at -80°C in the deep freezer for long-therm storage.

2.11 Growth curves

For the first growth curves, yeast cells were cultivated in SX-U medium to test the growth of yeasts on xylose. The first growth curves were obtained for the previous transformed yeast strains, including evolved and non-evolved yeasts. For these growth curves, three yeast colonies from each yeast strain, CEN.PK2-1C and IMX994, were used as three biological replicates. Yeasts cells were cultivated in pre-cultures of 10 mL SC-U media on Falcon tubes. Then, the pre-cultures were incubated at 30°C overnight. In the next day, 1 mL of yeast pre-cultures were collected and transferred to a cuvette to measure the OD value at 600 nm with a spectrophotometer, with a dilution of 1:20. Each yeast growth culture was inoculated with yeast cells to a OD = 0.1. Before the inoculation of the growth cultures, 10 mL of SX-U medium was added in 100 mL Erlenmeyer flasks, and then, the culture media were pre-warmed at 30°C. Yeast cells were cultivated in these cultures and incubated at 30°C for growth. The OD values of yeast cultures were measured using the spectrophotometer during 24 hours, in the following time points: 0, 2, 4, 5, 6, 7, 8, and 24 h. For absorbance measurements, dilutions of 1:1 (without dilution), 1:5, 1:10, and 1:20 for each time point were made (Table 10).

Table 10: Time points and dilutions for the 24 h growth curves of yeasts on SX-U medium.

Time (Hour)	Dilution factor
0	No dilution
2	No dilution
4	No dilution
5	1:5
6	1:5
7	1:10
8	1:10
24	1:20

Furthermore, growth curves for the evolved CEN.PK2-1C and IMX994 yeasts were obtained for 72 hours, with three technical replicates for each yeast strain. Yeast cells were first cultivated in SC-U pre-cultures of 5 mL, in 50 mL Falcon tubes. Then, the pre-cultures were incubated overnight at 30°C, and the OD values of each pre-culture were measured. Each growth culture was inoculated with yeast cells to a OD of 0.05. The cultures were prepared in glass tubes with 7 mL of SX-U medium, and they were then pre-warmed at 30°C. Then, yeast cells were cultivated in SX-U culture media and incubated at 30°C. The OD values of yeast growth cultures were measured in the time points and with the respective dilutions presented in table 11.

Table 11: Time points and dilutions for the 72 h growth curves of yeasts on SX-U medium.

Time (Hour)	Dilution factor
0	No dilution
12	1:5
16	1:5
20	1:10
24	1:10
36	1:20
40	1:20
44	1:20
48	1:20
60	1:50
64	1:50
68	1:50
72	1:50

Additionally, another growth curves were also obtained after the second ALE experiment, where yeasts were evolved in synthetic xylose media with and without drop-out. Two isolated colonies from each evolved CEN.PK2-1C and IMX994 strains were cultivated in SX-U medium for growth. These growth curves were obtained using the same procedure previously used, as well as the same time points and the respective dilutions presented in table 11. In this case, the growth curves were obtained using two technical replicates

for each isolated yeast colony, giving a total of four replicates for each yeast strain.

2.12 Plasmid loss in yeasts

Yeast cells from the previously evolved IMX994 yeasts were cultivated in YPD medium for plasmid loss in yeasts previously transformed with the plasmid pYPK0_TDH3_8054_2_ENO2. Yeast cells that were previously stored in SX-U media plates at 4°C were transferred to 5 mL of YPD media in 50 mL Falcon tubes. Then, the yeast cultures were incubated overnight at 30°C. In the next day, the OD values of yeast cultures was measured by the spectrophotometer, with a 1:20 dilution. 10 µL of each culture was transferred to a new YPD culture and incubated overnight at 30°C, and this process was repeated three times, making three serial passages of yeast cells in liquid YPD medium. At the end, 10 µL of yeast cultures were plated in solid YPD medium, with dilutions of 10^{-3} and 10^{-4}. Then, the cultures were incubated at 30°C overnight. After 3 days, yeast colonies were obtained, and 12 colonies from each yeast culture were transferred to solid YPD and SC-U media. Afterwards, the cultures were incubated overnight at 30°C for 3 days. Then, the plates were visualized and photographed in the GenoView/GenoSmart UV transilluminator. Finally, the plates were stored in the fridge at 4°C.

2.13 Spot assay analysis

For spot assay analysis, three groups of different types of yeasts were used: CEN.PK2-1C and IMX994 parental strains, evolved yeast strains, and yeasts without the plasmid pYPK0_TDH3_8054_2_ENO2. Initially, yeast cells were cultivated in 5 mL of YPD pre-cultures in 50 mL Falcon tubes, and they were then incubated overnight. In the next day, all pre-cultures were grown and centrifuged at 5000 rpm during 5 minutes to obtain the pellet. Then, the supernatant was discarded and 5 mL of sterile distilled water was added for washing the cells. The cultures were centrifuged again in same conditions, the supernatant discarded, and the pellets were resuspended in sterile water. After resuspension, the OD value at 600 nm of cell suspensions was measured using the spectrophotometer, with a dilution of 1:20. The yeast cells from pre-cultures were then transferred for inoculation in YPD medium to a OD = 1. Each yeast strain culture was diluted with four serial dilutions of 10^{-1}, 10^{-2}, 10^{-3}, and 10^{-4}, using sterile Eppendorff tubes. Then, yeast cells were plated in four solid culture media: SC-U, SX-U, SDX and YPX. For each plate, four strains were tested with five spots corresponding to serial dilutions of 10^{0} to 10^{-4}. The spot assays were carried out in sterile conditions with the use of a flux chamber. Then, the plates were incubated at 30°C for 3 days. Finally, the plates were observed, photographed and visualized in the GenoView/GenoSmart UV transilluminator. The plates were observed 3 days after the inoculation of yeast cells in culture media.

Chapter 3

Results and Discussion

3.1 Expression of xylose isomerase pathway in *S. cerevisiae*

3.1.1 Expression of xylose isomerase in yeasts with the pYPK0_TDH3_8054_2_ENO2 plasmid

The first step of this experimental work was the heterologous expression of the xylose isomerase pathway in *S. cerevisiae*. In order to accomplish that, two *S. cerevisiae* strains, CEN.PK2-1C and IMX994, were transformed with the plasmid pYPK0_TDH3_8054_2_ENO2. This plasmid contains the xylose isomerase expression cassette (TDH3_8054_2_ENO2), in which the TDH3 is the promoter, 8054_2 is the xylose isomerase gene, and ENO2 is the terminator. Before the transformation, the pYPK0_TDH3_8054_2_ENO2 plasmid was extracted from *E. coli* cells from the lab collection, which were previously transformed with this plasmid. After plasmid extraction, both yeast strains were tranformed with 1 µL of the extracted plasmid DNA. For the selection of transformants, yeasts were cultivated in solid synthetic complete medium without uracil (SC-U). For each transformation, dilutions of 1:1, 1:10 and 1:100 were made. In addition, negative controls were included, where yeasts were transformed with solely sterile water. Then, the transformed cells were plated in the SC-U media, and after 3 days of incubation at 30°C, the number of colonies in each plate was counted (Table 12). The transformation resulted in 245, 24 and 2 CEN.PK2-1C colonies, and 153, 15 and 1 IMX994 colonies, for the plates with dilutions of 1:1, 1:10 and 1:100, respectively.

Table 12: Number of yeast transformant colonies counted in transformation plates for yeasts transformed with the plasmid pYPK0_TDH3_8054_2_ENO2. The plates are represented according to the respective dilutions of 1:1, 1:10 and 1:100. C- is the negative control transformation plate.

	Plates			
Strain	1:1	1:10	1:100	C-
CEN.PK2-1C	245	24	2	0
IMX994	153	15	1	0

After the transformation, 10 colonies from each transformant yeast strain were picked and transferred to a new plate SC-U. Then, these yeast colonies were tested by colony PCR, in order to confirm the presence of the pYPK0_TDH3_8054_2_ENO2 plasmid. For this, the primers 1287 and 1341 were used to amplify the XI expression cassette contained on the plasmid. The resulting PCR samples were loaded onto an agarose gel and an image of the gel was acquired (Figure 9). Almost all yeast colonies, including the positive controls, had a band with a size between 500 and 750 bp, which is approximately the expected size of the PCR product (685 bp). Since the xylose isomerase gene was detected in almost all transformant colonies, the transformation of yeasts with the plasmid containing the xylose isomerase expression cassette was confirmed, and then, the transformation was successful. As the pYPK0_TDH3_8054_2_ENO2 plasmid was incorporated by transformant yeasts, they can express the XI pathway. Nevertheless, although the expression of xylose isomerase gene is required for yeasts to metabolize xylose, it is not sufficient for yeasts to carry out an efficient conversion of xylose and growth on xylose-containing media (S.-M. Lee et al., 2012). Therefore, the adaptive laboratorial evolution is still necessary to improve the XI-expressing yeasts growth on xylose. For this, three transformant colonies of each yeast strain were selected for the ALE experiment.

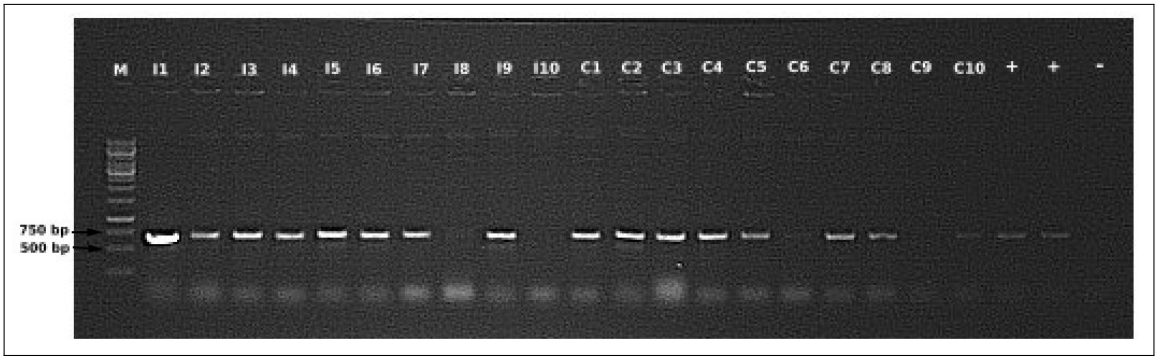

Figure 9: Image of agarose gel of colony PCR amplification for the XI expression cassette detection on yeasts transformed with the pYPK0_TDH3_8054_2_ENO2 plasmid. Each letter represent a gel lane, where M represents the molecular weight marker (Generuler 1 kb DNA Ladder [TermoFisher]), I (I1-I10) represents the IMX994 colonies, C (C1-C10) represents the CEN.PK2-1C colonies, + represents the positive controls, and - is the negative control. Almost all transformant yeast colonies, except the colonies I8, I10, and C9, had a visible band with a size of approximately 685 bp.

3.1.2 Genomic integration of xylose isomerase on *S. cerevisiae* by CRISPR/Cas9

The heterologous expression of any gene via an expression vector like a plasmid is an optimal strategy for genetic engineering in yeasts. However, a drawback associated with the use of plasmids for heterologous gene expression is the lack of stability. The reason for this is the fact that a plasmid requires the cultivation of transformed cells in selective media, with either antibiotic or auxotrophic selection, and it can easily

be lost if the selection factor is removed. When the transformed yeasts are cultivated in non-selective media, yeasts cells can lose the plasmid after various cell divisions, and then, the gene expression is also lost. The genomic integration of the xylose isomerase gene could led to a more stable expression of the XI pathway on yeasts, and it would allow the cultivation of engineered yeasts without the need of a selective pressure. In this way, the expression of the XI pathway in yeasts would be maintained after various cell divisions in any yeast culture media. Given that, the genomic integration of xylose isomerase gene on yeasts genome was attempted by the CRISPR/Cas9 technique. In this method, the plasmid pRCC-K was used to deliver the the Cas9 and the guide RNA (Generoso et al., 2016). In this case, it was designed a gRNA sequence that directs the Cas9 cut into the upstream region of the HXT11 gene (Figure 29 - Appendix B). However, the pRCC-K plasmid itself does not express the gRNA required to direct the DNA break to the desired location. Therefore, this plasmid was amplified in three parts by PCR using the three primer pairs 1646/253, 473/576, and 196/1645 (Figure 28 - Appendix A). Then, these three fragments were assembled to generate the plasmid pRCC-K_gDNA_HXT11. The gRNA-coding DNA was inserted in the plasmid by amplification using the primers 1645 and 1646 with the corresponding overhangs. Furthermore, the pRCC-K_gDNA_HXT11 fragments share homologous ends between them to allow the assembly of the plasmid fragments by homologous recombination. Thus, the three amplified fragments of the plasmid pRCC-K_gDNA_HXT11 were integrated in yeasts through transformation for *in vivo* assembly. In addition, the xylose isomerase expression cassette was also included in combination with the plasmid fragments for the transformation of yeasts, in order to integrate the XI expression cassette on yeasts genome.

Before yeast transformation, the plasmid pRCC-K was extracted from *E. coli* cells by the Miniprep protocol. After the plasmid extraction, the three fragments of plasmid pRCC-K_gDNA_HXT11 and the xylose isomerase expression cassette were amplified by PCR. The plasmid pYPK0_TDH3_8054_2_ENO2 was used as the template for the PCR amplification of the XI expression cassette. For this PCR, the primers 1643 and 1644 were used. Each primer contained a 30 bp homologous sequences in their 5' ends. Thus, the amplification of the XI cassette will result in a DNA segment that contains the XI expression cassette with homologous ends. This amplified DNA was used as a donor for the homologous recombination repair after the Cas9 DNA cut in the upstream region of the HXT11 gene (Figure 29 - Appendix B). The PCR samples were loaded onto an agarose gel, where a band for the amplified XI expression cassette was detected (Figure 10). This band is located just below to the 3000 bp marker band, which has approximately the expected size for the PCR product (2731 bp). This result indicates that the xylose isomerase expression cassette was amplified. However, a faint band on the negative control lane can be observed, nearly above to the marker band with 1500 bp. This band in negative control might indicate a contamination in PCR samples. Even though, if the PCR was contaminated, it would be expected to observe the negative control band for the XI expression cassette lane too. Nevertheless, this band was only detected in the negative control and did not appear in the XI expression cassette lane. Therefore, the PCR sample for the amplified

XI expression cassette was used for the further experimental steps.

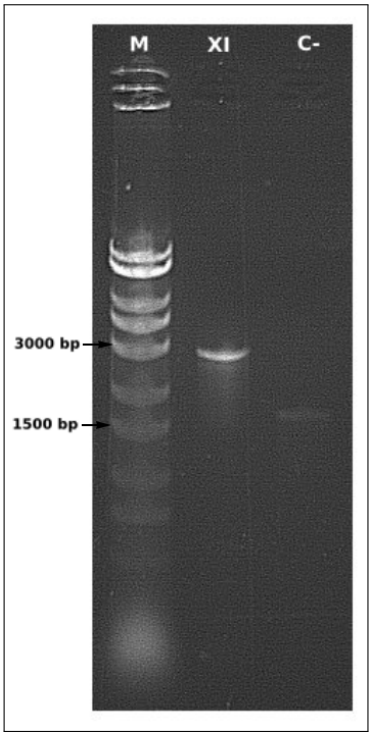

Figure 10: Image of agarose gel for the PCR amplification of the XI expression cassette. Each letter represent a gel lane, where M represents the molecular weight marker (PSU marker 1 kb DNA Ladder), XI is the amplified xylose isomerase expression cassette (2731 bp), and C- represents the negative control used for this PCR.

Then, the three parts of the plasmid pRCC-K_gDNA_HXT11 were amplified. For each plasmid fragment, the plasmid DNA was diluted three times, with dilutions of 1:100, 1:1000 and 1:10000. These dilutions were made due to the high concentration of pRCC-K plasmid, since the plasmid pRCC-K has a higher plasmid copy number (Generoso et al., 2016). Thus, the template DNA was diluted so that the amount of template was appropriate for the PCR, and to get a better chance of obtaining a PCR product for each plasmid fragment. In the figure 11, an agarose gel can be observed for the PCR where the three plasmid fragments were amplified. Each fragment was denominated according to the respective primer pair used for its amplification. For each plasmid fragment, there are three lanes corresponding to DNA dilutions of 1:100, 1:1000, and 1:10000. As can be observed in the gel, only the fragments 473/576 and 196/1645 had bands, while the fragment 1646/253 had no band. For the fragment 196/1645, two bands to with the same size of approximately 3000 bp can be visualized for the dilutions of 1:1000 and 1:10000. Whereas, the fragment 473/576 had two bands with equal size and just above the 2000 bp band, for the 1:100 and 1:1000 dilutions. The detected bands had approximately the expected sizes of the PCR products, as the fragment 473/576 has a size of 3020 bp and the fragment 196/1645 has 2068 bp. The 196/1645 and 473/576 fragments were successfully amplified, although there were no bands in

some lanes, specifically in the 1:100 dilution lane for the fragment 196/1645 and the 1:10000 dilution lane for the fragment 473/576.

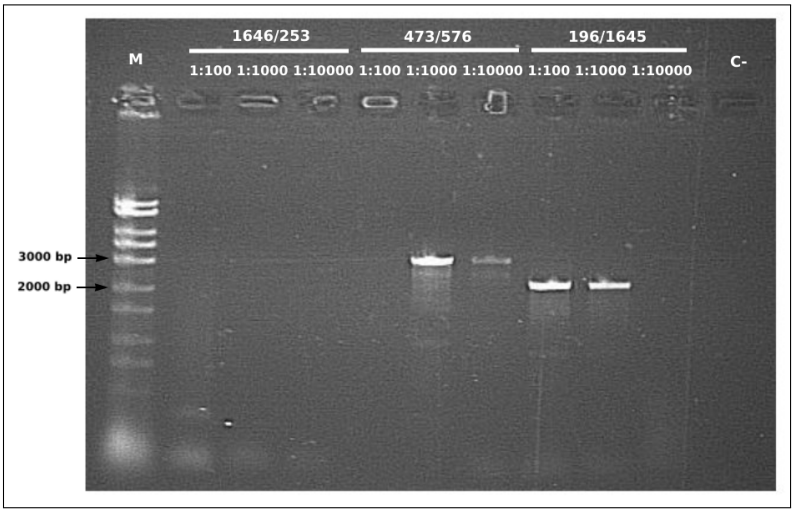

Figure 11: Image of agarose gel of the PCR amplification of three fragments of the plasmid pRCC-K_gDNA_HXT11. The lane represented by the letter M corresponds to the molecular weight marker (PSU marker 1 kb DNA Ladder). The 1646/253 (5295 bp), 196/1645 (3020 bp) and 473/576 (2049 bp) are the pRCC-K plasmid fragments amplified by the respective primer pairs. For each plasmid fragment to be amplified, dilutions of 1:100, 1:1000 and 1:10000 were made. The lane represented by C- is the negative control.

In order to amplify the remaining fragment (1646/253), the PCR conditions were optimized. The annealing temperature used for this PCR was raised from 54.5 °C to 58°C, and the extension time was increased to 2 minutes. Two PCR reactions were carried out with two dilutions of 1:100 and 1:1000. The PCR results were visualized in the agarose gel represented in the figure 12, where two bands can be observed with equal size and just above 5000 bp. This is approximately the expected size of the PCR product (5315 bp), indicating that the 1646/253 fragment was successfully amplified after the optimization of PCR conditions.

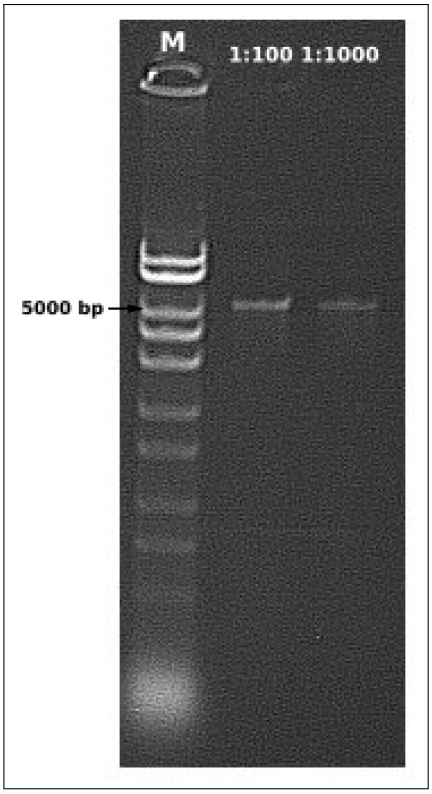

Figure 12: Image of agarose gel of the PCR amplification of the 1646/253 fragment of the plasmid pRCC-K_gDNA_HXT11. The lane represented by the letter M corresponds to the molecular weight marker (PSU marker 1 kb DNA Ladder). The other two lanes have the bands corresponding to the amplified 1646/253 fragment, with dilutions of 1:100 and 1:1000.

Afterwards, the PCR samples with the lowest dilutions were picked for enzymatic digestion, where the samples were treated with the restriction enzyme *Dpn*I. This digestion is necessary to degrade the remaining pRCC-K plasmid used as the template DNA for the previous PCRs. After 1 hour of digestion, the PCR samples were incubated at 80°C during 20 minutes for enzyme deactivation.

The next step was the transformation of yeasts, with the three pRCC-K_gDNA_HXT11 fragments and the XI expression cassette. The CEN.PK2-1C yeast strain was tranformed with 5 µL of each plasmid fragment and 45 µL of XI expression cassette DNA. For the selection of transformants, yeasts were cultivated in solid rich glucose medium with geneticin (YPD+G418). For each transformation, dilutions of 1:1, 1:10 and 1:100 were made. The transformant cells were plated, and after 3 days of incubation at 30°C, the number of colonies in each plate was counted. The transformation resulted in 20 colonies in total, in which 19 were obtained from the plate without dilution (1:1), and the other one was obtained from the plate with 1:10 dilution.

After the transformation, a colony PCR was carried out to confirm the integration of XI expression cassette on yeast genome. For this PCR, the primers 1354 and 1653 were used, where the primer 1354 pairs with the XI sequence, and the primer 1653 pairs with the HXT11 gene (Figure 7). The PCR samples were tested on agarose gel, but no positive yeast colonies were detected. This suggests that the XI expression

cassette was not integrated on yeasts genome. Then, another colony PCR was carried out to detect the presence of the pRCC-K plasmid on transformant yeast colonies. For this PCR, the primers 473 and 474 were used to amplify a pRCC-K portion (Figure 28 - Appendix A). The PCR results were observed in an agarose gel, where almost all colonies had a band nearly above the 1500 bp marker band (Figure 13). This band has approximately the expected size for the PCR product (1333 bp), indicating the presence of the plasmid on transformant yeast colonies.

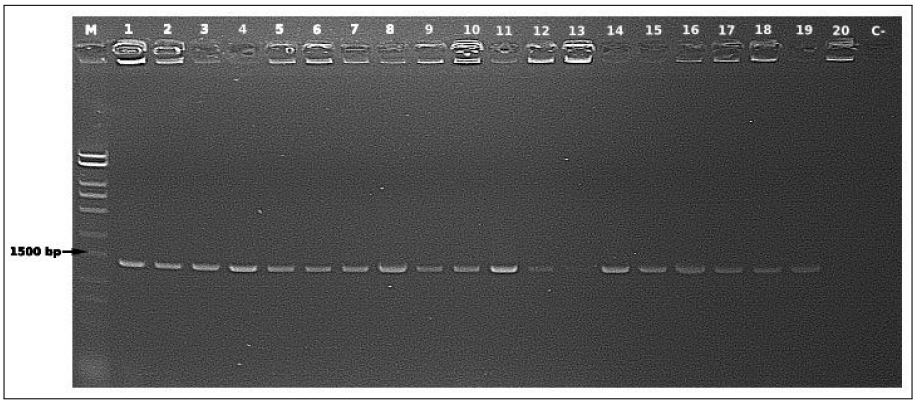

Figure 13: Image of agarose gel of PCR for detection of pRCC-K plasmid on transformant yeast colonies. The lane represented by the letter M corresponds to the molecular weight marker (PSU marker 1 kb DNA Ladder), the lanes represented by numbers 1-20 correspond to the transformant CEN.PK2-1C colonies, and the C- is the negative control. Almost all colonies, except the colony 20, had a band with a size of approximately 1333 bp.

Given the obtained results, the plasmid DNA was extracted from two transformant yeast colonies, in order to isolate the plasmid pRCC-K_gDNA_HXT11. After the plasmid extraction, two aliquotes of *E. coli* cells were transformed with 1 µL of the extracted plasmid DNA for plasmid rescue. The *E.coli* were transformed in LB-Amp medium and incubated overnight at 37°C. This *E. coli* transformation resulted in one hundred transformant colonies, and one colony from each transformation was then picked for plasmid DNA extraction. After the plasmid DNA extraction, the samples were used for sequencing in order to confirm the pRCC-K_gDNA_HXT11 DNA sequence, and to verify if the gRNA-coding DNA sequence was inserted into the plasmid. The sequencing results confirmed the plasmid sequence and the insertion of the gRNA-coding DNA into the plasmid (Figure 14). Two samples of the plasmid were sequenced and aligned with the predicted sequence. The obtained sequences were similar with the pRCC-K_gDNA_HXT11 sequence, and the gRNA-coding DNA was present in both samples.

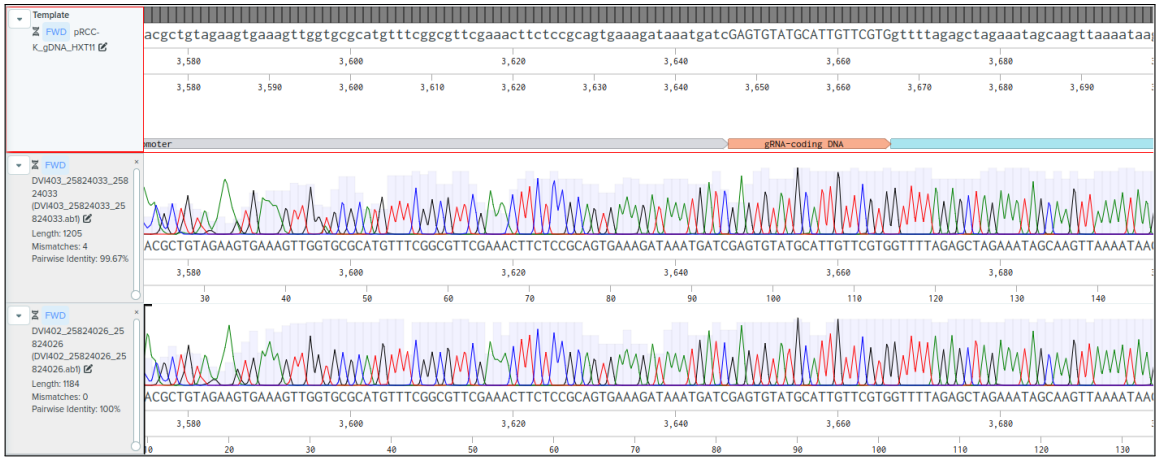

Figure 14: Alignment of the pRCC-K_gDNA_HXT11 sequences, including the predicted sequence and the obtained sequencing results. In this image, two DNA sequences obtained from the sequenced plasmid samples were aligned with the predicted sequence located on the top. For each sequence, the respective chromatogram is displayed, with the nucleotide bases marked with different colors. In addition, the length, base mismatches, and pairwise identity are also represented. The gRNA-coding DNA sequence, which is located between the SNR52 promoter and the gRNA scaffold sequences of pRCC-K plasmid, was detected for both obtained sequences. The sequenced region was located in the positions between 3575-4780 bp and 3575-4759 bp for the first and second sequences, respectively. This image was generated using the web platform software Benchling (https://www.benchling.com).

Then, a new yeast transformation was carried out, in which CEN.PK2-1C yeast cells were transformed with 1 µL of pRCC-K_gDNA_HXT11 plasmid DNA. The transformant cells were plated in rich glucose medium with geneticin (YPD+G418). After 3 days of incubation at 30°C, transformant colonies were obtained and counted. Three dilutions were made for the transformation, including dilutions of 1:1, 1:10 and 1:100. The transformation resulted in only 3 CEN.PK2-1C colonies from the 1:1 dilution plate. Furthermore, the obtained transformant colonies were tested to verify if the genomic integration of XI expression cassette occurred. For this, two PCRs were carried out, one to detect the presence of wild-type sequence of the HXT11 upstream region, and another to detect if the XI expression cassette was integrated on yeast genome. The detection of the wild-type sequence allows the exclusion of positive colonies for the XI integration, since the XI expression cassette is not integrated on yeast cells. The wild-type sequence amplification results in a band with a size of approximately 760 bp (Figure 8). The primers 1653 and 1654 were used for the wild-type sequence detection, while the primers 1354 and 1653 were used for the confirmation of XI expression cassette genomic integration. In the figure 15, an agarose gel for the detection of the wild-type sequence in transformant colonies can be observed. The colonies 1 and 3 had a faint band with a size near to the 750 bp marker band, which is approximately the expected size for the wild-type sequence. Thus, as these yeast colonies are positive for the wild-type sequence, the genomic integration of the XI expression cassette did not happen in these colonies.

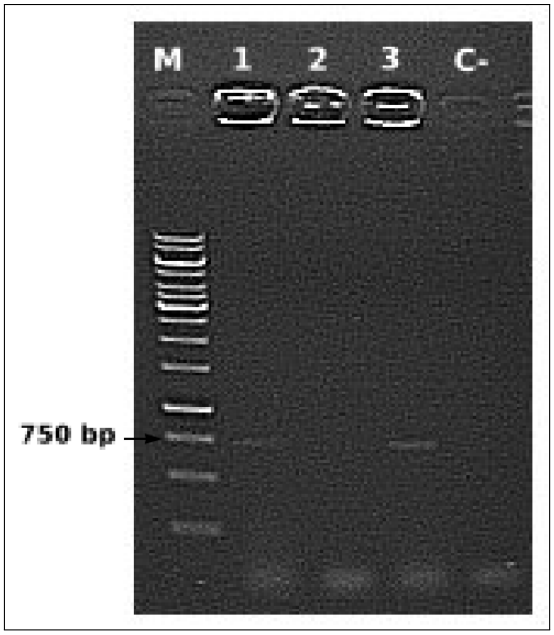

Figure 15: Image of agarose gel of PCR for detection wild-type sequence on transformant yeast colonies. The lane represented by the letter M corresponds to the molecular weight marker (Generuler 1 kb DNA Ladder [TermoFisher]), the lanes 1,2 and 3 represent the transformant CEN.PK2-1C colonies, and the C- is the negative control.

The remaining colony 2 was tested for the genomic integration of the XI cassette. However, no band was observed. These results indicate that the genomic integration of the XI expression cassette by the CRIPSPR/Cas9 method was not achieved. Nevertheless, since yeasts have previously been transformed with an expression vector containing the xylose isomerase expression cassette, XI-expressing yeasts were already obtained in this work. As mentioned before, the genomic integration could led to a more stable expression of xylose isomerase on yeasts, and the use of plasmids for gene expression requires the cultivation of transformed yeasts in selective media. Even tough, the integration of XI gene on yeasts genome did not work, and then, the yeast strains transformed with the plasmid pYPK0_TDH3_8054_2_ENO2 were used for the next experimental step. Besides, it must be taken into account that the CRISPR/Cas9 system has limitations, mainly with regard to the specificity of target sequences. The guide RNA can bind to non-specific sequences similar to the intended target sequence, and the Cas9 is recruited to make a double-strand break (DSB) into that non-specific regions of the genomic DNA (Sato and Kuroda, 2023). Then, this leads to a process called off-target effect, which decreases the precision of the genomic edition by the CRISPR/Cas9 system. Even so, the use of an alternative Cas9 with nickase activity is a possibility to overcome this limitation. This specific type of Cas9 is a core of emerging methods that have lower off-target effects on yeasts (Satomura et al., 2017). It only introduces single-strand breaks or nicks, as DSBs are more prone to off-target effects.

3.2 Adaptive laboratorial evolution of xylose-consuming *S. cerevisiae*

3.2.1 Evolution of yeasts for the optimization of growth on xylose

The first evolution experiment was carried out to improve the yeast growth on synthetic xylose media. For this, three yeast colonies from each of both CEN.PK2-1C and IMX994 yeast strains, which were previously transformed with the plasmid pYPK0_TDH3_8054_2_ENO2, were cultivated in pre-cultures of synthetic complete media without uracil (SC-U) with 2% of glucose. Then, the cultures were incubated overnight at 30°C, and in the next day, yeast cells were transferred to the growth cultures with synthetic complete medium without uracil. The concentration ratio of glucose/xylose was gradually changed over the time, as indicated in the table 2. The evolution experiment was carried out during a total period of 29 days, in which batch cultures were used for serial passages. The evolution ended after 10 successive transfers for CEN.PK2-1C yeast cells and 11 for IMX994 yeasts. During this time, the optical density of each transfer point were registered. These are the OD values achieved before the subsequent transfer, whereby each batch culture was inoculated with yeast cells to an initial OD of 0.05. The figure 16 shows the average of OD values registered for three yeast cultures of both yeast strains CEN.PK2-1C and IMX994. The glucose/xylose ratio and the days passed during serial passages are also represented. In the first two transfers, the concentration ratio was 0.5% glucose and 1.5% xylose, in which the OD values were the highest. The OD values for CEN.PK2-1C were slightly above 3, while the ODs of IMX994 yeasts were lower with about 2.7. Then, from the third transfer, the concentrations of glucose and xylose were changed to 0.25% and 1.75%, respectively. The OD values during these transfers were lower, being the values of approximately 2 for both strains. From the fifth transfer, a decrease in OD values to about 1 was observed for both strains, and the number of days between transfers was increased from about 2/3 days to 4 and 5 days. However, the time between transfers started to decrease from the ninth passage in IMX994 yeast strain. Until the eight transfer, the batch cultures still contained glucose and its concentration was reduced while the xylose concentration was increased. In this manner, yeasts can use the available glucose as a carbon source in combination with the xylose. Thus, it was expected that yeasts grow faster during the early stage of evolution, with higher OD values and less time between serial transfers. However, yeasts started to take longer to grow as the amount of glucose is reduced, as the OD values were lower and the time between transfers started to increase. This behaviour was observed in both strains until the eight passage. Finally, from the ninth transfer, glucose was completely removed from the medium and the xylose concentration was raised to 2%. For the CEN-PK2-1C yeast strain, the ODs were the lowest, being below 0.5. The time between transfers were the highest for the CEN.PK2-1C, being 4 and 5 days. Whereas, IMX994 cells displayed a significant increase in optical density from the ninth to tenth transfers. The optical density of IMX994 yeasts raised from 1 to 2.5, and then, a OD of 2 in the last transfer. Besides,

the time between transfers in IMX994 cells started to decrease from the ninth transfer with 4 days to 2 days in the last passage. Overall, these results indicate that IMX994 yeast cells apparently grow faster on xylose than CEN-PK2-1C yeasts, since IMX994 displayed higher OD values and lower time between transfers when cultivated with medium with solely xylose at 2%. Nevertheless, the yeasts growth on xylose can only be assessed more accurately through growth curves.

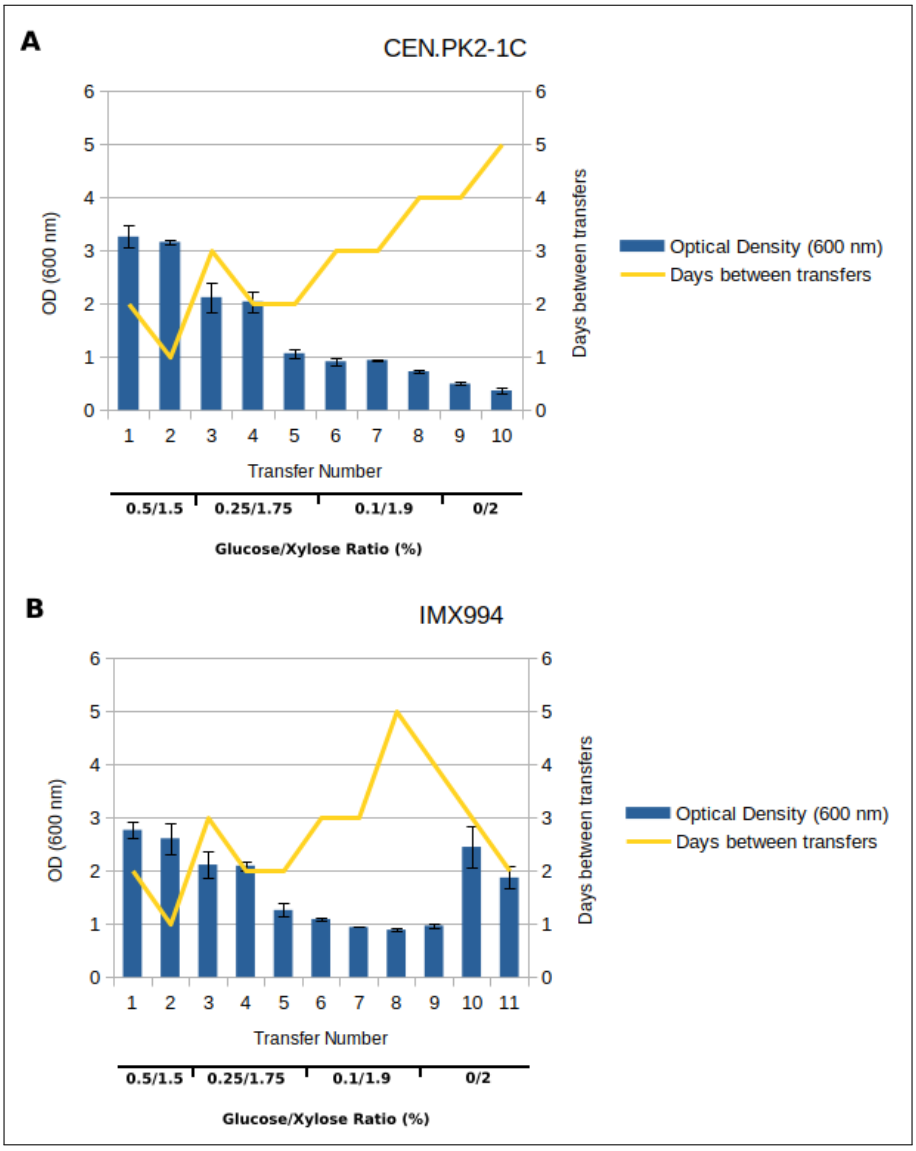

Figure 16: Overview of adaptive laboratorial evolution of two yeast strains CEN.PK2-1C (A) and IMX994 (B). The blue bars are the average of OD values for three colonies of each yeast strain used as biological replicates, which are the OD values measured before the subsequent transfer. The black lines are the error bars that represent the standard error of the three replicates used. The yellow line represents the time passed expressed in days between serial transfers. The the concentration ratio of glucose/xylose in the culture medium for the respective transfers is also represented.

In addition, the obtained OD values enable the estimation of the number of generations. The cumulative number of generations was calculated summing the number of generations for each time point with the number of generations of the previous ones. For this, the number of generations was calculated through the following formula:

$$\text{Number of generations} = \ln(OD_t) - \ln(0.05) \,/\, \ln(2)$$

The approximate total number of generations for both yeast strains over the evolution time is represented in figure 17. At the end of the evolution experiment, CEN.PK2-1C cells reached about 46 generations, while IMX994 achieved a higher number with about 57 generations.

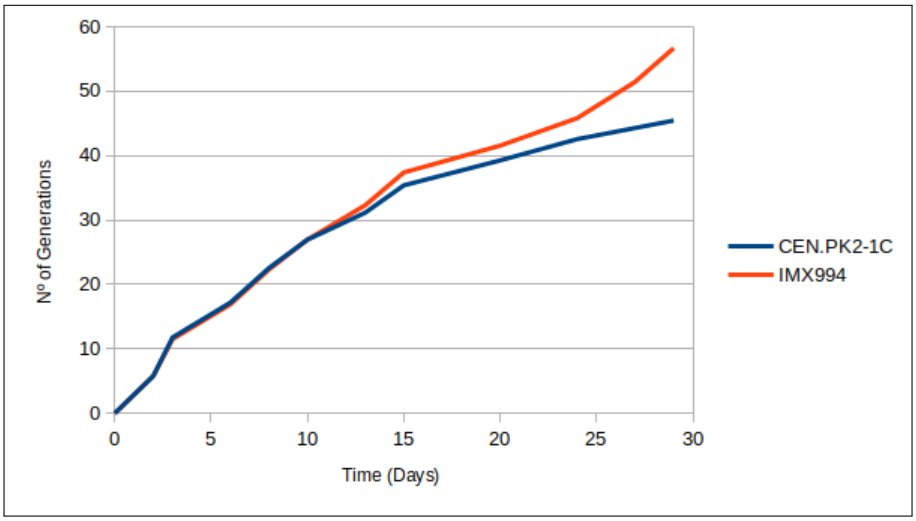

Figure 17: Cumulative number of generations of both yeast strains CEN.PK2-1C and IMX994 during the evolution experiment.

Then, growth curves were obtained in order to evaluate the growth of evolved yeasts and compare to the respective non-evolved parental strains. These curves were carried out during 24 hours, and the OD values were registered for each time point. Yeast cells were cultivated in synthetic xylose medium without uracil (SX-U) with 2% xylose as the sole carbon source, to an initial OD of 0.1. In the figure 18, four growth curves can be observed, including both yeast strains CEN.PK2-1C and IMX994 with the evolved and the respective non-evolved parental strains. It is possible to observe a lag phase for all growth curves in the first 8 hours, where the OD values were similar for all yeast strains. Then, a more pronounced growth takes place until the 24 hours, when significant differences between yeast strains, specially the evolved ones, can already be detected. As can be observed, the evolved strains displayed a higher growth in comparison with the non-evolved parental strains, being the IMX994 strain the one with higher growth. The evolved IMX994 yeasts reached a final OD of 2.7, while the evolved CEN.PK2-1C strain reached a final OD of about 1.2. Whereas, the IMX994 and CEN.PK2-1C parental strains reached final OD values of 0.8 and 0.6, respectively. These growth curves clearly demonstrate that the adaptive evolution of yeasts

had improved the yeast growth on xylose, as the evolved yeasts reached a higher optical density after 24 hours in comparison to the non-evolved strains.

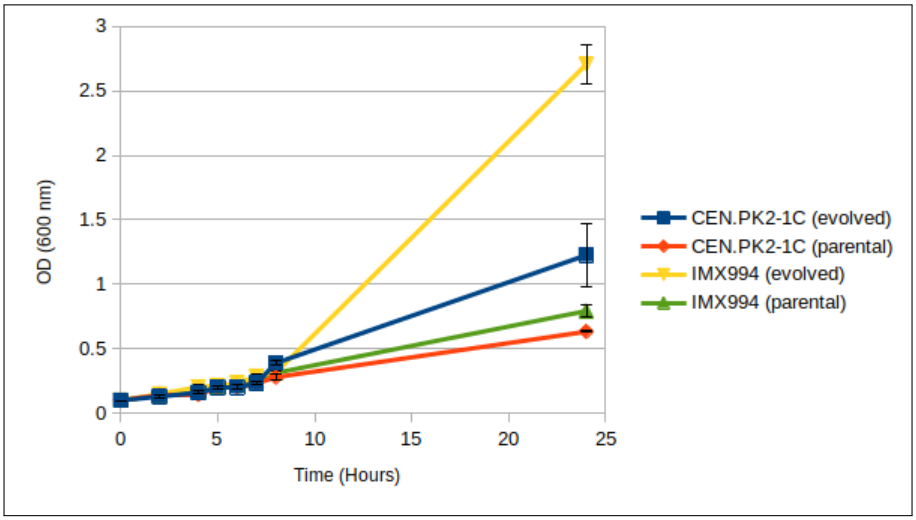

Figure 18: Growth curves of CEN.PK2-1C and IMX994 yeast strains on SX-U medium. In the figure, the evolved and non-evolved parental yeast strains are represented. The optical density was measured at 600 nm during 24 hours. The data points are the average OD of three biological replicates, which are three yeast colonies previously transformed with the XI expression vector. The black lines are the error bars that represent the standard error of the three replicates used.

Furthermore, another growth curves were obtained for the evolved yeast strains in the same culture medium, where the yeast colony with the highest growth was selected for both yeast strains. Yeasts were cultivated to an initial OD of 0.05, and the OD values were registered for the next 72 hours. In the figure 19, two curves for evolved CEN.PK2-1C and IMX994 cells can be observed. The IMX994 strain displayed higher OD values in comparison to the CEN.PK2-1C yeasts for almost all time points. After 72 hours, the CEN.PK2-1C cells reached a final OD of about 2.4, while the IMX994 cells reached a OD value of about 3.4. Thus, the IMX994 strain had the highest growth as it reached higher OD values than the CEN.PK2-1C strain.

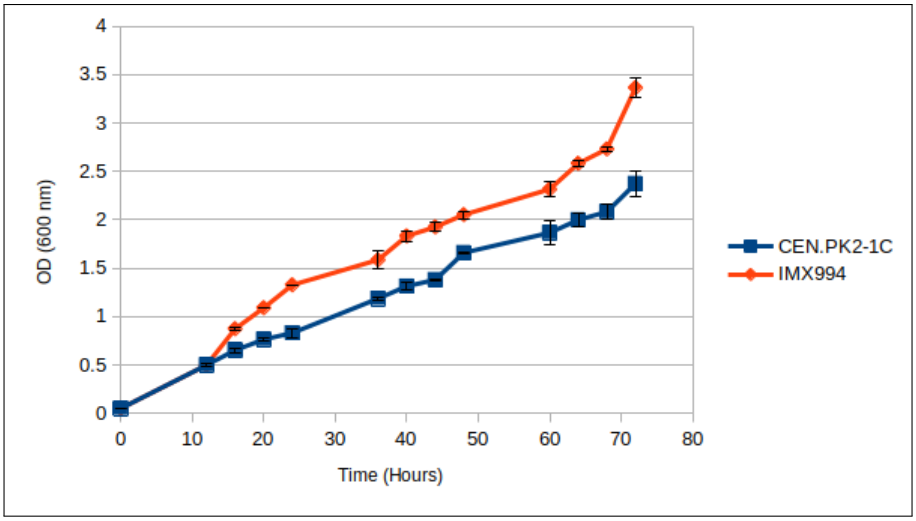

Figure 19: Growth curves of evolved CEN.PK2-1C and IMX994 yeast strains on SX-U medium during 72 hours. The data points are the average OD at 600 nm of three technical replicates of the yeast colony with the highest growth. The error bars corresponding to the standard error of the three replicates used are also represented.

3.2.2 Evolution of yeasts under nitrogen depletion

Another evolution experiment was carried out using the same yeast strains that were previously evolved. Yeast cells were initially cultivated in pre-cultures of SC-U with 2% glucose, and the pre-cultures were incubated overnight at 30°C. In the next day, cells were transferred to two types of synthetic medium, with and without drop-out. The evolution experiment was carried out during a period of 33 days. The evolution ended after 11 transfers for both strains in medium with drop-out, and 11 transfers for the IMX994 strain and 6 transfers for the CEN.PK2-1C strain in medium without drop-out. During serial passages, the batch cultures were inoculated to an initial OD = 0.05 and the final OD reached after a few days was registered (Figure 20). In the first two serial transfers, cells were cultivated with a concentration of xylose of 1.75% and glucose at 0.25%. Then, the concentration of xylose was raised to 1.9% with 0.1% glucose in the next two transfers, where a decrease in ODs was observed for all yeast strains. From the fifth transfer, all yeast strains were cultivated in medium with solely xylose (2%). For all yeast strains except CEN.PK2-1C in medium without drop-out there was a overall increase in optical density over passages, specifically between the fifth and sixth transfers. During this time, the time between transfers was of 3 days. In yeasts evolved in medium with drop-out, the ODs were higher than those cultivated in medium without drop-out, and this OD increase was slighter. In yeasts evolved in medium without drop-out, the OD of IMX994 strain was doubled from the fifth to the sixth transfer. Whereas, in the case of CEN.PK2-1C strain, cells took too long to grow, taking up to 17 days in the fifth transfer. Then, the sixth transfer was the last transfer for the CEN.PK2-1C without dropout, and the time between transfers was 5 days. From the seventh passage, the time between transfer was increased to 4 days for all yeast strains except the CEN.PK2-1C without

drop-out, which evolution ended in the sixth transfer. From this point, there was a gradual increase in ODs until the ninth transfer for all yeast strains. Then, in the last two transfers, the time between serial passages was reduced to 3 days, and a small increase in OD was observed from the tenth to the eleventh transfer. The IMX994 strain generally displayed higher OD values than the CEN.PK2-1C strain, having reached values between a range of 3 and 5 for the IMX994 cells with drop-out, and ODs between 2 and 3 in IMX994 yeasts in medium without drop-out. The CEN.PK2-1C cells had the lowest OD values, having OD values between 2 and 3 for cells cultivated with drop-out, and values about 0.5 for yeasts evolved in medium without drop-out.

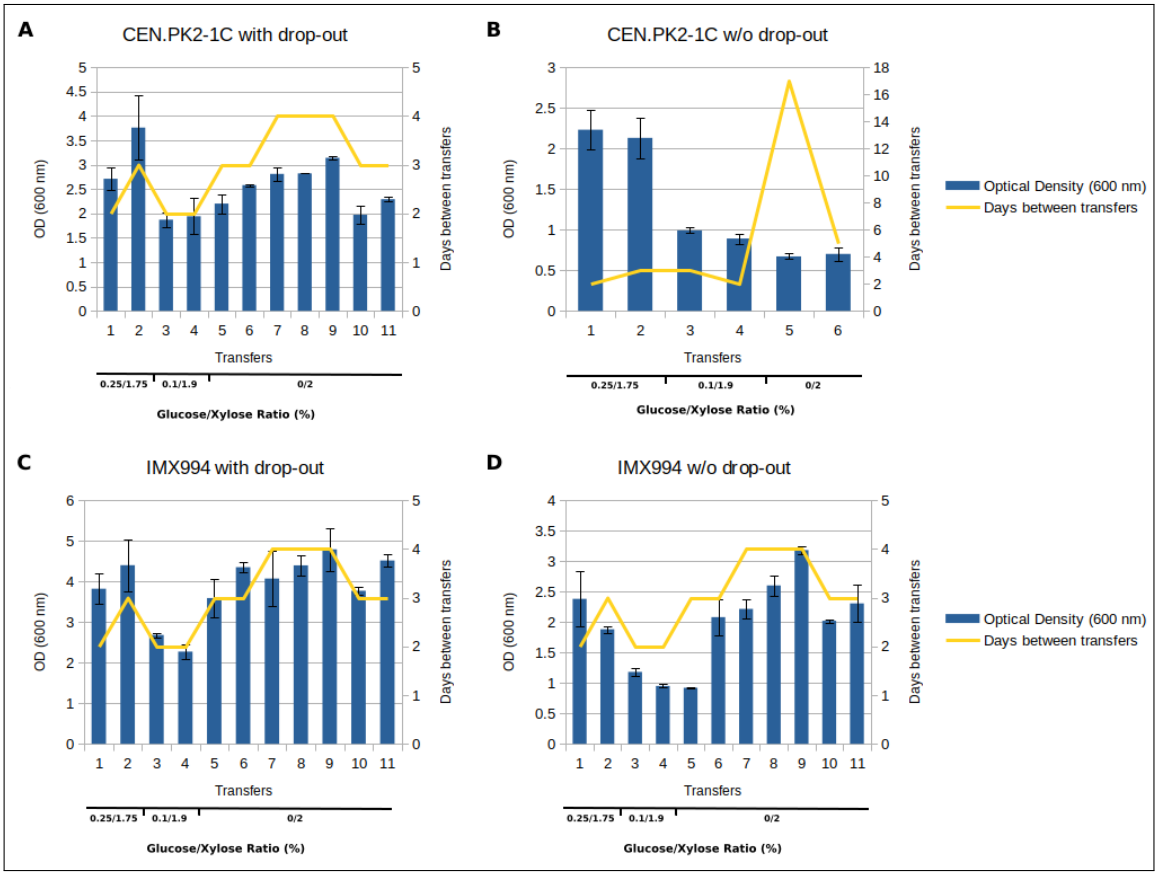

Figure 20: Overview of adaptive laboratorial evolution of two yeast strains CEN.PK2-1C and IMX994 in medium with and without drop-out. In this figure, there are four plots for each yeast strain and culture medium type, including CEN.PK2-1C with drop-out (A), CEN.PK2-1C without drop-out (B), IMX994 with drop-out (C), and IMX994 without drop-out (D). The blue bars are the average of OD values for three colonies of each yeast strain used as biological replicates, which are the OD values measured before the subsequent transfer. The black lines are the error bars that represent the standard error of the replicates used. The yellow line represents the time passed expressed in days between serial transfers. The the concentration ratio of glucose/xylose in the culture medium for the respective transfers is also represented.

Furthermore, the total number of generations for each evolved yeast strain was calculated using the aforementioned formula. In the figure 21, the cumulative number of generations over the time is represented. At the end of the evolution experiment, the CEN.PK2-1C strain reached of about 62 in medium with drop-out, and only 26 generations in medium without drop-out. The IMX994 strain reached a number of generations of 69 when cultivated with drop-out, and 57 in medium without drop-out. The number of generations between the two strains in drop-out medium is more similar, although the IMX994 cells reached 7 more generations. Whereas, the differences between the strains are much more remarkable in medium without drop-out, being the CEN.PK2-1C strain evolved in medium without drop-out the one with a much lower number of generations in comparison to the other yeast strains.

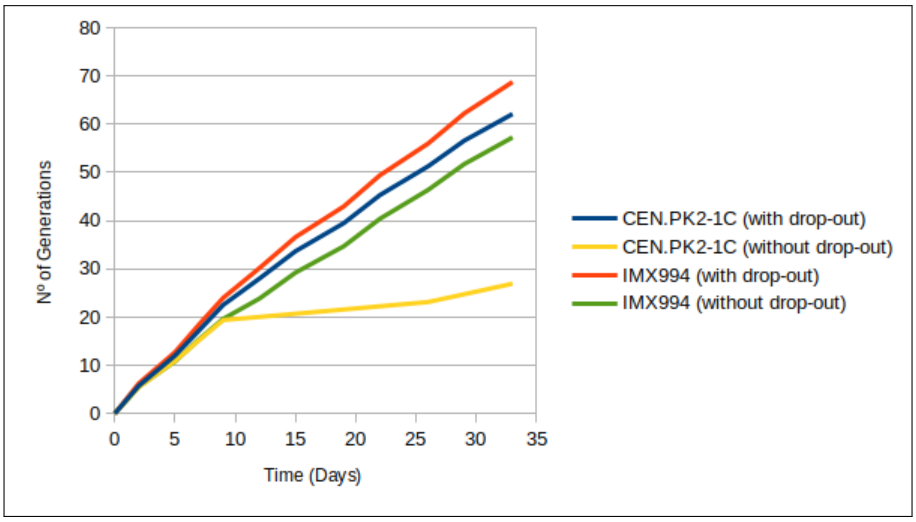

Figure 21: Cumulative number of generations of both evolved yeast strains CEN.PK2-1C and IMX994 cultivated with and without drop-out.

Additionally, growth curves were obtained for both yeast strains evolved in medium with and without drop-out. The cultures were inoculated with yeast cells to an initial OD = 0.05, and the OD values were registered during 72 hours. In the figure 22, four growth curves can be observed, with two curves for each strain evolved in both types of synthetic xylose medium. As can be observed, the IMX994 strain had a higher growth in comparison to the CEN.PK2-1C strains, reaching an OD of about 3.5 after 72 hours, while CEN.PK2-1C had reached an OD of about 2. It is possible to notice a similarity for the CEN.PK2-1C and IMX994 curves between both types of synthetic xylose media with and without drop-out, although slight differences in the OD values were observed between the growth curves of the IMX994 strain, being the IMX994 strain evolved without drop-out the one with the highest optical densities.

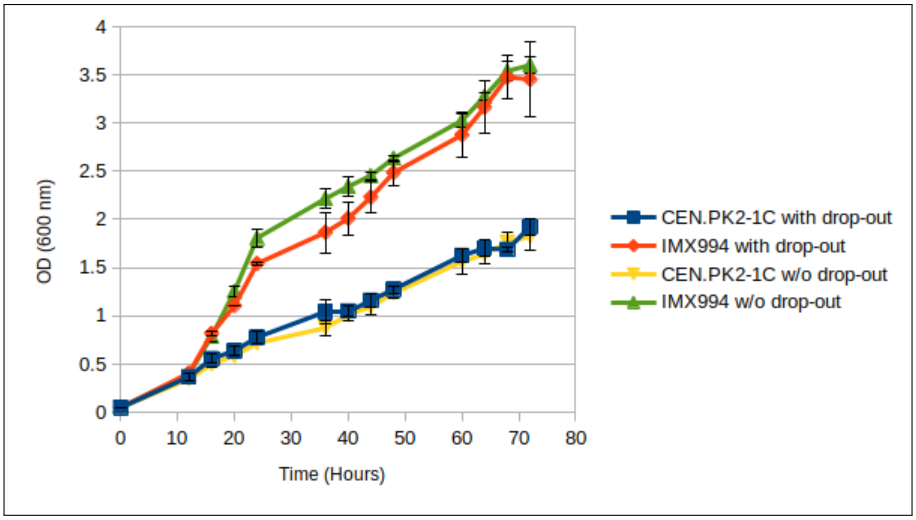

Figure 22: Growth curves of evolved CEN.PK2-1C and IMX994 yeast strains on SX-U medium during 72 hours. The data points are the average OD at 600 nm of two technical replicates per each two evolved yeast clones used as biological replicas, giving a total of four replicates. The error bars corresponding to the standard error are also represented.

3.3 Plasmid loss in yeasts with the pYPK0_TDH3_8054_2_ENO2 plasmid

After the ALE experiments of yeasts, IMX994 cells were cultivated in liquid rich glucose medium (YPD) in order to promote the plasmid loss, specifically the pYPK0_TDH3_8054_2_ENO2 plasmid which contains the xylose isomerase expression cassette. The cultivation of yeasts transformed with a plasmid in non-selective media can lead to plasmid loss, since cells that have not retained the plasmid after several cell divisions can proliferate on the medium. In this case, as the plasmid contains the auxotrophic selective marker *URA3*, yeasts were cultivated in an auxotrophic medium without uracil. After 3 serial passages in liquid rich medium, yeast cells were plated in solid rich medium and incubated at 30°C. After 3 days, yeast colonies were obtained for each yeast culture, with two yeasts colonies evolved in synthetic xylose media with and without drop-out. Then, 12 colonies from each yeast culture were picked and transferred to two culture media, rich glucose medium (YPD) and synthetic complete medium without uracil (SC-U). In this way, it is possible to know which colonies had lost the plasmid, which are those that did not grow in the selective medium SC-U. Whereas, if the colonies grew on both media, it means that colonies retained the plasmid. In the figure 23, the results obtained for the plasmid loss are represented. All yeast colonies grew on rich medium as expected, while some colonies survived and grew on selective medium SC-U. In the case of IMX994 yeasts evolved with drop-out, the colonies I5, II1, II2, II3, II10 and II12 had lost the plasmid. Whereas, in IMX994 yeasts evolved without drop-out, the colonies that lost the plasmid were I6, I10, II3, II5, II6, II10 and II11. Afterwards, 4 of these colonies were selected for spot assay analysis,

where different groups of yeast strains were tested, including parental yeast strains, evolved strains, and yeasts that lost the plasmid. These colonies include two yeast colonies evolved in medium with drop-out and other two colonies evolved without drop-out.

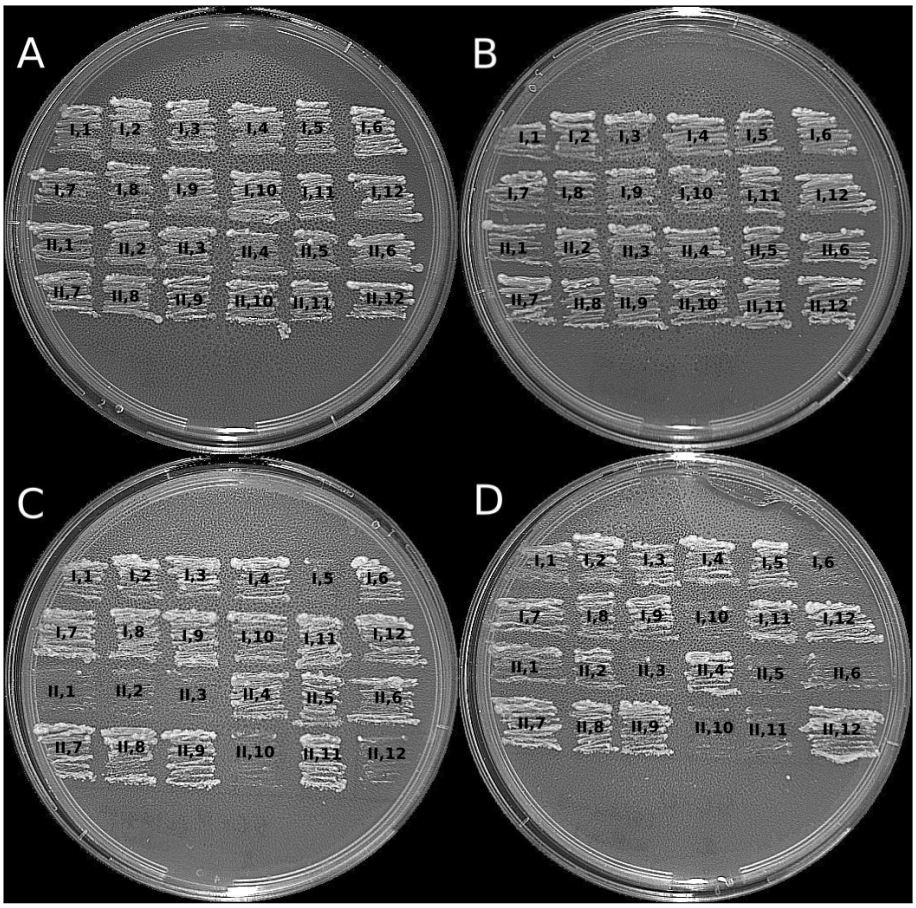

Figure 23: IMX994 yeast colonies cultivated in solid YPD and SC-U media after serial passages in liquid YPD medium to induce the plasmid loss. In this figure it is possible to observe four plates, two with YPD and another two with SC-U. Each plate was prepared in order to streak 12 yeast colonies from two isolated IMX994 parental clones, which were previously transformed with the pYPK0_TDH3_8054_2_ENO2 plasmid and evolved in synthetic xylose-containing media with and without, giving a total of 24 colonies per plate. The plates include: YPD medium for IMX994 cells evolved with drop-out (A); YPD medium for IMX994 cells evolved without drop-out (B); SC-U for IMX994 evolved with drop-out (C); and SC-U for IMX994 yeasts evolved without drop-out (D). The yeast colonies that lost the plasmid are indicated with the respective numbers observed in the figure. Each yeast colony was numbered by a roman numeral, which represents the evolved yeast parental clone I and II, and an arabic numeral representing each isolated yeast colony.

3.4 Spot assay analysis of *S. cerevisiae* strains

The spot assay analysis allows to obtain an visual insight into the growth of different types of microorganisms on a specific medium, typically by spotting a small amount of each strain on a plate and measuring the size of the colonies. It can be used to evaluate the growth of microbial cells in certain conditions, based on the size and shape of the cell colonies. In this case, the spot assay analysis was carried out to compare and characterize the growth of different yeast strains in four culture media: synthetic complete medium without uracil (SC-U); synthetic xylose medium without uracil (SX-U); synthetic defined xylose medium (SDX); and rich xylose medium (YPX). Four groups of yeast strains were tested, including the parental yeast strains CEN.PK2-1C and IMX994, evolved IMX994 yeast strains, and IMX994 yeasts that lost the plasmid. The SC-U and SX-U media were used to test the difference between yeasts transformed with the plasmid and those without the plasmid, while the SDX and YPX cultures were used as control media.

The first group of yeasts to be tested was the parental yeast strains CEN.PK2-1C and IMX994. These strains include the wild-type yeast strains and the non-evolved XI-expressing yeasts that were previously transformed with the pYPK0_TDH3_8054_2_ENO2 plasmid. In the figure 24, the plates where yeast cells were tested are presented, with five spots for serial dilutions from 10^{0} to 10^{-4}. According to the observed results, the parental XI-expressing IMX994 and CEN.PK 2-1C strains, denominated as IMX994 XI and CEN.PK2-1C XI, grew in SC-U and SX-U, while the wild-type yeast strains (CEN.PK2-1C WT and IMX994 WT) did not grow in these media. In addition, yeast colonies had a smaller size in SX-U when compared with the SC-U. According to the observations, in SC-U and SX-U culture media only the XI-expressing yeast strains grew since these yeasts were transformed with the pYPK0_TDH3_8054_2_ENO2 plasmid, which contains the auxotrophic marker *URA3* that enables the growth of transformant cells in the absence of uracil. Besides, the yeast growth on glucose is faster in comparison with the growth on xylose, which explains the different size of yeast colonies between the SC-U and SX-U. Whereas, the wild-type yeast strains did not survived and grew in both SC-U and SX-U since both CEN.PK2-1C and IMX994 strains are auxotrophic to uracil (Entian and Kötter, 2007; Papapetridis et al., 2018). In SDX medium, only the IMX994 strains displayed growth in this medium, and the colony size was smaller than in the other culture media. This happened since this medium only contains a minimal amount of ingredients, such as yeast nitrogen base without aminoacids, xylose, potassium hydrogen phtalate, and uracil. Besides, this medium does not have the aminoacids tryptophan, histidine and leucine. For this reason, the CEN.PK2-1C cells did not survived and grew in this medium since this strains has auxotrophy for these aminoacids (Entian and Kötter, 2007). Moreover, the wild-type IMX994 displayed a similar pattern with the XI-expressing IMXX94, although the colonies are slightly more visible for the IMX994 XI strain than in the wild-type in the 10^{-3} dilution. Finally, all yeast strains grew in YPX medium, without any significant differences between all yeast strains. These results demonstrate that the expression of XI gene through the plasmid pYPK0 gave to yeasts

the ability to metabolize the xylose and grow on medium where the xylose is the sole carbon source. It is possible to verify that the transformation of both yeasts with the pYPK0_TDH3_8054_2_ENO2 plasmid and the expression of the XI gene worked, as the XI-expressing strains grew in synthetic xylose medium.

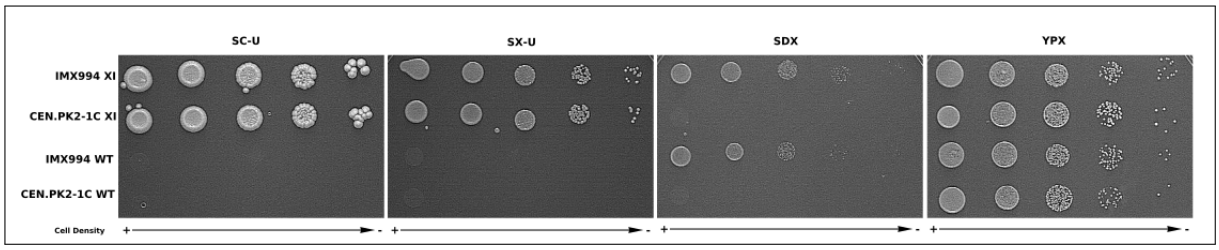

Figure 24: Spot assay analysis of parental yeast strains IMX994 and CEN.PK 2-1C, including the wild-type and the XI-expressing yeasts. In this figure, four plates with SC-U, SX-U, SDX and YPX are represented. Each plate has four strains, including IMX994 WT, CEN.PK2-1C WT, IMX994 XI, and CEN.PK2-1C XI. The variation of cell density is also represented, which results from the serial dilutions made, including dilutions of 10^{0} to 10^{-4}.

The evolved IMX994 yeasts were also tested by spot assays (Figure 25), where two clones of the evolved IMX994 were used (IMX994 I and II). These clones were obtained after the ALE experiment, in which yeasts were evolved in synthetic xylose medium with and without drop-out. As can be observed, all evolved yeast strains grew in both SC-U and SX-U medium as expected. Based on the size of the colonies, those that are observed in SC-U are larger than in SX-U medium, as yeasts grow more rapidly on glucose than on xylose. In addition, all yeasts, either evolved with drop-out or without, do not displayed any significant differences in spot assay analysis. Furthermore, all evolved yeasts also in SDX and YPX medium in same way, being the growth slower in SDX as the colony size was smaller than the other media.

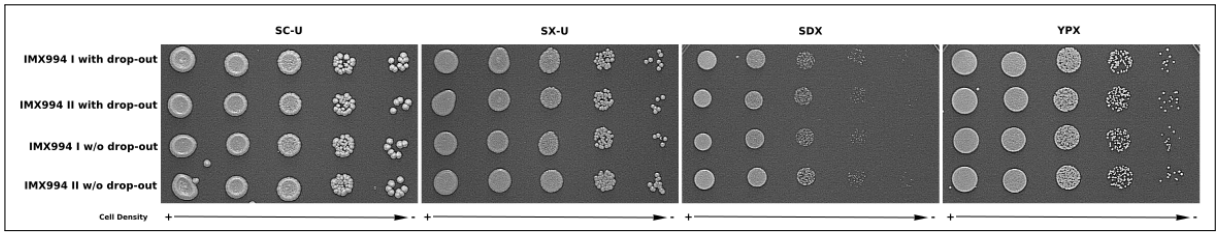

Figure 25: Spot assay analysis of evolved IMX994 yeasts. In this figure, the SC-U, SX-U, SDX and YPX media are represented. Each plate has four strains, including two clones of IMX994 yeasts (IMX994 I and II) evolved with and without drop-out. The variation of cell density is represented, which results from the serial dilutions made, including dilutions of 10^{0} to 10^{-4}.

In addition, the evolved yeast strains can be compared with the parental ones. The IMX994 evolved yeasts in comparison to the IMX994 parental yeasts did not have any significant difference in growth on SC-U and YPX media. However, the differences were clear in SX-U and SDX media. As can be observed, the evolved IMX994 cells displayed more colonies with a size larger than the parental IMX994 strains, indicating that the adaptive evolution of yeasts improved the growth of yeasts on xylose.

Finally, the same yeast strains used before but without plasmid were also tested. According to the figure 26, these yeast strains did not grow in SC-U and SX-U as expected. Nonetheless, these yeasts grew in SDX and YPX media, although the growth in SDX medium had been more reduced. Since these yeast strains lost the plasmid, they also lose the ability to survive and grow in uracil-auxotrophic media like SC-U and SX-U. Regarding to the SDX medium, it is possible to visualize some yeast colonies with a reduced size.

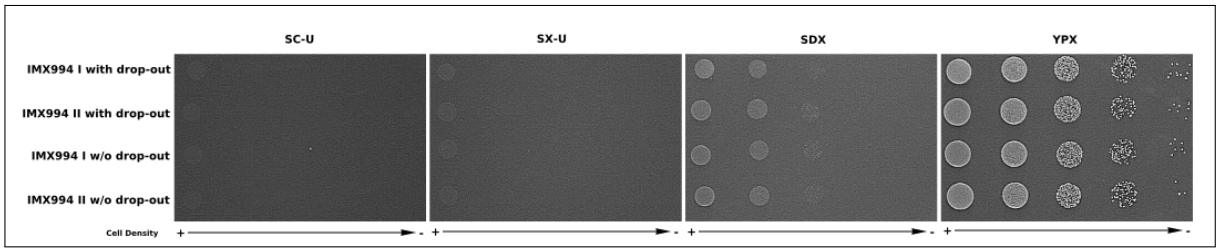

Figure 26: Spot assay analysis of yeasts that lost the plasmid pYPK0_TDH3_805_2_ENO2. In this figure, the SC-U, SX-U, SDX and YPX media are represented. Each plate has four strains, including the same yeast strains used before but without plasmid. The variation of cell density is represented, which results from the serial dilutions made, including dilutions of 10^{0} to 10^{-4}.

Interestingly, the yeasts that lost the plasmid displayed results that were similar to those of the parental wild-type IMX994 strain, showing similarities between the yeasts that lost the plasmid and the parental strains. Regarding to the evolved yeasts, the differences between these and the yeasts without plasmid were obvious. These results demonstrate that the loss of the pYPK0_TDH3_8054_2_ENO2 plasmid interferes with the ability of yeasts to grow in media where xylose is the sole carbon source. Consequently, yeasts without the plasmid are incapable to metabolize xylose as they cannot to express the xylose isomerase, and then, they lose the ability to grow efficiently on xylose.

Chapter 4

Conclusion and Future Perspectives

In this work, two yeast strains with the ability to metabolize xylose and grow efficiently on xylose-containing media were developed. The CEN.PK2-1C and IMX994 strains were first transformed with the expression vector pYPK0_TDH3_8054_2_ENO2 that contains the XI expression cassette. The transformation was successfully, giving the capability to yeasts to express the XI pathway. The genomic integration of XI gene by CRISPR/Cas9 was also attempted in the CEN.PK2-1C strain. Unfortunately, the CRISPR/-Cas9 technique did not work since the XI expression cassette integrated in yeast genome was not detected by PCR for any transformant colony. Giving that, the yeasts transformed with the pYPK0 expression vector with the XI gene were subsequently subjected to adaptive laboratorial evolution in order to optimize yeasts growth on xylose. After the ALE experiment, the analysis of yeast growth through growth curves and spot assay analysis indicate that the evolved yeast strains had a higher growth on xylose-containing media in comparison with the non-evolved parental strains. Therefore, the combination of the heterologous expression of XI pathway with the adaptive evolution led to the improvement of yeasts growth on xylose. Besides, in this work it was possible to verify the effect of plasmid loss, specially the pYPK0_TDH3_8054_2_ENO2 plasmid used for the XI pathway expression. The loss of the plasmid caused the inability for yeasts to assimilate xylose and grow properly on xylose media, demonstrating the relevance of the XI pathway expression. In conclusion, the heterologous expression of XI pathway in *S. cerevisiae* strains and the development of xylose-consuming yeasts was accomplished, although the ultimate goal of this work was not yet achieved. Thus, a link between the xylose catabolism and fatty acid production remains to be established.

This experimental work had successfully led to the development of new yeast strains capable to assimilate xylose and grow efficiently on xylose-containing media. However, there is still the possibility for future work that can be done to achieve the ultimate goal of this work, which is the production of fatty acids, specially branched-chain fatty acids. The FAs production will be connected to the xylose catabolism through some metabolic engineering strategies, including the integration of heterologous pathways in yeasts, such as the phosphoketolase pathway (PK) and the phosphate acetyltransferase (PTA). The introduction of these two metabolic pathways would enable the conversion of xylose until the production of acetyl-CoA, and then,

the FAs biosynthesis. Until the present moment, yeasts have the ability to convert xylose into xylulose via xylose isomerase. In turn, xylulose is phosphorylated into xylulose-5-phosphate by a native yeast metabolic pathway. From this point, the PK and PTA pathways would establish a link between the xylose catabolism and the FAs biosynthesis, as xylulose-5-phosphate is converted to glyceraldehyde-3-phosphate and acetyl phosphate that is then converted into acetyl-CoA. Since acetyl-CoA is a fundamental precursor of FAs biosynthesis, by directing the metabolism towards acetyl-CoA production it would lead to an enhancement of fatty acid production.

Thus, the heterologous expression of PK and PTA pathways can be used to achieve the main objective of this work. In this case, candidate genes of PK and PTA from source organisms available in the Department of Biology of the University of Minho will be expressed in XI-expressing *S. cerevisiae* strains that were already developed in this work. The source organisms for the extraction of the PK gene may include yeast species, such as *Schizosaccharomyces pombe*, *Schizosaccharomyces octosporus*, *Leuconostoc mesenteroides*, and *Rhodotorula glutinis*. Whereas, bacterial species such as *E. coli* and *Bacillus subtilis* can be used for the PTA gene extraction. Then, these genes should be first cloned using the pYPKa cloning vector and *E. coli* as the host organism. After gene cloning, the PK and PTA genes would be extracted, and then expressed in *S. cerevisiae* through the expression vector pYPK0. For this, there is a method that can be used for metabolic pathway assembly denominated as Yeast Pathway Kit (YPK) (F. Pereira et al., 2016). This method consist of a protocol where genetic elements for the expression of metabolic pathways, including genes and regulatory sequences, are assembled by making a set of single gene expression vectors that are further combined through homologous recombination. Then, the promoter-gene-terminator fragments, also denominated as transcriptional units, are generated and can be stitched together by a second round of homologous recombination. This is a method that enables the combination and expression of any desired metabolic pathways in *S. cerevisiae* in an efficient way.

Furthermore, the next step would be the characterization of yeast strains after the integration of PK and PTA pathways. In this task, the yeasts growth on xylose would be tested, with yeast strains expressing the PK/PTA pathway and with the deletion of acetyl-CoA syntethase pathway (ACS). In this screening task, the PK and PTA genes from the candidate source organisms that work best will be selected for characterization. Yeast strains with PK/PTA pathway, with and without the ACS pathway (*acs2Δ*), will be cultivated in culture media with glucose, ethanol or xylose. In order to characterize the PK and PTA enzymes with best performance, the growth of yeast strains expressing these enzymes will be evaluated in liquid cultures by the determination of the specific growth rates, and also in solid cultures by spot assay analysis. Then, the substrate consumption and metabolite production would be measured by HPLC. Besides, the lipid accumulation would be quantified by fluorescence, using nile red as a fluorescent marker.

In addition, the lipid production could be quantified for yeasts evolved under nitrogen depletion. Each yeast strain evolved in synthetic xylose medium with or without drop-out would be tested for lipid accumulation, which can be analysed and quantified by fluorescence microscopy using the BODIPY dye (Dan

et al., 2015). As mentioned before, the depletion of nitrogen sources in the yeast growth medium lead to an increase of lipid accumulation, and the results obtained by fluorescence microscopy could be then compared with those that are found in literature.

Moreover, various additional metabolic engineering strategies can be performed for the optimization of xylose consumption and fatty acids production. These strategies include the overexpression of acetyl-CoA carboxylase from *Yarrowia lipolytica* (H. Pereira et al., 2022), in order to increase levels of malonyl-CoA, which is a direct precursor of FAs synthesis. Besides, the deletion of the aldehyde dehydrogenase (*ALD6*), which converts acetaldehyde to acetate, can be carried out to limit the synthesis of acetyl-CoA through ACS, which consumes one ATP unit.

At the end, the accomplishment of the aforementioned tasks would lead to the improvement of FAs production from the conversion of xylose in yeasts. The combination of the heterologous pathways for assimilation of xylose and conversion into acetyl-CoA and the optimization of endogenous metabolic pathways would greatly expand the applications of metabolic engineering in *S. cerevisiae*. These approaches could lower the cost and reduce the carbon footprint for the overall process, leading to a sustainable and efficient use of natural resources. The FAs production by engineered *S. cerevisiae* would make possible an environment-friendly production of biofuels and fine chemicals derived from fatty acids.

Bibliography

Abad, S., Nahalka, J., Bergler, G., Arnold, S., Speight, R., Fotheringham, I., Nidetzky, B., & Glieder, A. (2010). Stepwise engineering of a *Pichia pastoris* D-amino acid oxidase whole cell catalyst. *Microbial Cell Factories*, *9*, 1–12. https://doi.org/10.1186/1475-2859-9-24

Allison, M. J., & Bryant, M. P. (1963). Biosynthesis of branched-chain amino acids from branched-chain fatty acids by rumen bacteria. *Archives of Biochemistry and Biophysics*, *101*(2), 269–277. https://doi.org/10.1016/S0003-9861(63)80012-0

Almeida, J., Bertilsson, M., Hahn-Hägerdal, B., Lidén, G., & Gorwa-Grauslund, M. (2009). Carbon fluxes of xylose-consuming *Saccharomyces cerevisiae* strains are affected differently by nadh and nadph usage in hmf reduction. *Applied Microbiology and Biotechnology*, *84*, 751–61. https://doi.org/10.1007/s00253-009-2053-1

Almeida, J., Runquist, D., Sànchez i Nogué, V., Lidén, G., & Gorwa-Grauslund, M. (2011). Stress-related challenges in pentose fermentation to ethanol by the yeast *Saccharomyces cerevisiae*. *Biotechnology Journal*, *6*, 286–299. https://doi.org/10.1002/biot.201000301

Amore, R., Wilhelm, M., & Hollenberg, C. P. (1989). The fermentation of xylose — an analysis of the expression of *Bacillus* and *Actinoplanes* xylose isomerase genes in yeast. *Applied Microbiology and Biotechnology*, *30*, 351–357. https://doi.org/10.1007/BF00296623

Bailey, J. E. (1991). Toward a Science of Metabolic Engineering. *Science*, *252*(5013), 1668–1675. https://doi.org/10.1126/science.2047876

Barnett, J. (2003). Beginnings of microbiology and biochemistry: The contribution of yeast research. *Microbiology*, *149*, 557–567. https://doi.org/10.1099/mic.0.26089-0

Barrangou, R., Fremaux, C., Deveau, H., Richards, M., Boyaval, P., Moineau, S., Romero, D., & Horvath, P. (2007). CRISPR Provides Acquired Resistance Against Viruses in Prokaryotes. *Science*, *315*, 1709–1712. https://doi.org/10.1126/science.1138140

Branduardi, P., Longo, V., Berterame, N., Rossi, G., & Porro, D. (2013). A novel pathway to produce butanol and isobutanol in *Saccharomyces cerevisiae*. *Biotechnology for Biofuels*, *6*, 1–12. https://doi.org/10.1186/1754-6834-6-68

Braun, A., Geier, M., Bühler, B., Schmid, A., Mauersberger, S., & Glieder, A. (2012). Steroid biotransformations in biphasic systems with *Yarrowia lipolytica* expressing human liver cytochrome p450 genes. *Microbial Cell Factories*, *11*, 1–16. https://doi.org/10.1186/1475-2859-11-106

Briggs, K., Lancashire, W., & Hartley, B. (1984). Molecular cloning, DNA structure and expression of the *Escherichia coli* D-xylose isomerase. *The EMBO Journal*, *3*(3), 611–616. https://doi.org/10.1002/j.1460-2075.1984.tb01856.x

Brown, T. A. (2016). *Gene Cloning & DNA Analysis: An Introduction (7th edition)*. John Wiley & Sons Ltd.

Carroll, D. (2011). Genome Engineering With Zinc-Finger Nucleases. *Genetics*, *188*, 773–782. https://doi.org/10.1534/genetics.111.131433

Chan, D., & Vogel, H. (2010). Current understanding of fatty acid biosynthesis and the acyl carrier protein. *The Biochemical Journal*, *430*, 1–19. https://doi.org/10.1042/BJ20100462

Chatterjee, R., & Yuan, L. (2006). Directed evolution of metabolic pathways. *Trends in Biotechnology*, *24*, 28–38. https://doi.org/10.1016/j.tibtech.2005.11.002

Christian, M., Cermak, T., Doyle, E., Schmidt, C., Hummel, A., Bogdanove, A., & Voytas, D. (2010). Targeting DNA Double-Strand Breaks with TAL Effector Nucleases. *Genetics*, *186*, 757–761. https://doi.org/10.1534/genetics.110.120717

Christie, W. W., & Han, X. (2012). Lipids: Their structures and occurrence (W. W. Christie & X. Han, Eds.; Fourth Edition). In W. W. Christie & X. Han (Eds.), *Lipid analysis (fourth edition)* (Fourth Edition). Woodhead Publishing. https://doi.org/10.1533/9780857097866.3

Cohen, S., Chang, A., Boyer, H., & Helling, R. (1973). Construction of biologically functional bacterial plasmids in vitro. *Proceedings of the National Academy of Sciences of the United States of America*, *70*(11), 3240–3244. https://doi.org/10.1073/pnas.70.11.3240

Cox, M., & Nelson, D. (2021). *Lehninger Principles of Biochemistry (8th edition)*. W. H. Freeman & Co Ltd.

Cunha, J., Soares, P., Romaní, A., Thevelein, J., & Domingues, L. (2019). Xylose fermentation efficiency of industrial *Saccharomyces cerevisiae* yeast with separate or combined xylose reductase/xylitol dehydrogenase and xylose isomerase pathways. *Biotechnology for Biofuels*, *12*, 1–14. https://doi.org/10.1186/s13068-019-1360-8

Dan, L., Song, J.-Z., Li, H., Shan, M.-H., Liang, Y., Zhu, J., & Xie, Z. (2015). Storage lipid synthesis is necessary for autophagy induced by nitrogen starvation. *FEBS Letters*, *589*, 269–276. https://doi.org/10.1016/j.febslet.2014.11.050

de Jong, B. W., Shi, S., Siewers, V., & Nielsen, J. (2014). Improved production of fatty acid ethyl esters in *Saccharomyces cerevisiae* through up-regulation of the ethanol degradation pathway and expression of the heterologous phosphoketolase pathway. *Microbial Cell Factories*, *13*(1), 1–10. https://doi.org/10.1186/1475-2859-13-39

Dragosits, M., & Mattanovich, D. (2013). Adaptive laboratory evolution — Principles and applications for biotechnology. *Microbial Cell Factories*, *12*(64), 1–17. https://doi.org/10.1186/1475-2859-12-64

Engel, S. R., Dietrich, F. S., Fisk, D. G., Binkley, G., Balakrishnan, R., Costanzo, M. C., Dwight, S. S., Hitz, B. C., Karra, K., Nash, R. S., Weng, S., Wong, E. D., Lloyd, P., Skrzypek, M. S., Miyasato, S. R., Simison, M., & Cherry, J. M. (2014). The Reference Genome Sequence of *Saccharomyces cerevisiae*: Then and Now. *G3 Genes|Genomes|Genetics*, *4*(3), 389–398. https://doi.org/10.1534/g3.113.008995

Entian, K.-D., & Kötter, P. (2007). 25 Yeast Genetic Strain and Plasmid Collections. *Methods in Microbiology*, *36*, 629–666. https://doi.org/10.1016/S0580-9517(06)36025-4

Fernandez-Moya, R., & Silva, N. (2017). Engineering *Saccharomyces cerevisiae* for High-Level Synthesis of Fatty Acids and Derived Products. *FEMS Yeast Research*, *17*, 1–15. https://doi.org/10.1093/femsyr/fox071

Fischer, C., Tseng, H.-C., Tai, M., Prather, K., & Stephanopoulos, G. (2010). Assessment of heterologous butyrate and butanol pathway activity by measurement of intracellular pathway intermediates in recombinant *Escherichia coli*. *Applied Microbiology and Biotechnology*, *88*, 265–275. https://doi.org/10.1007/s00253-010-2749-2

Fong, S., Burgard, A., Herring, C., Knight, E., Blattner, F., Maranas, C., & Palsson, B. (2005). In Silico Design and Adaptive Evolution of *Escherichia coli* for Production of Lactic Acid. *Biotechnology and Bioengineering*, *91*, 643–648. https://doi.org/10.1002/bit.20542

Gao, L., Cai, M., Shen, W., Xiao, S., Zhou, X., & Zhang, Y. (2013). Engineered fungal polyketide biosynthesis in *Pichia pastoris*: A potential excellent host for polyketide production. *Microbial Cell Factories*, *12*(77), 1–14. https://doi.org/10.1186/1475-2859-12-77

Generoso, W., Gottardi, M., Oreb, M., & Boles, E. (2016). Simplified CRISPR-Cas genome editing for *Saccharomyces cerevisiae*. *Journal of Microbiological Methods*, *127*, 203–205. https://doi.org/10.1016/j.mimet.2016.06.020

Gidijala, L., Kiel, J., Douma, R., Seifar, R., Gulik, W., Bovenberg, R., Veenhuis, D. M., & van der Klei, I. (2009). An Engineered Yeast Efficiently Secreting Penicillin. *PloS One*, *4*, e8317. https://doi.org/10.1371/journal.pone.0008317

Gietz, R. (2014). Yeast transformation by the LiAc/SS carrier DNA/PEG method. *Methods in Molecular Biology*, *1205*, 31–35. https://doi.org/10.1007/978-1-4939-1363-3_1

Hahn-Hägerdal, B., Karhumaa, K., Jeppsson, M., & Gorwa-Grauslund, M. (2007). Metabolic Engineering for Pentose Utilization in *Saccharomyces cerevisiae*. *Advances in Biochemical Engineering/Biotechnology*, *108*, 147–177. https://doi.org/10.1007/10_2007_062

Hallborn, J. (1996). Metabolic engineering of *Saccharomyces cerevisiae*: Expression of genes involved in pentose metabolism.

Hitzeman, R. A., Hagie, F. E., Levine, H. L., Goeddel, D. V., Ammerer, G., & Hall, B. D. (1981). Expression of a human gene for interferon in yeast. *Nature*, *293*, 717–722. https://doi.org/10.1038/293717a0

Hitzeman, R., Chen, C., Hagie, F., Patzer, E., Liu, C.-C., Estell, D., Miller, J., Yaffe, A., Kleid, D., Levinson, A., & Oppermann, H. (1983). Expression of hepatitis b surface antigen in yeast. *Nucleic Acids Research*, *11*, 2745–2763. https://doi.org/10.1093/nar/11.9.2745

Hu, Y., Zhu, Z., Nielsen, J., & Siewers, V. (2019). Engineering *Saccharomyces cerevisiae* cells for production of fatty acid-derived biofuels and chemicals. *Open Biology*, *9*, 1–10. https://doi.org/10.1098/rsob.190049

Inoue, H., Nojima, H., & Okayama, H. (1990). High efficiency transformation of *Escherichia coli* with plasmids. *Gene*, *96*(1), 23–28. https://doi.org/10.1016/0378-1119(90)90336-p

Jeong, D., Oh, E. J., Ko, J. K., Nam, J.-O., Park, H.-S., Jin, Y.-S., Lee, E. J., & Kim, S. R. (2020). Metabolic engineering considerations for the heterologous expression of xylose-catabolic pathways in *Saccharomyces cerevisiae*. *Plos One*, *15*, e0236294. https://doi.org/10.1371/journal.pone.0236294

Kaneda, T. (1991). Iso- and anteiso-fatty acids in bacteria: Biosynthesis, function, and taxonomic significance. *Microbiological Reviews*, *55*(2), 288–302. https://doi.org/10.1128/mr.55.2.288-302.1991

Karathia, H., Vilaprinyo, E., Sorribas, A., & Alves, R. (2011). *Saccharomyces cerevisiae* as a model organism: A comparative study. *PloS One*, *6*(2), 1–10. https://doi.org/10.1371/journal.pone.0016015

Karhumaa, K., Garcia Sanchez, R., Hahn-Hägerdal, B., & Gorwa-Grauslund, M. (2007). Comparison of the xylose reductase-xylitol dehydrogenase and the xylose isomerase pathways for xylose fermentation by recombinant *Saccharomyces cerevisiae*. *Microbial Cell Factories*, *6*(5), 1–10. https://doi.org/10.1186/1475-2859-6-5

Kjeldsen, T., Balschmidt, P., Diers, I., Hach, M., Kaarsholm, N., & Ludvigsen, S. (2001). Expression of Insulin in Yeast: The Importance of Molecular Adaptation for Secretion and Conversion. *Biotechnology & Genetic Engineering Reviews*, *18*, 89–121. https://doi.org/10.1080/02648725.2001.10648010

Knothe, G. (2010). Biodiesel and renewable diesel: A comparison. *Progress in Energy and Combustion Science*, *36*, 364–373. https://doi.org/10.1016/j.pecs.2009.11.004

Kocharin, K., Siewers, V., & Nielsen, J. (2013). Improved polyhydroxybutyrate production by *Saccharomyces cerevisiae* through the use of the phosphoketolase pathway. *Biotechnology and Bioengineering*, *110*, 2216–2224. https://doi.org/10.1002/bit.24888

Kratzer, R., Egger, S., & Nidetzky, B. (2008). Integration of enzyme, strain and reaction engineering to overcome limitations of baker's yeast in the asymmetric reduction of α-keto esters. *Biotechnology and Bioengineering*, *101*(5), 1094–1101. https://doi.org/10.1002/bit.21980

Kuyper, M., Harhangi, H. R., Stave, A. K., Winkler, A. A., Jetten, M. S. M., de Laat, W. T., den Ridder, J. J. J., op den Camp, H. J. M., van Dijken, J. P., & Pronk, J. T. (2003). High-level functional expression of a fungal xylose isomerase: The key to efficient ethanolic fermentation of xylose by *Saccharomyces cerevisiae*? *FEMS Yeast Research*, *41*, 69–78. https://doi.org/10.1016/S1567-1356(03)00141-7

Kuyper, M., Hartog, M., Toirkens, M., Almering, M., Winkler, A., Dijken, J., & Pronk, J. (2005). Metabolic engineering of a xylose-isomerase-expressing *Saccharomyces cerevisiae* strain for rapid anaerobic xylose fermentation. *FEMS Yeast Research*, *5*, 399–409. https://doi.org/10.1016/j.femsyr.2004.09.010

Kwak, S., & Jin, Y.-S. (2017). Production of fuels and chemicals from xylose by engineered *Saccharomyces cerevisiae*: A review and perspective. *Microbial Cell Factories*, *16*(1). https://doi.org/10.1186/s12934-017-0694-9

Lahue, C., Madden, A., Dunn, R., & Heil, C. (2020). History and Domestication of *Saccharomyces cerevisiae* in Bread Baking. *Frontiers in Genetics*, *11*, 1–15. https://doi.org/10.3389/fgene.2020.584718

Lee, D.-H., & Palsson, B. (2010). Adaptive Evolution of *Escherichia coli* K-12 MG1655 during Growth on a Nonnative Carbon Source, L-1,2-Propanediol. *Applied and Environmental Microbiology*, *76*, 4158–4168. https://doi.org/10.1128/AEM.00373-10

Lee, S.-M., Jellison, T., & Alper, H. S. (2012). Directed evolution of xylose isomerase for improved xylose catabolism and fermentation in the yeast *Saccharomyces cerevisiae*. *Applied and Environmental Microbiology*, *78*(16), 5708–5716. https://doi.org/10.1128/AEM.01419-12

Li, X., & Heyer, W.-D. (2008). Homologous recombination in DNA repair and DNA damage tolerance. *Cell Research*, *18*, 99–113. https://doi.org/10.1038/cr.2008.1

Lian, J., & Zhao, H. (2015). Recent advances in biosynthesis of fatty acids derived products in *Saccharomyces cerevisiae* via enhanced supply of precursor metabolites. *Journal of Industrial Microbiology and Biotechnology*, *42*(3), 437–451. https://doi.org/10.1007/s10295-014-1518-0

Lomakin, I., Xiong, Y., & Steitz, T. (2007). The Crystal Structure of Yeast Fatty Acid Synthase, a Cellular Machine with Eight Active Sites Working Together. *Cell*, *129*, 319–332. https://doi.org/10.1016/j.cell.2007.03.013

Lucena, G., Sánchez-López, A., Barberán-Aceituno, C., Carrillo, J., Lopez-Guerrero, J., & Aguilar-Quesada, R. (2016). DNA Source Selection for Downstream Applications Based on DNA Quality Indicators Analysis. *Biopreservation and Biobanking*, *14*, 1–7. https://doi.org/10.1089/bio.2015.0064

Mans, R., van Rossum, H., Wijsman, M., Backx, A., Kuijpers, N., Broek, M., Daran-Lapujade, P., Pronk, J., Van Maris, A., & Daran, J.-M. (2015). CRISPR/Cas9: A molecular Swiss army knife for simultaneous introduction of multiple genetic modifications in *Saccharomyces cerevisiae*. *FEMS Yeast Research*, *15*(2), 1–15. https://doi.org/10.1093/femsyr/fov004

Mattanovich, D., Sauer, M., & Gasser, B. (2014). Yeast Biotechnology: Teaching the Old Dog New Tricks. *Microbial Cell Factories*, *13*, 34. https://doi.org/10.1186/1475-2859-13-34

Mavrommati, M., Daskalaki, A., Papanikolaou, S., & Aggelis, G. (2021). Adaptive laboratory evolution principles and applications in industrial biotechnology. *Biotechnology Advances*, *54*, 1–31. https://doi.org/10.1016/j.biotechadv.2021.107795

McCarty, M., Dinicolantonio, J., & O'Keefe, J. (2015). Capsaicin may have important potential for promoting vascular and metabolic health. *Open Heart*, *2*, 1–7. https://doi.org/https://doi.org/10.1136/openhrt-2015-000262

Meisinger, C., Pfanner, N., & Truscott, K. (2006). Isolation of Yeast Mitochondria. *Methods in Molecular Biology*, *313*, 33–39. https://doi.org/10.1385/1-59259-958-3:033

Mizushima, N., & Komatsu, M. (2011). Autophagy: Renovation of Cells and Tissues. *Cell*, *147*(4), 728–741. https://doi.org/10.1016/j.cell.2011.10.026

Moes, C. J., Pretorius, I. S., & van Zyl, W. H. (1996). Cloning and expression of the *Clostridium thermosulfurogenes* D-xylose isomerase gene (xylA) in *Saccharomyces cerevisiae*. *Biotechnology Letters*, *18*, 269–274. https://doi.org/10.1128/aem.56.9.2638-2643.1990

Mosier, N., Wyman, C., Dale, B., Elander, R., Lee, Y., Holtzapple, M., & Ladisch, M. (2005). Features of promising technologies for pretreatment of lignocellulosic biomass. *Bioresource Technology*, *96*, 673–686. https://doi.org/10.1016/j.biortech.2004.06.025

Moysés, D. N., Reis, V. C. B., Almeida, J. R. M. d., Moraes, L. M. P. d., & Torres, F. A. G. (2016). Xylose Fermentation by *Saccharomyces cerevisiae*: Challenges and Prospects. *International Journal of Molecular Sciences*, *17*(3), 1–18. https://doi.org/10.3390/ijms17030207

Mu, W., Hassanin, H., Zhou, L., & Jiang, B. (2018). Chemistry Behind Rare Sugars and Bioprocessing. *Journal of Agricultural and Food Chemistry*, *66*, 13343–13345. https://doi.org/10.1021/acs.jafc.8b06293

Nandy, S. K., & Srivastava, R. K. (2018). A review on sustainable yeast biotechnological processes and applications. *Microbiological Research*, *207*, 83–90. https://doi.org/10.1016/j.micres.2017.11.013

Nevoigt, E. (2008). Progress in Metabolic Engineering of *Saccharomyces cerevisiae*. *Microbiology and Molecular Biology Reviews*, *72*, 379–412. https://doi.org/10.1128/MMBR.00025-07

Nielsen, J., & Keasling, J. (2016). Engineering Cellular Metabolism. *Cell*, *164*, 1185–1197. https://doi.org/10.1016/j.cell.2016.02.004

Nikolau, B., Perera, A., Brachova, L., & Shanks, B. (2008). Platform chemicals for a biorenewable chemical industry. *The Plant Journal : For Cell and Molecular Biology*, *54*, 536–545. https://doi.org/10.1111/j.1365-313X.2008.03484.x

Ohgren, K., Bengtsson, O., Gorwa-Grauslund, M., Galbe, M., Hahn-Hägerdal, B., & Zacchi, G. (2007). Simultaneous saccharification and co-fermentation of glucose and xylose in steam-pretreated corn stover at high fiber content with *Saccharomyces cerevisiae* tmb3400. *Journal of Biotechnology*, *126*, 488–498. https://doi.org/10.1016/j.jbiotec.2006.05.001

Ostergaard, S., Olsson, L., & Nielsen, J. (2000). Metabolic Engineering of *Saccharomyces cerevisiae*. *Microbiology and Molecular Biology Reviews*, *64*(1), 34–50. https://doi.org/10.1128/MMBR.64.1.34-50.2000

Paddon, C., Westfall, P., Pitera, D., Benjamin, K., Fisher, K., McPhee, D., Leavell, M., Tai, A., Main, A., Eng, D., Polichuk, D., Teoh, K., Reed, D., Treynor, T., Lenihan, J., Fleck, M., Bajad, S., Dang, G., Diola, D., & Newman, J. (2013). High-level semi-synthetic production of the potent antimalarial artemisinin. *Nature*, *496*, 528–532. https://doi.org/10.1038/nature12051

Papapetridis, I., van Dijk, M., Dobbe, A., Metz, B., Pronk, J., & Van Maris, A. (2016). Improving ethanol yield in acetate-reducing *Saccharomyces cerevisiae* by cofactor engineering of 6-phosphogluconate dehydrogenase and deletion of *ALD6*. *Microbial Cell Factories*, *15*, 1–16. https://doi.org/10.1186/s12934-016-0465-z

Papapetridis, I., Verhoeven, M., Wiersma, S., Goudriaan, M., Van Maris, A., & Pronk, J. (2018). Laboratory evolution for forced glucose-xylose co-consumption enables identification of mutations that improve mixed-sugar fermentation by xylosefermenting *Saccharomyces cerevisiae*. *FEMS Yeast Research*, *18*, 1–47. https://doi.org/10.1093/femsyr/foy056

Paques, F., & Duchateau, P. (2007). Meganucleases and DNA Double-Strand Break-Induced Recombination: Perspectives for Gene Therapy. *Current Gene Therapy*, *7*, 49–66. https://doi.org/10.2174/156652307779940216

Pereira, F., Azevedo, F., Skorupa Parachin, N., Hahn-Hägerdal, B., Gorwa-Grauslund, M., & Johansson, B. (2016). The Yeast Pathway Kit: A method for metabolic pathway assembly with automatically simulated executable documentation. *ACS Synthetic Biology*, *5*, 386–394. https://doi.org/10.1021/acssynbio.5b00250

Pereira, H., Azevedo, F., Domingues, L., & Johansson, B. (2022). Expression of *Yarrowia lipolytica* acetyl-coa carboxylase in *Saccharomyces cerevisiae* and its effect on in-vivo accumulation of malonyl-coa. *Computational and Structural Biotechnology Journal*, *20*, 779–787. https://doi.org/10.1016/j.csbj.2022.01.020

Porro, D., Bianchi, M., Brambilla, L., Menghini, R., Bolzani, D., Carrera, V., Lievense, J., Liu, C.-L., Ranzi, B., Frontali, L., & Alberghina, L. (1999). Replacement of a Metabolic Pathway for Large-Scale

Production of Lactic Acid from Engineered Yeasts. *Applied and Environmental Microbiology*, *65*(9), 4211–4215. https://doi.org/10.1128/AEM.65.9.4211-4215.1999

Portnoy, V., Bezdan, D., & Zengler, K. (2011). Adaptive laboratory evolution—harnessing the power of biology for metabolic engineering. *Current Opinion in Biotechnology*, *22*, 590–594. https://doi.org/10.1016/j.copbio.2011.03.007

Portnoy, V., Herrgård, M., & Palsson, B. (2008). Aerobic Fermentation of D-Glucose by an Evolved Cytochrome Oxidase-Deficient *Escherichia coli* Strain. *Applied and Environmental Microbiology*, *74*, 7561–7569. https://doi.org/10.1128/AEM.00880-08

Ran-Ressler, R., Devapatla, S., Lawrence, P., & Brenna, T. (2008). Branched Chain Fatty Acids Are Constituents of the Normal Healthy Newborn Gastrointestinal Tract. *Pediatric Research*, *64*, 605–609. https://doi.org/10.1203/PDR.0b013e318184d2e6

Redman, M., King, A., Watson, C., & King, D. (2016). What is CRISPR/Cas9? *Archives of Disease in Childhood*, *101*, 1–3. https://doi.org/10.1136/archdischild-2016-310459

Rezanka, T. (1989). Very-long-chain fatty acids from the animal and plant kingdoms. *Progress in Lipid Research*, *28*(3), 147–187. https://doi.org/10.1016/0163-7827(89)90011-8

Roca, C., Nielsen, J., & Olsson, L. (2003). Metabolic Engineering of Ammonium Assimilation in Xylose-Fermenting *Saccharomyces cerevisiae* Improves Ethanol Production. *Applied and Environmental Microbiology*, *69*, 4732–6. https://doi.org/10.1128/AEM.69.8.4732-4736.2003

Rude, M. A., & Schirmer, A. (2009). New microbial fuels: A biotech perspective. *Current Opinion in Microbiology*, *12*(3), 274–281. https://doi.org/10.1016/j.mib.2009.04.004

Sandberg, T., Salazar, M., Weng, L., Palsson, B., & Feist, A. (2019). The emergence of adaptive laboratory evolution as an efficient tool for biological discovery and industrial biotechnology. *Metabolic Engineering*, *56*, 1–16. https://doi.org/10.1016/j.ymben.2019.08.004

Sarthy, A., McConaughy, B., Lobo, Z., Sundstrom, J., Furlong, C., & Hall, B. (1987). Expression of the *Escherichia coli* xylose isomerase gene in *Saccharomyces cerevisiae*. *Applied and Environmental Microbiology*, *53*(9), 1996–2000. https://doi.org/10.1128/aem.53.9.1996-2000.1987

Sato, G., & Kuroda, K. (2023). Overcoming the Limitations of CRISPR-Cas9 Systems in *Saccharomyces cerevisiae*: Off-Target Effects, Epigenome, and Mitochondrial Editing. *Microorganisms*, *11*(4), 1–19. https://doi.org/10.3390/microorganisms11041040

Satomura, A., Nishioka, R., Mori, H., Sato, K., Kuroda, K., & Ueda, M. (2017). Precise genome-wide base editing by the CRISPR nickase system in yeast. *Scientific Reports*, *7*(1), 1–10. https://doi.org/10.1038/s41598-017-02013-7

Sheldon, R., & Woodley, J. (2017). Role of Biocatalysis in Sustainable Chemistry. *Chemical Reviews*, *118*, 801–838. https://doi.org/10.1021/acs.chemrev.7b00203

Sherman, F. (2002). Getting Started With Yeast. *Methods in Enzymology*, *350*, 3–41. https://doi.org/10.1016/s0076-6879(02)50954-x

Silva, P., Ceja-Navarro, J., Azevedo, F., Karaoz, U., Brodie, E., & Johansson, B. (2021). A novel D-xylose isomerase from the gut of the wood feeding beetle *Odontotaenius disjunctus* efficiently expressed in *Saccharomyces cerevisiae*. *Scientific Reports*, *11*, 1–12. https://doi.org/10.1038/s41598-021-83937-z

Singh, P., & Kumar, S. (2019). Microbial Enzyme in Food Biotechnology (M. Kuddus, Ed.). In M. Kuddus (Ed.), *Enzymes in food biotechnology*. Academic Press. https://doi.org/10.1016/B978-0-12-813280-7.00002-5

Sitnicka, D., Figurska, K., & Orzechowski, S. (2010). Functional Analysis of Genes. *Advances in Cell Biology*, *2*, 1–16. https://doi.org/10.2478/v10052-010-0001-y

Sonderegger, M., Schümperli, M., & Sauer, U. (2004). Metabolic Engineering of a Phosphoketolase Pathway for Pentose Catabolism in *Saccharomyces cerevisiae*. *Applied and Environmental Microbiology*, *70*, 2892–2897. https://doi.org/10.1128/AEM.70.5.2892-2897.2004

Stephanopoulos, G., & Vallino, J. (1991). Network Rigidity And Metabolic Engineering In Metabolite Overproduction. *Science*, *252*, 1675–1681. https://doi.org/10.1126/science.1904627

Stephanopoulos, G., Aristidou, A. A., & Nielsen, J. (1998). *Metabolic Engineering: Principles and Methodologies*. Academic Press.

Taormina, V., Unger, A., Schiksnis, M., Torres-Gonzalez, M., & Kraft, J. (2020). Branched-Chain Fatty Acids-An Underexplored Class of Dairy-Derived Fatty Acids. *Nutrients*, *12*, 1–16. https://doi.org/https://doi.org/10.3390/nu12092875

Tehlivets, O., Scheuringer, K., & Kohlwein, S. (2007). Fatty acid synthesis and elongation in yeast. *Biochimica et Biophysica Acta*, *1771*, 255–270. https://doi.org/10.1016/j.bbalip.2006.07.004

Trotter, P. (2001). The genetics of fatty acid metabolism in *Saccharomyces cerevisiae*. *Annual Review of Nutrition*, *21*, 97–119. https://doi.org/10.1146/annurev.nutr.21.1.97

Van Maris, A., Winkler, A., Kuyper, M., de laat, W., Dijken, J., & Pronk, J. (2007). Development of Efficient Xylose Fermentation in *Saccharomyces cerevisiae*: Xylose Isomerase as a Key Component. *Advances in Biochemical Engineering/Biotechnology*, *108*, 179–204. https://doi.org/10.1007/10_2007_057

Wahlbom, C., Eliasson, A., & Hahn-Hägerdal, B. (2001). Intracellular fluxes in a recombinant xylose-utilizing *Saccharomyces cerevisiae* cultivated anaerobically at different dilution rates and feed concentrations. *Biotechnology and Bioengineering*, *72*, 289–296. https://doi.org/10.1002/1097-0290(20010205)72:3<289::aid-bit5>3.0.co;2-9

Walfridsson, M., Bao, X., Anderlund, M., Lilius, G., Bülow, L., & Hahn-Hägerdal, B. (1997). Ethanolic fermentation of xylose with *Saccharomyces cerevisiae* harboring the *Thermus thermophilus* xylA gene, which expresses an active xylose (glucose) isomerase. *Applied and Environmental Microbiology*, *62*, 4648–4651. https://doi.org/10.1128/AEM.62.12.4648-4651.1996

Wang, Y., Halls, C., Zhang, J., Matsuno, M., Zhang, Y., & Yu, O. (2011). Stepwise increase of resveratrol biosynthesis in yeast *Saccharomyces cerevisiae* by metabolic engineering. *Metabolic Engineering*, *13*(5), 455–463. https://doi.org/10.1016/j.ymben.2011.04.005

Winkler, J., Reyes, L., & Kao, K. (2013). Adaptive Laboratory Evolution for Strain Engineering. *Methods in Molecular Biology*, *985*, 211–22. https://doi.org/10.1007/978-1-62703-299-5_11

Wisselink, H., Toirkens, M., Berriel, M., Winkler, A., Dijken, J., Pronk, J., & Van Maris, A. (2007). Engineering of *Saccharomyces cerevisiae* for Efficient Anaerobic Alcoholic Fermentation of L-Arabinose. *Applied and Environmental Microbiology*, *73*, 4881–4891. https://doi.org/10.1128/AEM.00177-07

Woolston, B., Edgar, S., & Stephanopoulos, G. (2013). Metabolic Engineering: Past and Future. *Annual Review of Chemical and Biomolecular Engineering*, *4*, 259–288. https://doi.org/10.1146/annurev-chembioeng-061312-103312

Wuest, D., Hou, S., & Lee, K. (2011). Metabolic Engineering (M. Moo-Young, Ed.; Second Edition). In M. Moo-Young (Ed.), *Comprehensive biotechnology (second edition)* (Second Edition). Burlington, Academic Press. https://doi.org/10.1016/B978-0-08-088504-9.00229-4

Xiao-Jie, L., Hui-Ying, X., Zun-Ping, K., Jin-Lian, C., & Li-Juan, J. (2015). CRISPR-Cas9: A new and promising player in gene therapy. *Journal of Medical Genetics*, *52*, 289–296. https://doi.org/10.1136/jmedgenet-2014-102968

Xiberras, J., Klein, M., Hulster, E., Mans, R., & Nevoigt, E. (2020). Engineering *Saccharomyces cerevisiae* for Succinic Acid Production from Glycerol and Carbon Dioxide. *Frontiers in Bioengineering and Biotechnology*, *8*, 11–13. https://doi.org/10.3389/fbioe.2020.00566

Ziv, N., Brandt, N., & Gresham, D. (2013). The Use of Chemostats in Microbial Systems Biology. *Journal of Visualized Experiments*, *80*, 1–10. https://doi.org/10.3791/50168

Appendix A

Appendix 1 - Plasmid maps

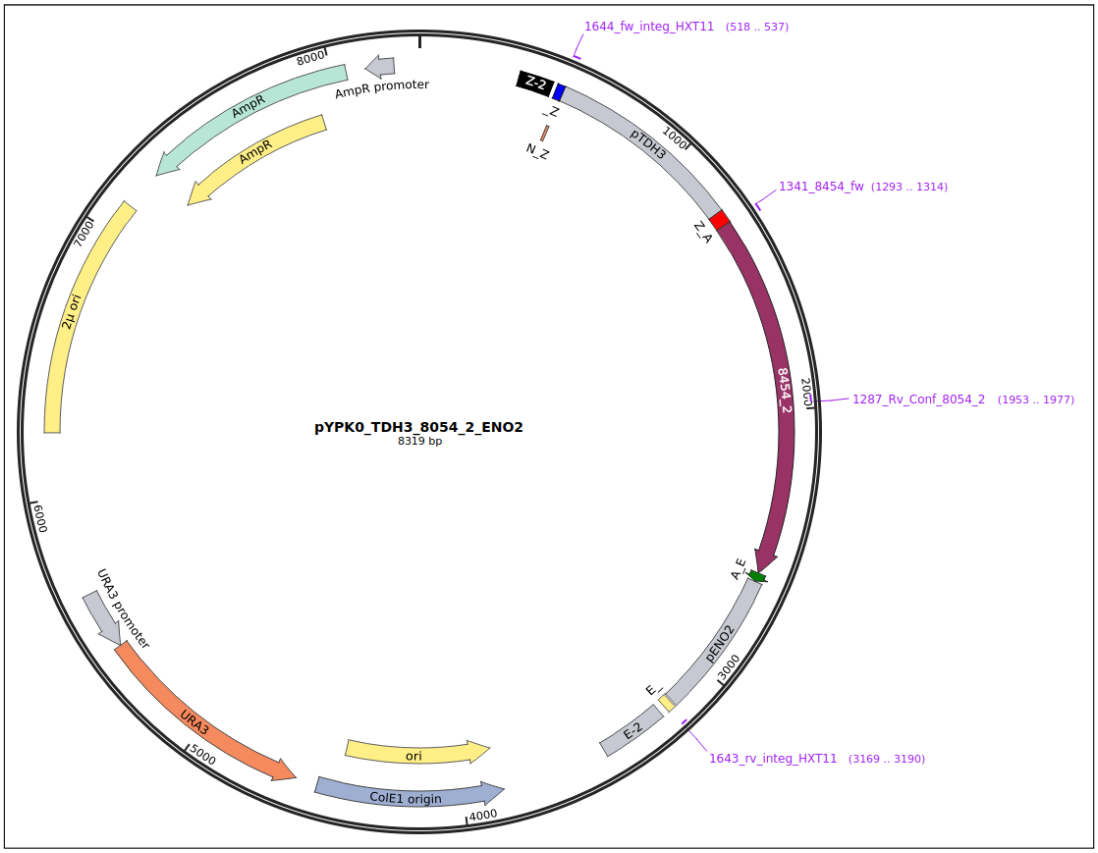

Figure 27: pYPK0_TDH3_8054_2_ENO2 plasmid map. This plasmid contains the xylose isomerase expression cassette (TDH3_8054_2_ENO2), with the promoter TDH3, the xylose isomerase gene 8054_2 extracted from the gut of the wood feeding beetle *Odontotaenius disjunctus* (Silva et al., 2021), and the terminator ENO2. In addition, this plasmid also have other important features, such as the selection marker *URA3* that confers the ability to produce uracil and survive in uracil auxotrophic media, the *AmpR* marker that gives ampicillin resistance, and the sequences for the origins of replication, including the 2µ ori (2 micron origin) and ColE1 origin. The primers used for PCRs where this plasmid was used are also represented. The plasmid map was designed using the software SnapGene®.

Figure 28: pRCC-K plasmid map. This plasmid is a CRISPR-Cas9 vector that contains a sequence for the expression of Cas9 protein, and the guide RNA expression cassette, which is composed by the SNR52 promoter, the gRNA scaffold, and the terminators SUP4 and CYC1. The pRCC-K also have other relevant sequences, including: the *AmpR* selection marker that gives ampicillin resistance; the KanMX expression cassette, composed by the *KanR* selection marker, which confers antibiotic resistance to geneticin, and the promoter and terminator TEF sequences; and origins of replication ori and 2µ ori (2 micron origin). The primers used for PCRs where this plasmid was used are also represented. The plasmid map was designed using the software SnapGene®.

Appendix B

Appendix 2 - Genomic integration of the XI expression cassette on HXT11 locus

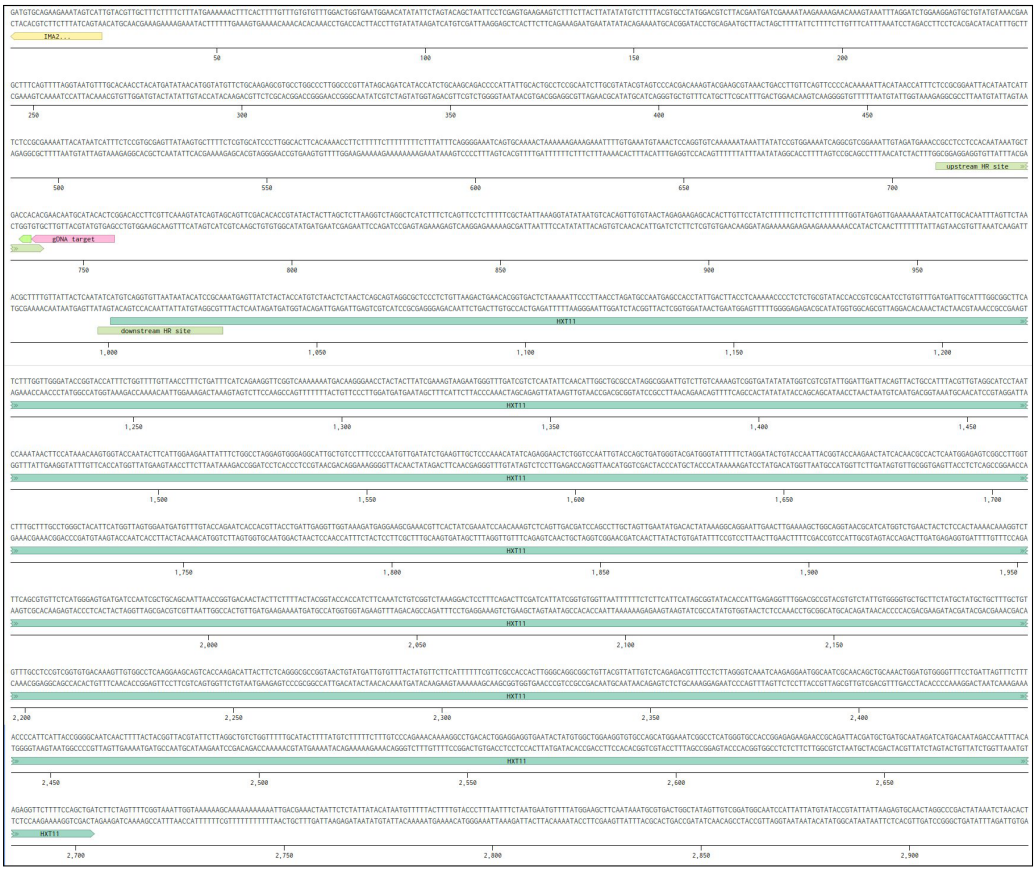

Figure 29: Schematic representation of the HXT11 locus on *S. cerevisiae* genome. The relevant features include the HXT11 gene, gDNA target, the PAM sequence (green arrow adjacent to the gDNA target), and the upstream and downstream homologous recombination sites used to integrate the xylose isomerase cassette expression by homologous recombination after the Cas9 cut. This image was generated using the web platform software Benchling (https://www.benchling.com).

Appendix C

Appendix 3 - Drop-out -HULT aminoacid mix

Table 13: Drop-out -HULT aminoacid mix composition.

Aminoacid	Concentration (mg/L)
L-Adenine	19.74
L-Arginine	78.96
L-Asparagine	78.96
L-Aspartic acid	78.96
L-Cysteine	78.96
L-Glutamic acid	78.96
L-Glutamine	78.96
L-Glycine	78.96
L-Isoleucine	78.96
L-Lysine	78.96
L-Methionine	78.96
L-Phenylalanine	78.96
L-Proline	78.96
L-Serine	78.96
L-Threonine	78.96
L-Tyrosine	78.96
L-Valine	78.96
Myo-inositol	78.96
Para-aminobenzidine	7.896

Appendix D

Appendix 4 - Primers list

Table 14: Primers list with the nomenclature and the respective sequences.

Name	Sequence (5' → 3')
196_pMEC_MX4_fwd	ACTTTTCGGGGAAATGTGC
253_kanC3	CCTCGACATCATCTGCCCAGAT
473_MSW_rev	GTATAGCGACCAGCATTC
474_MSW_fwd	TCCTTGACAGTCTTGACG
576_pBR322_2	GAAAAATAAACAAATAGGGGTTCCG
1287_Rv_Conf_8054_2	GAAAGTTGCCCTTAAAGCCTTTACT
1341_8454_fw	ATGACATACTTTCCCACAGTGG
1354_fw_seq_8454	CTTGCGACCATCTTAACC
1356_sgDNA_seq_pRCC-K_v2	CACACCCTACAATGTTCTG
1643_rv_integ_HXT11	TGCGGATGTATTATTAACACCTGACATGATTGATTCAGGTAAATCCGGAT
1644_fw_integ_HXT11	CGCCTCCTCCACAATAAATGCTGACCACACTGCGGCCGCTGACTTAAATA
1645_rv_HXT11_gDNA	CACGAACAATGCATACACTCGATCATTTATCTTTCACTGCGGAG
1646_fw_HXT11_gDNA	GAGTGTATGCATTGTTCGTGGTTTTAGAGCTAGAAATAGCAAGTTAAAAT
1653_rv_HXT11_conf	TAGAGTCACCGTGTTCAGTC
1654_fw_upstream_HXT11	CTGCAAGCAGACCCCATTATTG